Journal of Nanostructure in Chemistry (2023) 13:197–242
https://doi.org/10.1007/s40097-022-00479-0

REVIEW

Nanostructured metal–organic framework-based luminescent sensor for chemical sensing: current challenges and future prospects

Sopan N. Nangare[1] · Ashwini G. Patil[2] · Sachin M. Chandankar[3] · Pravin O. Patil[4]

Received: 12 November 2021 / Accepted: 14 February 2022 / Published online: 26 February 2022

Abstract

From its inception, an astonishing movement has been made in the architecture and fabrication of a fresh category of nanostructured material acknowledged as luminescent metal–organic frameworks (MOFs). Luminescent MOFs are self-assembled nanostructure by coordinating suitable metal cations or clusters and ideal organic linkers, which exhibited an abundance of merits for sensing of interest of analytes, such as chemicals, metal ions, biomarkers, etc. Herein, tunable surface morphology and diverse functionality of luminescent MOFs offer high sensitivity, high selectivity, good stability, recyclability, real-time applicability, etc. Additionally, the accessible porosity and luminescence property of nanostructured MOFs provides the transducing potential from host–guest chemistry to recognizable improvement in nanosize MOFs luminescence. Therefore, in this review article, we have summarized the nanostructured design of MOFs-based luminescent sensors for chemical and metal ions sensing. At first, the requirement of monitoring of chemical residues and metal ions exposure has been discussed that demonstrates the topical necessity for the chemical and metal ions recognition. Afterward, the current trends of MOFs-centered sensors, synthesis types, and their properties have been elaborated in brief. It revealed that several theoretical sensing mechanisms, such as electron transfer, energy transfer, ligand interaction, overlapping effect, oscillation effect, inner filter effect, decomposition, etc., are accountable for sensing of metal ions and chemical residues. The applications of nano-architectured MOFs-based luminescent sensors for chemical as well as metal ions sensing have been illustrated, which exhibit the lowest detection limit (μM–nM) for both metal ions and chemicals. Interestingly, the nanostructured MOFs relied on luminescent sensors that exhibited high sensitivity and selectivity for the chemical and metal ions in presence of diverse interfering substances. Surface functionality presented on the surface of nano-size MOFs, types of ligands, and selected metal ions provides precise recognition of real-time samples containing metal ions and chemicals. On the whole, the nanostructured design of a MOFs-based luminescent sensor will release a fresh preference for sensing of a target analyte.

✉ Pravin O. Patil
rxpatilpravin@yahoo.co.in

[1] Department of Pharmaceutics, H. R. Patel Institute of Pharmaceutical Education and Research, Dist: Dhule (MS), Shirpur 425405, India

[2] Department of Microbiology, R. C. Patel Arts, Commerce and Science College, Dist: Dhule (MS), Shirpur 425405, India

[3] Department of Pharmaceutics, R. C. Patel Institute of Pharmaceutical Education and Research, Dist: Dhule (MS), Shirpur 425405, India

[4] Department of Pharmaceutical Chemistry, H. R. Patel Institute of Pharmaceutical Education and Research, Dist: Dhule (MS), Shirpur 425405, India

Graphical abstract

Nanostructured metal-organic frameworks based luminescent sensor for chemical and metal ions sensing

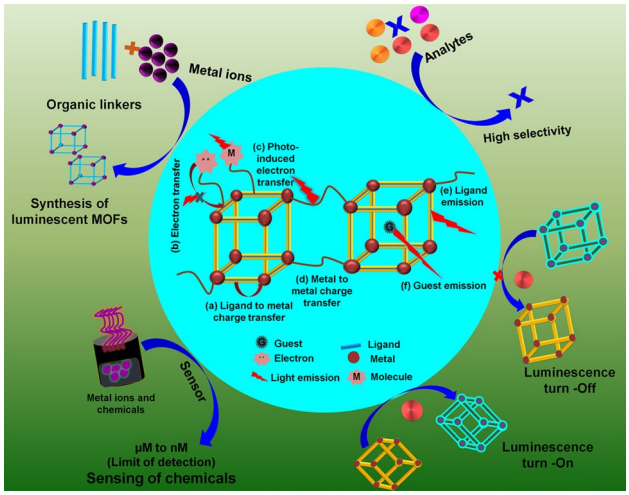

Keywords Nano-structure · Metal–organic framework · Luminescent sensor · Sensitivity · Chemical sensing · Metal ions sensing

Introduction

Need to monitor chemical residues and metal ions exposure

Recently, metal ion recognition in biological processes has received a lot of emphasis from the scientific community [1]. In this element, the World health organization reported that the occurrence of high levels of metal ions in water can influence the quality of water and end with the human being and aquatic life also [2]. With the speedy augmentation of human civilization since the industrial revolution, the concern of environmental pollution has been accompanied like a shadow. Herein, the most imperative source of water contamination is the inappropriate outflow of industrialized and household water [3]. For example, the cobalt and chromium exposures in the workplace and environment have recently been related to a variety of inflammatory and degenerative disorders, as well as cancer [4]. Importantly, the existing heavy metals can cause cancer that may be because of their physiological properties. Therefore, the revealing of such metal ions is decisive to restrict several health issues [5]. Besides this, the continuous exposure of polycyclic aromatic hydrocarbons to humans and animals shows the abundant health issue that covers neurotoxicity, immunotoxicity, endocrine disruption, genotoxicity, carcinogenicity, etc. [6]. The consumption of food and water intake with pesticide residue results in different kinds of cancer, organ/tissue toxicity, etc. Therefore, they require to authorize the availability of pesticides residues in food and water samples [7]. In this vein, a literature survey reported that food safety is an international issue that received massive consideration in the past two decades owing to exposure and high use of heavy metal ions, chemicals, etc. in different fields [8]. The residue of antibiotics in the food is a challenging task in the case of food safety wherein it may cause diverse adverse effects [9]. In a nutshell, there is an opinion to shun the revelation of chemicals and metal ions. Recently, the assessment of chemical residue and metal ion is attention-grabbing arena that reported diverse approaches for identification and quantification of target chemical and metal ions. In the next section, we have addressed the development of estimation strategies for chemicals and metal ions in brief.

Estimation of chemical residues and metal ions

Literature assessment revealed that the revealing of chemical moieties at trace levels with high selectivity and sensitivity is the mushrooming field in the research area [10]. In addition, the selective recognition of explosive chemicals is extremely demanding from society as well as health-related agencies. In this regard, several toxic chemicals, such as picric acid, trinitrotoluene (TNT), di-nitro-toluene, etc., have been detected using both qualitative and quantitative methods [11]. It has been reported that if the analyte is exited in form of a volatile organic substance, then it is reasonably complicated to quantify the amount of analyte using spectroscopic methods. In this hint, the application of

the fluorescent-mediated detection methods offers numerous benefits in terms of sensitivity, selectivity, detection speed, cost factor, etc. [12]. As per literature, colorimetric sensing has been reported for sensing metal ions but the making use of dye for visualizing the metal ions affects its sensitivity. Subsequently, it impacts the sensitivity of the interest analyte. Therefore, the application of the colorimetric method in metal ion and chemical sensing is restricted [1, 13]. In addition, there are diverse methods, principally qualitative methods and quantitative methods that endow with poor detection limits and low selectivity [7]. Traditional recognition methods including liquid chromatography, mass spectrometry, gas chromatography, etc., are suffering from plenteous disadvantages in the vein of a time-consuming process, huge workload, and high costs [3, 14]. Moreover, surface-enhanced Raman spectroscopy, ion mobility spectrometry, gas chromatography coupled with mass spectrometry, and cyclic voltammetry have been reported for sensing explosives. There are chances of false-positive output and therefore it requires immediate calibration. Also, such methods are labor-intensive, expensive, and not feasible for non-stop assessment [15]. As a result, it is vital in developing adequate and speedy identification approaches for metal ions and chemical sensing. Recently, the luminescent sensors have exhibited the aptitude to identify a plethora of pollutants in diverse media with towing sensitivity, high selectivity, simplicity, etc. [3]. In this shade, environmentally sustainable biomimetic composites with exceptional merits, such as high sensitivity, great biocompatibility, and precise selectivity, are extremely appealing for health monitoring. However, addressing these traits at the same time frame is a daunting problem [16]. Presently, an abundance of modified nano-materials has been developed for diverse applications in science [17, 18]. In this field, rapid progress in technology is offering diverse advanced approaches to surmount the problems associated with customary methods [19].

The sensing of interest analyte qualitatively and quantitatively can be achievable using modified nano-materials [20]. Therefore, several nano-composites have been structured for recognition of toxic pollutants [21], such as explosives and flammable gases [22]. The employment of optical sensing particularly, the fluorescence-based sensor for interest analyte sensing in complexed media is held countless shares in the last few years. In this line, diverse theoretical sensing mechanisms are reported that include chelation enhanced fluorescence, metal-to-ligand charge transfer, and photo-induced electron transfer. Furthermore, the metal–ligand coordination-mediated luminescent property is an attention-grabbing approach for highly sensitive and selective recognition of chemical moieties and metal ions [23]. Therefore, making use of fluorescent nano-materials for the recognition of metal ions in biological systems can furnish high sensitivity [1]. Consequently, there is a pressing necessity to expand fluorescent nanomaterials-mediated sensors for the tracking of metal ions and chemical traces in provided samples. From the last few years, published scientific researchers have seen significant effort in implementing metal–organic frameworks (MOFs)-derived nanosize materials (Fig. 1) [24]. Due to their regulatability, modifiability, and designability potential, it is playing an imperative part in environmental applications [25]. According to the peer-reviewed literature, MOFs are laying the groundwork for immensely sensitive and selective monitoring of toxic chemicals and metal ions. As a result, we explained the luminescent MOFs facilitated detecting tactic for chemicals, primarily metal ions, and toxic chemicals, in this systematic review. At first, we have summarized current MOF developments, divergent approaches for MOF synthesis, and then notified its distinctive features that render it a promising forum for detecting applications. The assorted sensing mechanisms implicated in the luminescent MOFs-based recognition system are then discussed. Following that, luminescent MOF-mediated sensing stations for chemicals and metal ions are evidenced. Areas of improvement of these luminous MOFs-based metal ions and chemical sensing will not only benefit the environment, but will also emerge as a prospective nano-platform for further scientific applications.

Trends of MOFs-based sensor

Structural design of MOFs

From its inception, remarkable progress has been made in the architecture and fabrication of a novel category of nanostructured material acknowledged as MOFs [26]. Most

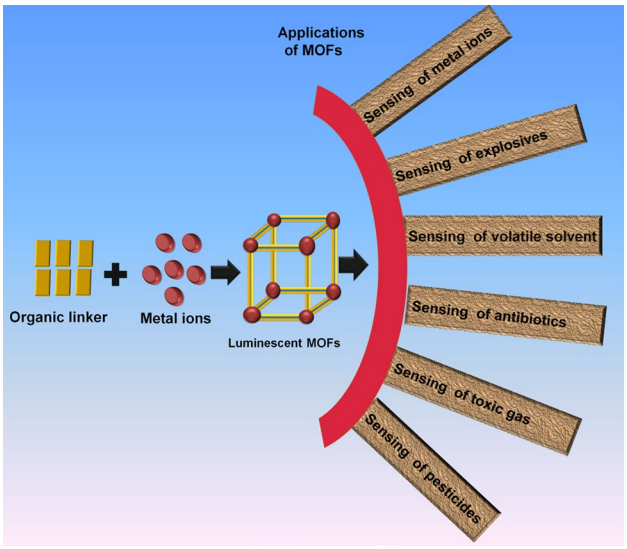

Fig. 1 Schematic presentation of MOFs synthesis using metal ions and organic ligands and their application in sensing.

relevantly, nanostructured MOFs are self-assembly that can design by coordinating appropriate metal cations or clusters and ideal organic linkers (Fig. 1) [27, 28]. Principally, MOFs are a highly porous [25] and crystalline material that contains tunable chemical compositions plus frameworks [24, 29]. Herein, an exceptional type of organic linker offers the bridging among two metal ions or clusters [30, 31]. It is obvious that the application of appropriate organic ligands, such as bi-, tri-, tetra-, or multi-dentate ligands, provides effective nanostructures with an ultrahigh porosity, elevated specific area, and appropriate pore dimensions. Furthermore, it offers luminescence property to MOFs [32]. From the last two decades, thorough studies on these kinds of species have resulted in the development of a huge number of MOFs with multifaceted architectures and architectural magnificence [33]. Accordingly, it provides a practical engineering tactic for creating porous systems with tailorable sizes, formulaic structures, and enhanced surface areas [27, 34].

A published literature survey demonstrated that MOFs are a new breed of hybrid nanomaterials composed of precise metal-connecting points and appropriate organic bridging ligands via different methods. In the last decade, it has gotten a lot of interest from the scientific fraternity due to its nanosize dimensions. The pore sizes of MOFs have been obtained from few angstroms to nanometer (nm) that principally relied on the ligand size and network connectivity [35]. Because of such abundant properties, nanosize MOFs are gaining notable consideration in diverse fields, such as catalysis, sensing, imaging, separation, gas storage, etc. [26, 28]. Moreover, based on the purpose of the study, the size of MOFs can be controlled. Herein, the length of a preferred ligand is playing a significant function in the tuning of the size of MOFs [36]. It has been reported that the nano-MOFs with tiny sizes furnishes the additional accessible active sites. In addition, it provides the better mass diffusion of analytes towards/from the active sites as compared to the typical MOFs those having MOFs size micrometer. As a result, it enhances the ability of electrocatalytic activity and detection sensitivity [37]. Based on the MOFs' nature, it is classified into two types mainly crystalline MOFs and amorphous MOFs. In a nutshell, crystalline MOFs are hollow structures made up of a limitless number of metal networks united through organic linkers. On the other hand, amorphous MOFs maintain the crucial structural components and connections of their crystalline counterparts while lacking any brief regular structure [38]. Such non-crystalline MOFs are currently receiving enormous awareness as a substitute for the upcoming generation of different technologies [39], drug delivery [40], etc. Up to 2014, there are only 28 amorphous MOFs are available [41]. According to a literature review, amorphous MOFs comprise inorganic networks mainly clusters or metal ions interlinked by appropriate organic linkers that extended in two/three dimensions and have the propensity for porosity [38, 39]. Remarkably, amorphous MOFs incorporate features often seen in crystalline MOFs, such as large surface areas, exceptional porosities, superior thermal stability as well as chemical stabilities. Furthermore, it furnishes the potential of tunable pore size and shapes. In addition, the plentiful active sites, abundant defects, free from gain boundaries, etc. provide the uniqueness to amorphous MOFs [39]. As of their comparable tetrahedral connectivities, zeolitic imidazolate frameworks (ZIFs) are excellent prospects for amorphization due their architectures are tightly connected to zeolitic silica polymorphs [42]. Moreover, different amorphous MOFs have been reported for example zirconium (Zr)-based modified MOFs [43], iron MOFs (NEU-2: Fe(BPDI)$(Py)_2$, BPDI: N, N′bis(glycinyl) pyromellitic diimide; Py: pyridinE) [44], NEU-3 [NEU-3: Zn(PMDA)$(Py)_2$, PDMA: N,N′-pyromelliticdiimido-di-L-alanine], NEU-4 [NEU-4: Fe(PMDA)$(Py)_2$] [45], etc.

Presently, advances in MOFs-based composites resulted in nanostructured MOFs that endow abundant attributes which are useful for sensing applications as compared to the naked MOFs. Consequently, nanostructured MOFs are paving the mode for their usage in an ample variety of applications, such as sensing heavy metals, chemicals, etc. [46]. Herein, ultra-porous structure and large surface area of nanostructured MOFs focus on the specific sample marker. Subsequently, it enables improved reactive sites, and finally augments the sensor's responsiveness [46]. Generally, MOFs can undergo thermal change, yielding a range of nanostructures, such as carbon-based materials, metal oxides, metal carbides, metal chalcogenides, etc. Particularly, the nano-MOFs with adequate size and topology can be synthesized with different strategies. In most cases, the pyrolysis of MOFs chemically converts the MOFs-based nanostructures into a variety of shapes [47]. Besides, it offers the potential of dispersibility in diverse solvents as well as water. Such nano-MOFs can be coated for improved biocompatibility of MOFs. Additionally, it provides the size associated with optical, magnetic, and electrical properties. Such nano-MOFs can be constructed using different synthesis methods mainly microwaves method or sonochemistry methods. Despite this advancement, the control on size and morphology of nano-MOFs is challenging to researchers [48]. Literature survey revealed that the 12,000 types of novel MOFs have been synthesized in early 2005 [32]. In 2021, Deng and co-authors reported that the 20,000 types of MOFs have been designed for several applications [49]. Table 1 enlisted the summary of different types of MOFs based on their metal ions and linker available for several applications.

Recently, a center of attention is the development of luminescent MOFs wherein the luminescence produces from the ligands. Herein, it is originated from a rigid ligand with aromatic moieties. In addition, in presence of metal ions, guest molecules, or extended π systems it shows the

Table 1 List of a verity of MOFs based on their metal ions and linker

MOFs	Metal	Linker	Synthesis method	Refs
$Bi_2Cd(2,6\text{-}pdc)_4\text{-}(H_2O)_2H_2O$	Bismuth-Cadmium (Bi-Cd)	Pyridine-2,6-dicarboxylate (2,6-H_2pdc)	Hydrothermal synthesis	[51]
$Pb_3(bpt)_2\text{-}(phen)_2.phen$	Lead (Pb)	Biphenyl-3,4′,5-tricarboxylic acid (H_3BPT)	Solvothermal synthesis	[52]
{[$Ln_4(tmba)_6(phen)_4$]·m(H_2O) (phen)}n	Lanthanide (Ln)	Thiobis(4-methylene-benzoic acid) (H_2tmba), 1,10-Phenanthroline (phen)	Not reported	[53]
[Cd(BPDC)(BP_4VA)·2DMF]n	Cd	9,10-Bis((E)-2-(pyridin-4-yl) vinyl)anthracene (BP_4VA), Biphenyl-4,4′-dicarboxylic acid (H_2BPDC)	Not reported	[54]
$Al(OH)(O_2C\text{–}C_{10}H_6\text{–}CO_2)]\infty$	Aluminum (Al)	2,6-Naphthalenedicarboxylate (2,6-ndc)	Solvothermal synthesis	[55]
Yb-MOFs	Ytterbium (Yb)	Biphenyl-3,40,5-tricarboxylate (BPT)	Solvothermal synthesis	[56]
$[Cd(tpbpc)_2]\cdot 2H_2O\cdot DMF$	Cd	4′-[4,2′;6′,4″]-terpyridin-4′-yl-biphenyl-4-carboxylic acid (Htpbpc)	Hydrothermal synthesis	[57]
$Tb_{0.99}Eu_{0.01}(BDC)_{1.5}(H_2O)_2$	Europium (Eu), Terbium (Tb)	1–4-Benzendicarboxylate (BDC)	Reverse micro-emulsion technique	[58]
{[Ln(HL)]·3DMF·$3H_2O$}n [LZG-Eu and LZG-Tb]	Ln = Eu, Ln = Tb	1,4-bis(2′,2″,6′,6″-tetracarboxy-1,4′:4,4″-pyridyl)benzene (H_4L)	Solvothermal synthesis	[59]
$Cd_3Ln_2(btc)_4(H_2O)6(DMF)_4$	Cd–Tb	1,3,5-benzenetricarboxylic acid (H_3btc)	Solvothermal synthesis	[60]
$Li_3[Li(DMF)_2]$ $(CPMA)_2\}\cdot 4DMF\cdot H_2O$	Lithium (Li)	Bis(4-carboxyphenyl)-*N*-methyl-amine (H_2CPMA)	Solvothermal synthesis	[61]
{[Tb(HL)(H_2O)$_2$]·x(solv)}n	Tb	5,5′-(((1,4-phenylenebis(a zanediyl))bis(carbonyl)) bis(azanediyl)) diisophthalic acid (H_4L)	solvothermal synthesis	[62]
OX-2 MOFs	Silver (Ag)	Terephthalic acid (BDC)	Sonochemical Synthesis	[63]
Mg(H_2DHBDC)	Magnesium (Mg)	2,5-dihydroxybenzene-1,4-dicarboxylate (H_2DHBDC^{2-})	Solvothermal synthesis	[64]
Zn_2(TCPE)	Zinc (Zn)	Tetrakis(4-carboxyphenyl)ethylene (TCPE)	Solvothermal synthesis	[64]
{[Eu_3(BTDC)$_4$(HCOO) (H_2O)$_2$]·solvents}n or (JXUST-9)	Eu^{3+}	2,1,3-benzothiadiazole-4,7-dicarboxylic acid (H_2BTDC)	Solvothermal synthesis	[65]
$[(Cu^I_4I_4)_3(Cu^I_6)_2(3\text{-}ptt)_{12}]_{n^*}24nDEF^*12nH_2O$	Copper (Cu)	5-(pyridin-3-yl)-1H1,2,4-triazole-3-thiol (3-Hptt)	Solvent precipitation method	[66]
$Cu_2(\mu_3\text{-}tmds)_2(imH)_4]\cdot H_2tmds$	Cu	1,3-Bis(3-carboxypropyl)tetramethyldisiloxane (H_2tmds)	Solvothermal synthesis	[67]
$MV[Mn_2Cu_3(mpba)_3(H_2O)_3]\cdot 20H_2O$	Manganese (Mn)-Cu	*N*,*N*′-1,3-phenylenebis(oxamate) ($mpba^{4-}$)	Solvothermal synthesis	[68]
NU-1000	Zirconium (Zr)	Tetraethyl 4,4′,4″,4‴-(pyrene-1,3,6,8-tetrayl) tetrabenzoic acid (TBAPy)	Solvothermal synthesis	[69]
$[Eu_2L_3(DMF)(H_2O)_3]\cdot$x(solvent)	Eu	Eu_2L_3 (Obtained from methyl 4-amino-2 methoxybenzoate and *N*, *N*′-Carbonyldiimidazole)	Solvothermal synthesis	[70]
$Zn_5(L_1)_2\cdot(\mu OH)\cdot(HCO_2)\cdot DMF\cdot 2H_2O$]·$6H_2O$	Zn, Ruthenium (Ru)	Ru(4,4′-CO_2H-bpy)$_2CN_2$ (L_2-H_4)	Solvothermal synthesis	[71]
nano-ZIF-8 (Zeolitic imidazolate framework: ZIF)	Eu	2-methylimidazole	Electrochemical synthesis	[72]

Table 1 (continued)

MOFs	Metal	Linker	Synthesis method	Refs
In(OH)(bdc)]n	Indium (In)	1,4-benzenedicarboxylate (bdc)	Not reported	[73]
Ln_2(D-cam)(Himdc)$_2$(H_2O)$_2$	Ln	D-H_2cam = D-camphoric acid, H_3imdc = 4,5-imidazole dicarboxylic acid	Hydrothermal synthesis	[74]
Ti_2(HDOBDC)$_2$(H_2DOBDC)	Titanium (Ti)	2,5-dihydroxyterephthalic acid (H_4DOBDC)	Solvothermal synthesis	[75]
TbTATB	Tb	4,4′,4″-striazine-2,4,6-triyl-tribenzoic acid (H_3TATB)	Solvothermal synthesis	[76]
[Zn_3(TCPB)$_2$(H_2O)$_2$]·2H_2O·4DMF	Zn	1,3,5-tri(4-carboxyphenoxy) benzene (H_3TCPB)	Solvothermal synthesis	[77]

luminescence. In this, an application of MOFs as sensory materials offers abundant advantages in contrast to the free form of organic ligands. In brief, MOFs available in solid can diminish the rate of non-radiative decay. Accordingly, it boosted the fluorescence intensity, as well as quantum efficiency. Furthermore, post-synthetic modulation in MOFs can offer multi-functional MOFs that can release more open sites for sensing (or absorption) of the target analyte. Interestingly, luminescent MOFs can furnish the natural habit to target analyte owing to the sustainable pores that exist in prepared MOFs [50].

Overall, the MOFs-templated method offers a potential chance to create a wide range of nanostructured MOFs. Fascinatingly, tuning the topologies, architectures, and characteristics of MOFs-derived nanostructures can enable them to operate better. To promote this technique, more compelling and adaptable, future research and development should focus on a deeper analysis of MOFs-derived nanostructures and a superior understanding of the underlying processes. In this next subsection, we addressed the different methods of synthesis of MOFs.

MOFs synthesis

Methods of MOF synthesis

Importantly, the procedure of MOFs synthesis is playing an imperative function in the assembly of novel MOFs [32]. These advancements in the domain of material are facilitating the prudent construction of porous and nanosized MOFs with adequate functional sites that play a key role in precise host recognition. Accordingly, it is allowing us to customize their functional characteristics [33]. It is crystal clear that the design approach of MOFs along with intentional surface morphology is related to the incorporation of different properties mainly optical, porosity, magnetic, electrical, catalytic, chiral, etc. In addition to this, the metal-to-ligand ratio is also a crucial parameter in the design of MOFs. It has been reported that the nature of selected metal ions, electronic attributes, coordination number, geometry, etc. affects the design of MOFs. In the case of ligands, the nature of the linker mainly shape, geometry, length, flexibility or rigidity, functional groups, etc. plays an imperative role in sensing a target with high sensitivity and selectivity [26]. In this regard, the MOFs synthesis methods are playing an imperative role to tune surface morphology and other properties of MOFs [78]. Hence, it needed accurate control on the molecular level during MOFs synthesis that provides the precise frameworks and compositions. Countless studies have chronicled the synthetic techniques of MOFs and their derivatives by adjusting parameters, such as reaction environment, temperature conditions, solvent types, etc., opening the path for innovative tailored functional materials [32]. Figure 2 shows the MOF's synthesis methods using different types of metal ions and ligands.

Different MOFs synthesis methods include conventional synthesis, microwave-assisted synthesis, electrochemical synthesis, sonochemical synthesis, and mechanochemical synthesis (Fig. 2) [78]. Out of these methods, it has been suggested that hydrothermal synthesis is a feasible method for pristine MOFs synthesis that contains organic water-soluble ligand [27, 32]. In the case of organic ligands soluble in a diverse organic solvent can be used for MOFs synthesis via a solvothermal method. Besides this, advanced in situ thermal treatment can be used for the synthesis of MOFs derivatives. In this method, diverse types of substances can be incorporated through surface modification and simple chemical modifications [32]. Published literature accounted that the MOFs are outstanding nanoporous materials composed of hybrid materials mainly inorganic–organic counterparts [78, 79]. To begin with, the slow evaporation method has been suggested as a conventional method to synthesize MOFs (Fig. 3A). In this case, there is no requirement for external energy to design the MOFs. Therefore, this method has been extensively used in the initial moment. Importantly, the whole process requires room temperature for the process. Here, utilized solvent or solution of initial mixtures is get

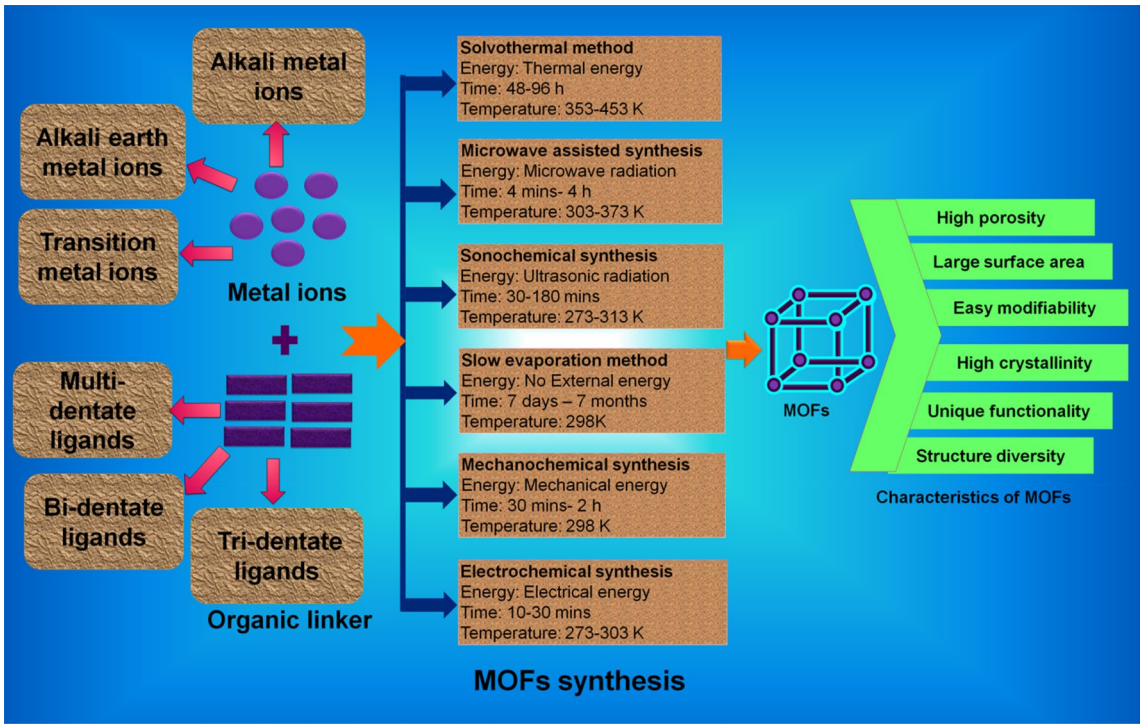

Fig. 2 Presentation of MOFs synthesis using different methods, their reactions conditions, and characteristics of MOFs

concentrated due to slow evaporation of used solved at constant temperature or room temperature. In this case, the solubility of the initial precursor in a solvent is also a major limitation step that can be resolved using a mixture of two or more solvents. It can aid in the speedy evaporation of solvent content from the product. Despite the plenty of merits, it needed additional time for the synthesis of MOFs [80, 81]. Traditional synthesis methods comprise the use of heat/temperature for MOFs synthesis. Based on the preferred environment for synthesis, it is called as solvothermal method and non-solvo-thermal method. Essentially, the solvothermal method is based on a simplistic reaction setup. It is useful to synthesize the crystalline form of MOFs. Also, it provides a high yield that may be because of elevated temperature. In the case of non-solvothermal reactions, the reaction solvent is a prime criterion that plays an imperative role in the size and shape of MOFs [82, 83]. Herein, the improved practical yield and unique space crystal generation are important for the catalysis of target analytes. Herein, the proper solvent preference in the synthesis method helps to control the toxicity of MOFs and other quality parameters [78]. In brief, solvothermal synthesis is achieved at definite conditions primarily enclosed vessels plus autogenous pressure above the solvent boiling point (Fig. 3B). Nanoscale MOFs morphologies can be practicable using solvothermal conditions that cannot be promising by traditional methods. Herein, chemical changes in initial precursor materials put forward the nanosize dimensions to materials. In several reactions, high boiling point solvents are also utilized for the design of MOFs with specific nanosize dimensions. Moreover, other solvents including acetone, methanol, ethanol, acetonitrile, diethyl formamide, and dimethylformamide are frequently used for the fabrication of nanosize MOFs. In addition, we can prefer the mixture of the abovementioned solvents to surmount the solubility concern of the precursor [81]. It has been reported that the conventionally used methods are suffering from major limitations that comprise time-consuming processes and the total extent time is lengthy. To resolve the demerits, recently microwave-assisted methods have been reported that offer a small reaction time (Fig. 3C). In the case of microwave-assisted synthesis, the selection of solvent has relied on the aptitude of microwave absorption [78, 84]. Briefly, the electromagnetic energy conversion into heat has relied on the microwave absorption aptitude of the solvent. And based on the heat generation, the reaction is achieved. Herein, the size of reaction vessels and stirring of the reaction mixture is the foremost factor involved in the synthesis of MOFs [7, 84]. Using this method, we can propose nanostructure MOFs within a few minutes to a few hours. It has been broadly reported for the synthesis of nanosize metal oxide-based MOFs. In this method, majorly heating of solvent and procure mixture involved

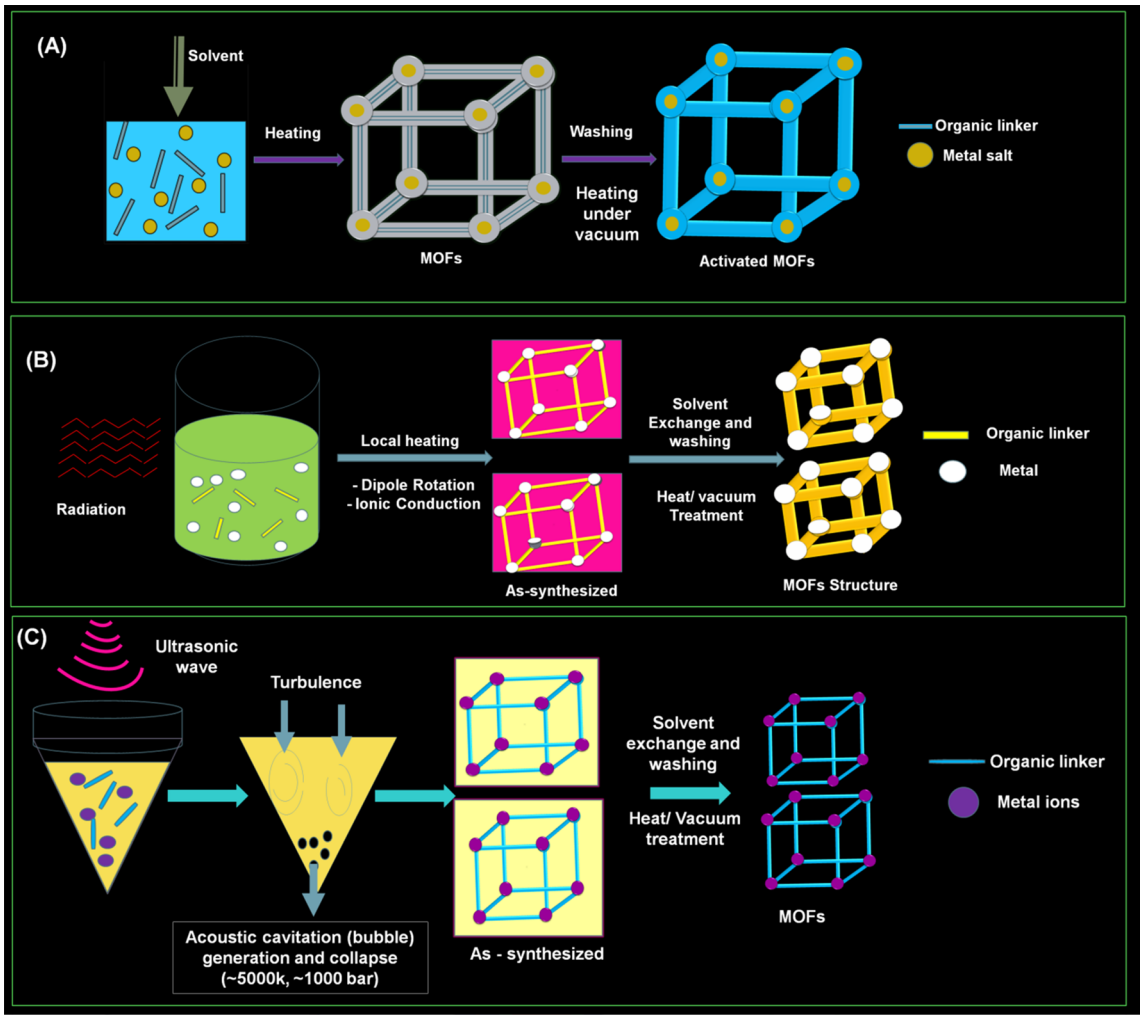

Fig. 3 Synthesis of MOFs **A** slow evaporation method, **B** solvothermal synthesis, **C** microwave-assisted methods

along with microwaves for a predefined time interval that offers the nanosized crystalline MOFs. It is also acknowledged as the microwave-assisted solvothermal synthesis method for the fabrication of nanosize MOFs [81].

Electrochemical synthesis has importantly relied on the delivery of preferred metal ions in form of the anode (Fig. 4A). The selected linker needs to dissolve in a prepared reaction mixture along with a specific electrolyte. The central benefit of electrochemical synthesis is to provide evidence of the non-stop synthesis of intended MOFs. In this synthesis, the application of protic solvents in the prepared reaction mixture aid to suppress the metal ion deposition from anode on the surface of the cathode [7]. Formerly, electrochemical synthesis techniques were investigated for the creation of porous nanostructured materials, such as platinum and platinum-based alloys. This technique of synthesis of MOFs may be paired with porous nanostructured materials to create a novel class of porous core–shell MOFs that can be investigated in further sensing and catalysis applications [78]. Sonochemical production is the application of high-intensity ultrasound to a reaction mixture [7]. The usage of the sonochemical technique of synthesis is extremely restricted, and only a few MOFs have been synthesized using this approach (Figure AB) [85]. Literature survey revealed that sonochemistry is the chemical transformation of molecules. In this, the application of intense ultrasonic energy from 20 kHz to 10 MHz helps to synthesize nanomaterials. Interestingly, ultrasound causes chemical transformations as well as physical transformations in a liquid through a cavitation process. Accordingly, it involves the production, growth, and quick collapse of bubbles. Finally, it results in local hot spots with a brief lifetime and high temperature plus pressure. Extreme circumstances can augment chemical reactions by causing an overabundance of crystallization nuclei to develop. When compared to standard hydrothermal procedures, sonochemical approaches can fabricate homogenous nucleation centers and a significant reduction in crystallization instant [81]. In this method, different kinds

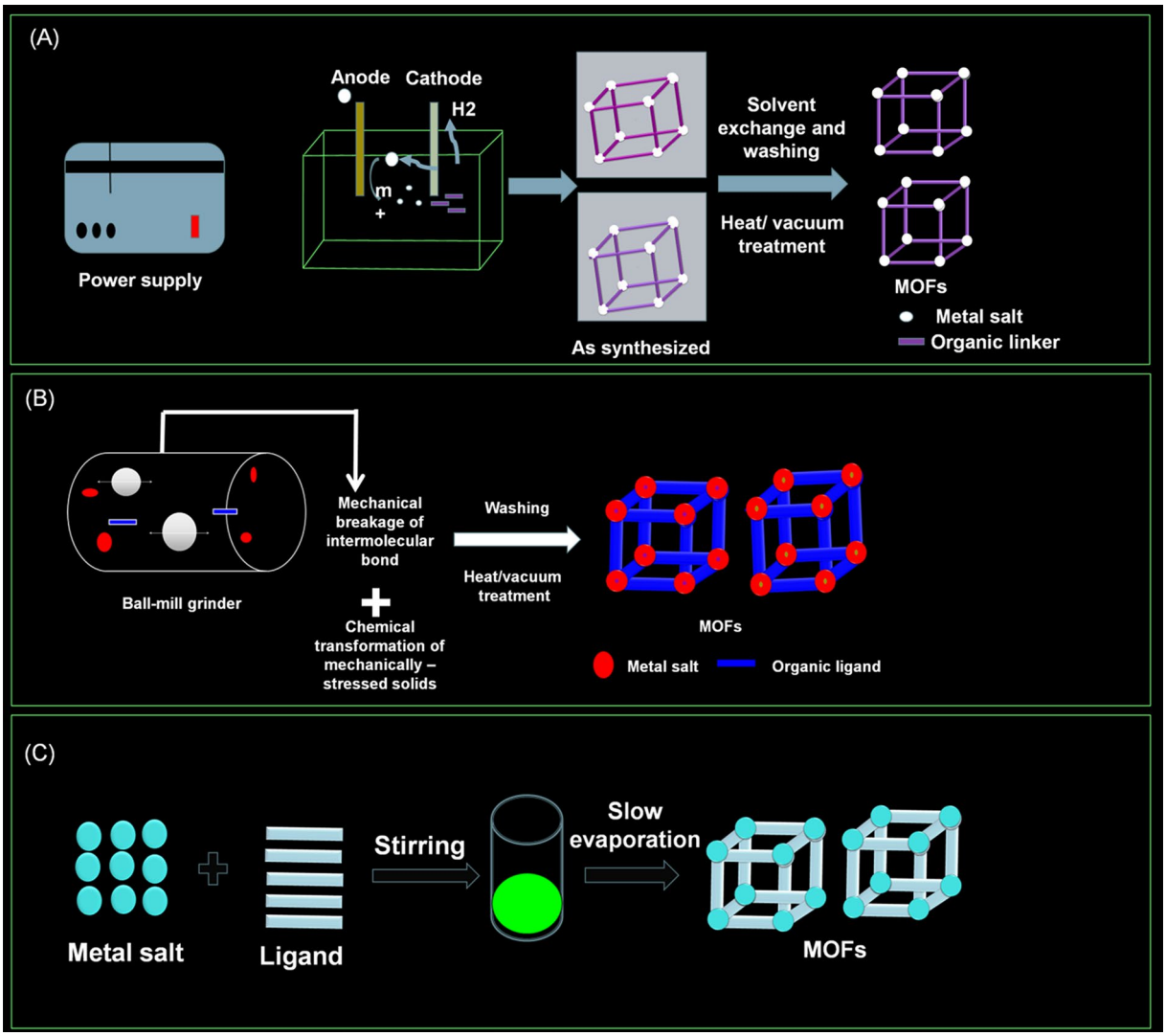

Fig. 4 Synthesis of MOFs **A** electrochemical synthesis; **B** sonochemical synthesis, and **C** mechanochemical synthesis

of structures can be obtained, such as interpenetrated structures and non-interpenetrated structures. Interestingly, the optimum sonication power furnishes the combined form interpenetrated-non-interpenetrated structures. Moreover, the non-interpenetrated and interpenetrated structures have been obtained at low and high sonication power, respectively [78]. The term "mechanochemical synthesis" refers to the involvement of mechanical energy in the process (Fig. 4C). Mechanical breaking of intramolecular bonds is occurred proceeded by a chemical transition. The benefits of mechanochemical synthesis comprise the aptitude to execute it at ambient temperature and instead of the requirement of the solvent [86]. In addition to allowing for solvent-free synthesis, this approach allows for the utilization of metal oxide salts in form of precursors. Ultimately, it provides an excellent substitute for the utilization of metal salts. In addition, it yields just water as a byproduct therefore there is no toxicity issue and pollution. In the case of solvent-based synthesis, the low solubility of metal oxides limits the applications. Interestingly, mechanochemical synthesis of MOFs can refer to the metal oxide as an adequate salt precursor [87, 88].

Important factors for MOFs synthesis

Importantly, it is generally understood that the crystallization, architecture, and topology of MOFs are often not determined by the modulus building elements, but also by a variety of synthesizing circumstances, such as solvent type [89], types of metal ions and organic linker, reaction condition [90], pH [91], temperature [92], etc. Based on these parameters, it is categorized under two classes including compositional parameters and process parameters. Briefly, compositional parameters include a concentration of components, counterions, reaction materials, etc. whereas the

process factor includes temperature, time, and pressure [93]. In solvothermal methods, the particle size can be diverse with temperature and other reaction conditions. As per the literature, cyclodextrin-based MOFs synthesis at 50 °C shows a uniform size distribution (2–3 μm). Therefore, it confirmed that the optimized temperature condition assists to control the size distribution. Moreover, the assortment of solvents, such as methanol or other aqueous solution, also affects the size distribution of MOFs. Cyclodextrin-based MOFs relied on the reaction of potassium hydroxide and cyclodextrin with methanol vapor diffusion resulting in the particle size within the range of micrometer (200–400 μm, at room temperature). In addition, the longer incubation time for MOFs synthesis furnishes the smaller size cyclodextrin-based MOFs (40 μm) [94]. While synthesis of MOFs using diverse methods, several critical parameters affect the size, morphology, porosity, stability, dispensability, etc. Fascinatingly, the sufficient particle size of MOFs is crucial for the development of sensors and other industrial applications. In the case of the sonication method, several synthesis parameters including the molar ratio of reactants, irradiation frequency, concentration of reactants, sonication time, etc. are essential to controlling the MOFs size. As per literature, at 30 kHz, irradiation frequency, the MOFs aggregation has been obtained whereas, 60 min sonication time provides the uniform distribution of nanosize MOFs. Importantly, ultra-sonication aid to control the crystallization process as well boosts the mass transfer, and finally increases the molecular diffusion [95]. The choice of adequate solvent is the imperative part in MOFs synthesis wherein it affects the ligand and metal ions coordination directly or indirectly. The number of applications claimed that each solvent influence the coordination approach of metal ions and linkers. In addition, it plays the position of guest molecules in MOFs whereas few of them act as a framework modulating agent. Moreover, deprotonation of the preferred organic linker (carboxylate linker) owing to the selection of solvents chiefly DMF resulted in the alteration in MOFs structure [96]. In most cases, the decomposition of ligands has been obtained that may due to the presence of solvents shows the less or absence of coordination between linker and metal ions [93]. During the synthesis of MOFs, the addition of numerous types of organic and inorganic additives resulted in the modulation of crystallinity of MOFs and that provides the control on particle size. For example, the adding of benzoic acid with lower concentration provides the lower size of MOFs namely UIO-66-NH_2 (UIO: Universitetet I Oslo). Moreover, 20 nm particle size containing MOFs has resulted in aggregation [97]. The preference of proper metal size and ligand-to-metal bond length provides the effectual morphology of MOFs. In the case of the synthesis of MOFs, the versatility nature of metal ions and ligands assists to modify the structure of MOFs as well as the composition of MOFs-mediated composite [90]. In addition to this, the molar ratio of reactants is given the superior topological pattern in MOFs-mediated sensors. In 2019, Seetharaj and co-authors suggested that the molar ratio of ligand and metal offers the 1D zigzag polymeric chain-mediated copper-based MOFs [93]. The acidic and basic pH of the media aids in the crystallization of materials as well as helps in the formation of organic and inorganic conjugates. It has been revealed that the pH of the reaction medium acts as an external stimulus that affects the coordination among linker and metal ions [98]. Principally, the coordination potential of 1,3-adamantanediacetic acid (H_2ADA, linker) depends on the pH of the media. Furthermore, the color of MOFs can be varying with the pH of the reaction condition. Overall, structural diversity is directly related to the pH of the reaction solution [93]. In conclusion, the preference of appropriate method for the synthesis of MOFs requires the optimization of different compositional and process-related critical factors that affect the MOFs-related parameters including porosity, particle size, particle size uniformity, dispersibility, crystal growth, etc.

Properties of MOFs

Owing to the bonding between an organic ligand and inorganic metal ions, we can be designed the one-dimensional (1D), two-dimensional (2D), and three-dimensional (3D) topologies. Such topologies are crucial for sensing and adsorption of interest analyte [28]. It has been revealed that the surface architectured MOFs offer abundant advantages including tunable pore size, larger surface area, plenty of biding sites, etc. [99]. Because of these benefits, it confirms the potential of gas adsorption, catalysis, luminescent detection, etc. [7, 78]. Owing to the inherent advantages primarily speedy detection, high sensitivity, economic, ease of manipulation, etc., luminescent MOFs have recently been regarded as a form of emerging material for finding chemicals and metal ions [100]. It has been revealed that the MOFs can support the removal of interest analyte via a different mechanism that essentially includes hydrogen bonding, electrostatic interaction, π–π stacking interaction, size exclusion, etc. [28]. As per published literature, MOFs are exhibited in crystalline form. It furnished the precise space geometry that can support pharmaceutical applications. It has been revealed that the MOFs possess high porosity and a larger surface area (about 7140 m^2/g) [101] that might be because of long ligands preferred in MOFs synthesis. Moreover, the porosity of MOFs is high (about 94%) as compared to the other reported materials [28, 102]. Zhang and co-authors reported the BET (BET: Brunauer, Emmett, and Teller) area MOFs within the range of 3800 m^2/g to 9140 m^2/g whereas pore volume has been reported up to 5.02 cm^3/g. In this case, dissimilar techniques have been reported to measure the

porosity of MOFs wherein numerous probe molecules have been suggested, such as nitrogen, carbon dioxide, argon, etc. [103]. Interestingly, it furnishes the elevated host–guest interaction that is helpful for sensing of interest analyte [104]. The pore size of MOFs can be modified into larger pores using a proper ligand with a sufficient length. Hence, ligand length is a critical fact in the porosity of MOFs. Mainly, it regulates the pore size, as well as different porosity modulators, can be utilized wherein preference of additives, template agent size, and ligand type is a decisive factor [90]. In addition, MOFs structural units can be integrated by assorted bridging ligands and metal ions/clusters in occurrence of diverse coordination structures via coordination bonding that furnishes the diversified structure. Overall, it assists to synthesize MOFs with a precise framework using simplistic synthetic assembly as well as monomer design [28, 78]. It furnishes exceptional spectroscopic attributes principally high quantum yield, wide emission range, long lifetime, etc. Owing to this, it gained diverse opportunities in sensing applications [105]. Figure 2 depicts the different MOFs properties that are useful for sensing metal ions and chemical residues.

Presently, the functionalization of organic ligands provides the potential for amending in MOFs structure. Moreover, chemical functionalization can be more accommodating for pore surface and framework functionalization [27, 28]. It has been divulged that the MOFs exhibits multiple chemical and physical functions. Possibly, it might be because of the porous and pure form of inorganic–organic hybrid modified MOFs conjugates [7, 106]. The application of long size and σ bonding containing unique organic ligands furnishes prominent properties to MOFs, such as deformability and reversibility. Hence, such MOFs exhibited the high flexibility that resulted in the instant physicochemical changes after contact with the interest analyte. In addition, it provides the multi-level adsorption process as well as desorption process [28]. In material science and chemistry, MOFs have gained huge interest owing to their excellent biocompatibility. Therefore, it can be used for plenty of biomedical applications, such as biomarkers sensing, targeted delivery, bioimaging, etc. [78, 104]. As we know, the surface functionalization of MOFs is providing plenty of merits in sensing and removal of interest analytes with elevated performance in terms of sensitivity, selectivity, and so on. In the case of surface functionalization of MOFs, the coordination modulation and post-synthetic surface functionalization of MOFs are two main approaches that are helpful for sensor presentation improvement. In the case of post-synthetic modulation, covalent bonding and non-covalent bonding participate an important role that gives nanostructured MOFs [78]. Bimetallic MOFs are a new form of MOFs that has aroused a lot of interest recently. It can be synthesized by altering the synthesis technique of particular MOFs and incorporating appropriate quantities of second metal ions. In brief, the interaction among two metal ions with identical charge density plus electronic configuration and organic linkers furnish the bimetallic MOFs. Bimetallic MOFs might be an exceptional replacement for monometallic MOFs. [107]. For the last two decades, luminescence-based approaches extensively reported for the identification of interest markers. Briefly, it is the phenomenon of spontaneous light emission caused by energy absorption. In this phenomenon, the organic molecule absorbs the photon with sufficient energy that provides plenty of photo-physical phenomena. Recently, luminescence-centered materials gained gigantic attention from researchers that may be because of versatility, economic factor, simplistic process, and single-molecule sensing ability [104]. Especially, luminescent MOFs are composed of metal ions and multi-dentate fluorescent organic ligands that endow stupendous and adjustable photoluminescent attributes [108]. Mainly, it relied on structural composition, host–guest interactions, pore surface, and their volume [104]. Overall, the brief illustration of the design of luminescent MOFs and their sensing mechanisms provides insights for the development of new sensing strategies.

Stability of MOFs

Published literature revealed that the deal substances for sensing applications are intended to have a strong selectivity and wide surface area. In addition, such substances must provide us the high mechanical, chemical, thermal, and mechanical stability under process [109]. Therefore, plenty of literature surveys announced that the stability of developed MOFs is critical in basically all applications. MOFs' chemical, mechanical, and thermal stability are all vital considerations [110, 111]. The chemical stability of MOFs has been revealed to relate to their susceptibility to the consequences of interaction with different substances in their surroundings, including humidity, bases, solvents, acids, and aqueous solutions. In this line, MOFs have preferably been utilized in catalysis applications wherein stability of MOFs is imperative to challenge to the scientific fraternity. In the case of MOF thermal and mechanical stability, they generally correspond with a propensity of MOFs to sustain the stability of the structure when subjected to heating, vacuum, or pressure processing. Nevertheless, in the aforementioned operational settings, the majority of the documented MOFs had limited durability. This restriction severely limits the actual applicability of MOFs. As a result of the necessity and immediacy, the expansion and implementation of durable MOFs have earned a lot of emphasis [110]. In the case of thermal stability, it can confirm using different thermal analytical methods with different reaction conditions. Herein, the destruction temperature of MOFs is obtained at continuous increment in temperature.

Furthermore, the elemental composition changes, as well as solid-state nuclear magnetic response, etc. have been reported for the same. Initially developed MOFs have been suffered the issue of thermal stability in industrial applications such as the process of catalysis. As a result, it restricted the applications of MOFs in industry. Modern synthesizing development has evolved in thousands of frameworks with great thermal stability. Such enhanced heat endurance of the structure gives access to the catalysis of diverse active molecules [112]. Even though numerous MOFs are susceptible to architectural degradation simply under ambient air conditions owing to the coordination bonds liability involving ligands and metal ions [110]. In recent years, it rising range of MOFs with extraordinary chemical stability in the gas storage process, water desalination, ion exchange application, etc. [111]. The literature survey claimed that the solvent system is decisive in MOF synthesis. It helps to determine the surface and internal morphology of prepared MOFs. Moreover, solvents can either coordinate with selected metal ions as well as behave as space filler molecules. It is worthy to mention that the employment of water into a synthesis of MOFs plays the role of structure-directing agent for MOFs. As per literature, the solvents employed in MOFs synthesis should have an adequate polar nature and a high boiling point. The list of solvents, such as alcohols, dimethyl sulphoxide (DMSO), acetone, acetonitrile, dimethylacetamide (DMA), dimethylformamide (DMF), diethylformamide (DEF), etc., can be used alone as well as in combination for the synthesis of MOFs. Majorly, it is associated with the solubility of metal ions, organic ligands, and other components [113]. As per the literature, the chemical stability of MOFs can be confirmed via different techniques such as powder X-ray diffraction (PXRD) patterns. In this, prepared MOFs PXRD pattern after and before treatment in solvents provides the idea about chemical stability [114]. Notably, several MOFs are suffering from stability issues after addition into the aqueous system including acidic, water, and basic solutions. Literature survey demonstrated that the MOFs with good thermal stability (400 °C), larger surface area (2900–3400 m^2/g) are suffering from the collapse of an initial structure after contact with moisture or air [115]. It has been divulged that the improvement of chemical stability of MOFs can be improved using different strategies mainly including synthesis of MOFs using suitable metal ions and linkers combination, post-synthetic modification, incorporation of stability modifier, surface treatment, etc. [110]. The utilization of high charge density containing small and hard ions including Cr^{3+}, Zr^{4+}, Al^{3+}, etc. offers strong bonding with selected ligands and resulted in adequate chemical stability. Literature survey reported that the use of green solvents, such as water, ethyl lactate, methyl lactate, di-phenyl sulfoxide (DMSO), ionic liquids, etc., is extensively preferred for the synthesis of MOFs. Among all reported solvents, water is generally employed for the synthesis of MOFs. Despite this, the stability of final MOFs in water is quite less whereas the crystallinity loss, interaction with MOFs containing hydrophilic molecules, high specific heat, etc. influences the stability of MOFs [116]. Currently, supercritical liquids have been enlisted that offer tunable characteristics including surface tension, viscosity, and polarity. Majorly, MOFs can be developed with defined morphology that is principally associated with the MOFs synthesis method. Using such supercritical solvents can affect the pore interconnectivity, density, and pore size of MOFs [117]. Owing to the rapid crystallization, it resulted in the formation of larger size MOFs. Therefore, the utilization of supercritical liquids in the synthesis of nano-size MOFs is suffering stability problems [116]. Presently, plentiful literature reported the utilization of ionic liquids to replace the harsh solvents for the synthesis of MOFs [118]. Application of ionic liquids can be used as designer solvents for MOFs synthesis wherein it aid to modify the composition of ionic liquids as per requirement. Moreover, it offers a larger surface area, high yield, and reasonable cost [116]. The growth of the crystal is a major factor that affects the stability of MOFs and it can be modified using the coordination modulation approach. Herein, utilization monodentate linker offers a similar surface functionality to the multidentate organic linker. Interestingly, such modulators furnish the enhancement and turn down in MOFs crystal growth that resulted into diverse size crystals [113]. The MOFs mechanical stability at different reaction conditions, such as vacuum, pressure, etc., at diverse applications, is also essential fact in MOFs synthesis. Herein, the higher surface area and superior porosity of MOFs resulted in the stability issue. Principally, there are plenty of chances of partial collapse of pores, phase changes possibility, etc. Whereas, there are plenty of chances of loss of crystalline nature of MOFs during synthesis of MOFs via a mechanical process, such as ball mill process and mechanical milling [119]. Overall, with a continued focus on durable MOFs and a thorough knowledge of the underlying mechanisms influencing structural durability, emerging MOFs with improved physical and chemical stability are being generated. In addition, the ever-increasing number of stable MOFs has greatly increased the scope of MOF applications including sensing, catalysis, drug delivery, etc.

Luminescent MOFs

Luminescent materials have long piqued the interest of both scientists and laypeople. Such compounds emit energy in the form of light, rather than heat radiation when stimulated by external stimuli, such as UV light, electron beams, X-rays, or even mechanical phenomena [120]. The abundance of organic and metal elements provides

practically endless options for producing countless different types of luminous MOFs, the functionality of which may be easily planned and built [121]. Luminescent MOFs is attention-grabbing types of MOFs that are utilized in the construction of fluorescent sensor for the identification of interest analyte [122]. Notably, luminescent MOFs shine out as a distinct form of the sensor when compared to other typical luminous sensors owing to their crystalline structure, architectural variety, everlasting porosity, and tunable capability [120]. It has been divulged that the luminescence of MOFs is generated owing to the unique characteristic of different metal ions, types of organic linkers, and different charge transfer processes [15]. The post-synthetic modification (PSM) and host–guest chemistry-based MOFs have been reported such as luminescent lanthanide (Ln^{3+})-based MOFs (Ln-MOFs) that furnish the high sensitivity and speedy detection [123]. Currently, different categories of guest species including chromophores, quantum dots, and organic dyes have been suggested as a new approach in the host framework of Ln-MOFs that also contribute to the optical properties of MOFs [124].

Several MOFs have been designed using transition metal ions for example Cr^{3+}, Fe^{3+}, Zn^{2+}, etc. whereas alkali earth or alkali metal ions have also been reported for MOFs construction (Fig. 2). In this instance, the oxidation state, coordination geometry, and coordination number of metal are also important for MOFs design. In the case of metal coordination geometry mainly cubic, octahedral, tetrahedral, square planner, etc. are essential for the construction of MOFs [125]. Figure 5 depicts the different luminescence response mechanisms of MOFs. In brief, MOF's luminescence can be caused by either organic linkers or metal ions due to their intrinsic hybrid makeup. The main prevalent kind is linker-mediated luminescence, which has three subcategories: linker emission, ligand-to-metal charge transfer, and metal-to-ligand charge transfer [15]. Due to the general ability of metal–ligand bonds, the formation of coordination bonds between the metal ions and the organic linkers can proceed reversibly to allow the rearrangement of metal

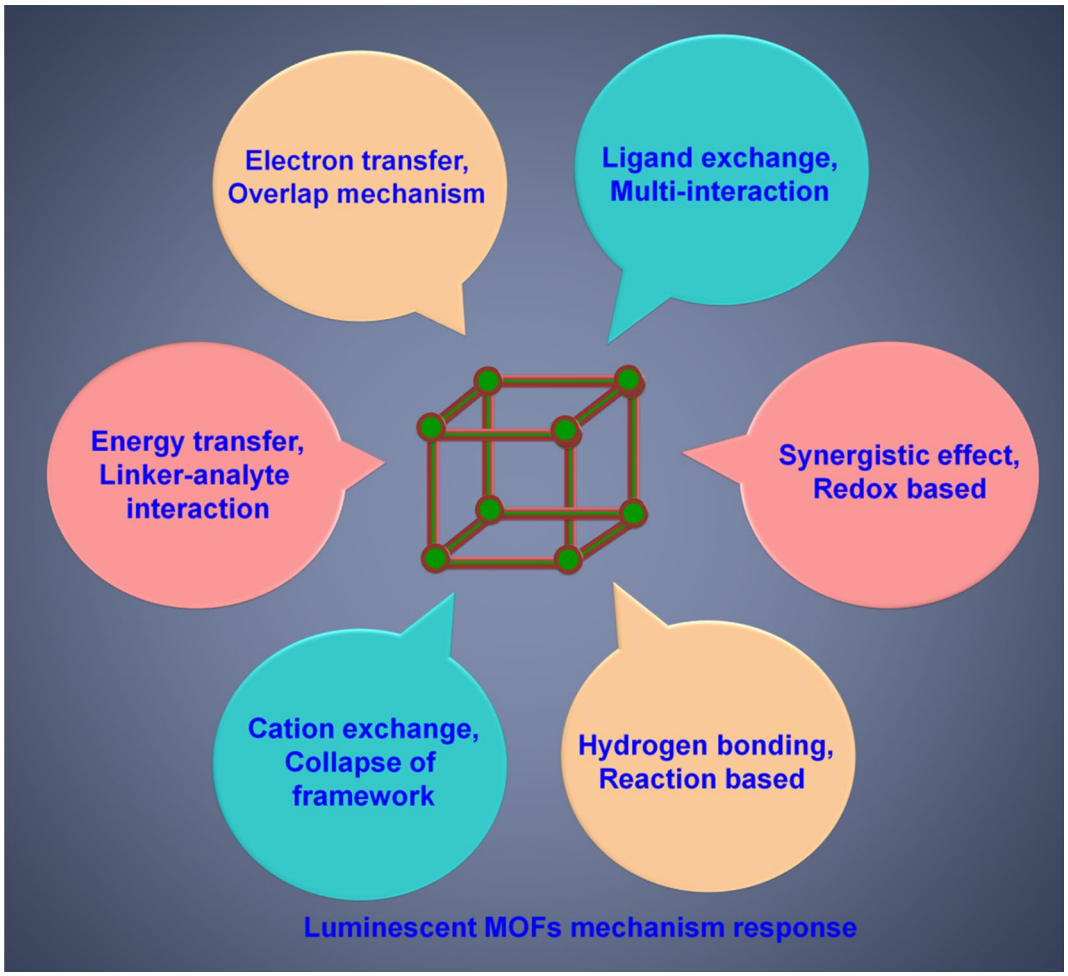

Fig. 5 Demonstration of luminescent MOFs mechanism responses

ions and organic linkers during the process of polymerization. This in turn allows MOFs to possess highly ordered framework structures [7, 8]. Different types of organic linkers, such as sulphonate, phosphates, nitrites, amines, carboxylates, etc., have been accounted for MOFs preparation. Notably, the adequate selection of organic linkers is based on the relative angularity of binding sites, several Lewis basic sites of ligands, etc. [125].

In several documented luminescent MOFs, fluorescent linkers have aromatic backbones or p-conjugated backbones, resulting in linker emission upon irradiation [126]. Owing to chemical stability, higher surface area, and easily induced luminescence, luminescent MOFs are highly appealing nanomaterials for diverse applications. The structural diversity of assembly of metal and ligands is playing an imperative part in luminescent MOFs that can also be modified into functionalized MOFs. Such functionalized luminescent MOFs exhibited improved sensitivity and selectivity as compared to bare luminescent MOFs [120]. MOFs' porous properties consent to them to adsorb and pre-concentrate solutes, enhancing the likelihood of host reactions and boosting sensor responsiveness [127]. Recently, zirconium (Zr)-based luminescent MOFs such as UiO-66-NH_2 have been designed for sensing applications. It has inimitable features mainly chemical stability, high luminescent quantum efficiencies, porosity, and improved surface area. Notably, it relies on secondary building units (SBU) that have high stability. Notably, the luminescent MOFs contain luminescence characteristics associated with different mechanisms including charge transfer transition. It covers the metal-to-ligand charge transfer and ligand-to-metal charge transfer. Moreover, the functionalization of amino groups in MOFs exhibited the charge transfer interaction due to auxochromic and bathochromic roles in the aromatic ring structure of MOFs [128]. Luminescent MOFs act as a sensor for recognition of interest analyte via different mechanisms that include guest-induced luminescence, metal-to-ligand charge transfer, ligand-to-metal charge transfer, ligand-centered emission, and photo-induced electron transfer [104, 129]. Figure 6 shows the presentation of luminescence sensing from MOFs.

It has been claimed that the luminescent MOFs offer plenty of superior merits, such as high sensitivity, lower detection limit, as compared to traditional fluorescent materials. Possibly, it may be because of intrinsic porosity and exceptional functionalities available in MOFs that are supportive for analyte binding and focused on the guest molecules [130]. Using the porosity of MOFs, precise monitoring of analytes may be accomplished by size exclusion, at which openings of the MOFs function as a separator to enable certain molecules to enter, hence modifying photoluminescence [131]. Literature survey demonstrated that the MOFs can also selectively target certain molecules. Such processes are frequently observed while detecting ionic species such as metal ions. Because of the significant affinity between pyridyl and copper (Cu^{2+}) ions, pyridyl-containing MOFs can be employed for Cu^{2+} detection [120]. The most prevalent method of analyte-sensor coupling is electron transfer between host and guest. Because the energy level of most

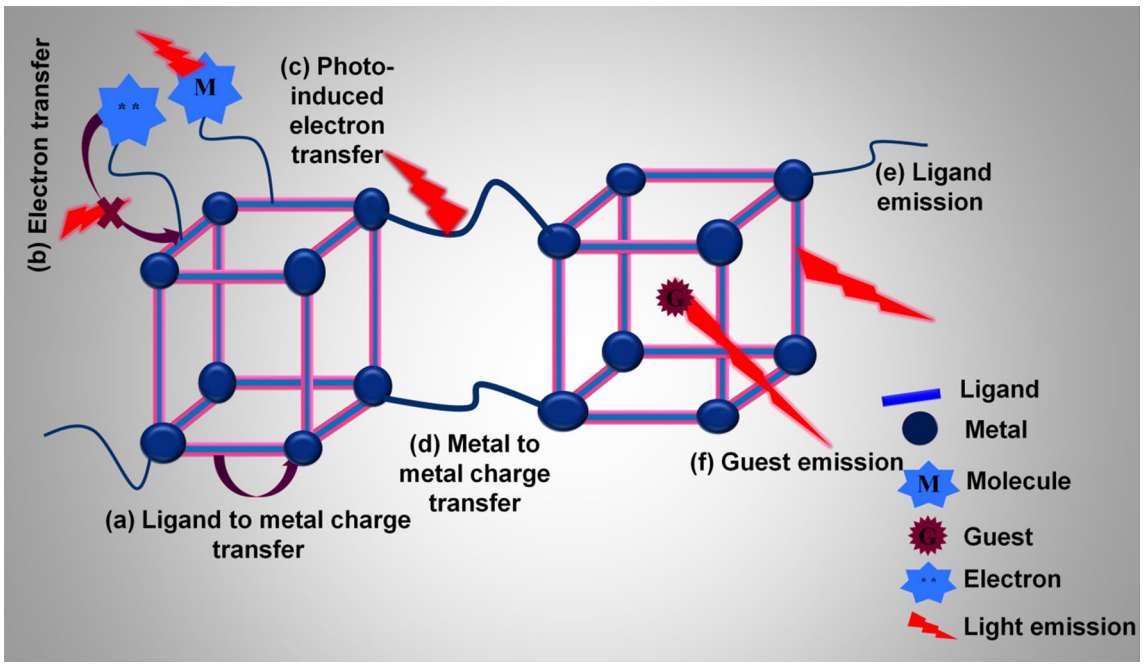

Fig. 6 Presentation of luminescence sensing from MOFs. **a** Ligand-to-metal charge transfer; **b** Electron transfer; **c** Photo-induced electron transfer; **d** Metal-to-metal charge transfer; **e** Ligand emission; **f** Guest emission

analytes' lowest unoccupied molecular orbital's (LUMO) is often lower than that of MOFs' LUMOs or conduction bands (CBs), in which the electron transfer from preferred MOFs to interest guest molecules is conceivable [132]. Energy transmission across host and guest is indeed critical for detection, which is strongly reliant on the degree of overlap amongst analyte absorption and sensor output (emission) [133]. Besides this, the fluorescent turn-off mechanism has been reported wherein the fluorescent quenching in the original emission peak resulted in poor sensitivity. Majorly, the alteration in the intensity in the existence of analyte is challenging to monitor. In most of these cases, the molecules with identical electronic and structural attributes illustrate the trouble to segregate such molecules. Presently, there is turn approach is widely employed for sensing of interest analyte wherein the interaction with MOFs part furnishes the induction in intensity, or new emission peak generation, or wavelengths shifts [64, 134]. Literature survey reported the overlap response mechanism which is capable of signal transduction. Importantly, the overlapping of analyte UV–Vis absorption band and luminescent MOFs containing photoluminescence excitations/emission band is offered the sensing of an analyte. It has been mentioned that the effective overlapping of the non-emissive analyte absorption band with donor resulted in resonance energy transfer [130].

The sensing mechanism of luminescent MOFs can be altered with respective metal ions and types of ligand used for designing MOFs. Despite this mechanism, the decomposition of the sensor is a vital strategy that has been reported for sensing a target analyte. In this context, the polymorphic lanthanide complexes synthesized as a multifunctional nanomaterial. Herein, the metal ion (such as Co^{2+}) induces the decomposition of luminescent nanostructures. It may be because of the unique outer electronic configuration of the interest analyte (for example Co^{2+}). [135]. In the recently published literature, a luminescent lanthanide complex has been prepared wherein mercuric ions (Hg^{2+}) cannot quench the luminescence. On contrary, the methyl form of analyte (CH_3Hg^+) quenched the luminescence of the Ln-complex. Possibly, it may be because of the coordination of CH_3Hg^+ with uncoordinated carboxyl oxygen of the Ln-complex. Moreover, the oscillation of C-H in the methyl group would consume the energy of lanthanide ions and finally, it resulted in quenching of luminescence [136]. Moreover, the presence of luminescence quenching groups such as O–H with a high concentration in the region of lanthanide ions ($Eu^{3+)}$ resulted in the quenching of luminescence of Eu^{3+} via oscillation effect [137]. Another sensing mechanism of lanthanide MOFs (Ln-MOFs) includes the strong inner filter effect. In this study, the strong absorption of interest analyte overlaps with MOFs excitation spectrum. It demonstrated that the UV light is absorbed by interest analyte in selected sensing medium of analyte and MOFs. Herein, the UV light is not able to get at the prepared sensor and then excite MOFs via antenna effect. Therefore, the recognition of the target analyte by prepared MOFs has been done via a strong inner filter effect [138]. In the inner filter effect mechanism, during overlapping, the target analyte will filter the excitation photons followed by decline or return the photons for the excitation of MOFs [139]. It has been proposed that the open channel nanostructure and controlled hole size of luminescent MOFs offer guest-induced luminescence during sensing of interest analyte [15].

Zheng and co-authors reported the quenching mechanism of lanthanide (Ln^{3+}) complexes in presence of an interest analyte. The luminescence of prepared Ln-complexes has been observed due to the antenna effect. It is based on three major steps that include the absorption of photons by antenna (selected linker/ligand) this coordinated the Ln ions. After that, it absorbed energy transfer from linker to Ln^{3+} ions, and finally, it resulted in a generation of luminescence. Herein, the quenching can be occurred by the ligand-to-metal charge transfer mechanism [140]. Taken as a whole, the Ln-centered MOFs offer the energy transfer from Ln^{3+}-to-Ln^{3+} and ligand-to-Ln^{3+}. In addition, the emission of Ln-MOFs relies on the non-radiative energy relaxation from the 4f excited state (upper) to the emitting level of Ln^{3+} [141].

As we know the luminescence of MOFs has relied on either metal or linker and both metal and linker. For example, in the context of zinc-based luminescent MOFs (Zn-MOFs), luminescence is generated from emission organic linkers. Here, linker-based emissions are originated from selected single ligands, as well as it may be because of ligand to ligand charge transfer. Interestingly, 3D MOFs offer augmented ligand interactions as well as modify the energy that resulted in the emission behavior [142]. Literature survey reported that the Zn-MOFs furnishes the different theoretical sensing mechanisms, such as π–π interaction among analyte and MOFs, charge transfer from linker to the analyte (electron-deficient), diffusion-controlled, etc. In another case, the luminescence to MOFs has been observed due to the intra- as well as inter-ligand charge transfer process. Principally, indium and lithium-based MOFs have been reported in this category [15]. Moreover, the nano-form of MOFs (nano-MOFs) has been reported in bulk form (nanoparticles) that furnishes the boosted performance in terms of towering sensitivity. In this category, europium (Eu)-based rod shape nano-MOFs (diameter: less than 20 nm) have been constructed using 1,4-benzenedicarboxylic acid as a ligand (H_2bdc) [143]. It is worthy to mention that the nano-MOFs containing luminescence lifetime cannot be affected after the introduction of interest targets in diverse concentrations. Subsequently, it confirmed the absence of analyte and metal center electronic interaction. In this case, the analyte shows the strong absorbance at a specific wavelength that

may be because of different transitions (like π–π* transition). It reduces the energy transfer from the ligand to the metal center and finally, there is a quenching of emission [15]. Overall, we have addressed the different luminescent MOFs-mediated sensors for metal ions and chemical sensing applications. In the next section, we have discussed the applications of luminescent MOFs for sensing chemicals and metal ions in brief.

Nano-architectured MOFs-based luminescent sensor

Recently, the extensive applicability of MOFs into sensing is holding huge awareness from scientific fraternities due to their high sensitivity, high stability (thermal and chemical), high selectivity, high surface area, reusability, post-synthetic modification ability, etc. Accordingly, MOFs are of particular interest for impending applications in environmental applications for sensing of gas, pesticide, vapor, etc. In addition, it is used for biosensing and drug delivery applications [144–146]**.** Nevertheless, there is a demand for essential prerequisites for the novel or optimized functionalities to prolong the foremost applications of MOFs towards recent areas of sensors, biomedicine, magnetic and electronic devices, proton conduction, etc. [50, 147, 148]. Figure 5 depicts the different luminescent MOFs-mediated mechanism responses involved in the detection of metal ions and chemicals. Table 1 summarizes the different kinds of luminescent with types of metal ions, ligands, synthesis methods, analyte, and the limit of detection, linearity range, and sensing mechanism.

Structural design of MOFs luminescent sensor for chemical sensing

Sensing high explosives is a prime requirement for monitoring environments and human life. In this line, in 2009, Lan et al. developed the highly luminescent MOFs, namely microporous MOFs (MMOF) or $Zn_2(bpdc)_2$-(bpee)-mediated luminescent sensor, for recognition of high explosives in the vapor. Herein, the $[Zn_2(bpdc)_2$-(bpee)]·2DMF has been prepared via a solvothermal method. Interestingly, the redox quenching mechanism using ligand (bpdc: 4,4'-biphenyldicarboxylate and bpee = 1,2-bipyridylethene) helps to sense the target analyte. Besides, both preferred ligands provided the luminescence property, analyte detection capability, and high conjugated *pi* systems. Principally, the 3D structure plus porosity of nanosized MOFs affords highly sensitive recognition of nitro explosives. Consequently, the nitroaromatic explosive, plastic explosive, 2,4-dinitrotoluene (DNT), as well as 2,3-dimethyl-2,3-dinitrobutane (DMNB) recognition has been accomplished via using this developed MOFs-mediated sensor. Herein, host–guest chemistry plays a key role in sensing a target analyte. In the case of DMNB sensing, stronger interaction among analyte and MOFs has been found that may be because of pore confinement of DMNB inside the MOFs cavities. As result, it shows good fluorescence quenching in presence of DMNB. Owing to the affinity towards the high electron-deficient compound, the prepared MOFs offer high selectivity towards the analyte species in presence of other interfering substances. In the future, owing to reversible and speedy detection, high sensitivity, etc., the abovementioned luminescent MOFs-mediated sensors can be preferred for different explosive sensing [149]. The luminescent Cu^{2+}-based MOFs, namely Cu-TCA, have been designed using tri-carboxy-tri-phenyl amine (H_3TCA) via solvo-thermal reaction for recognition of nitric oxide (NO) in an aqueous plus in living cells. Herein, the TCA has been employed as an emitter. Briefly, the Cu^{2+} ions' paramagnetic nature would quench the ligand-based fluorescence. Whereas, the NO and metal ion's coordination on the MOFs surface reduces the Cu^{2+} to Cu^{+}. Accordingly, it improved the luminescence of Cu-TCA. Herein, two MOFs-mediated sensors for NO have been reported based on the tri-phenyl-amine (TCA) moiety mainly Cu-TCA and Eu-TCA. In that, the Cu^{2+} get reduced after an existence of NO that showed luminescence in aqueous solution which can provide the high selectivity and sensitivity towards the bioimaging application in the living cells. Quenching of the paramagnetic center has resulted in the reduction of emission of the ligands. In the sensing case, Cu^{2+} generates the diamagnetic species and that was responsible for quenching of luminescence of MOFs. Furthermore, Eu-TCA explored the NO sensing application as a ratiometric luminescent chemosensor. In the future, it will release new avenues for highly sensitive and selective sensing of chemicals using a ratiometric luminescent sensor [150].

Yang and their team reported terbium (Tb)-based MOFs (Tb-MOFs-76) for acetone sensing (Fig. 7). Initially, Tb-MOFs-76 has been prepared via the microwave-assisted method with amino acid namely proline as capping agents (Fig. 7A). Fascinatingly, it contains only one carboxylic group as compared to the other organic linkers (H_3BTC:1,3,5-benzene tricarboxylic acid). The increased proline concentration reduced the crystal size of composites after a certain concentration (Fig. 7B). Herein, the proline offered a reduction in crystal size due to modulating effect among 'Ln' ions and linkers. Hence, proline is a more suitable capping agent for MOFs-based sensors that may be because of its solubility, and size reduction capability. Furthermore, pillar-like rods of nanoscale MOFs (30 µm) exhibited photoluminescence in solution and explored the platform for solvent sensing like acetone in presence of other solvents. Herein, the rise in the concentration of acetone shows a decline in luminescent properties of MOFs

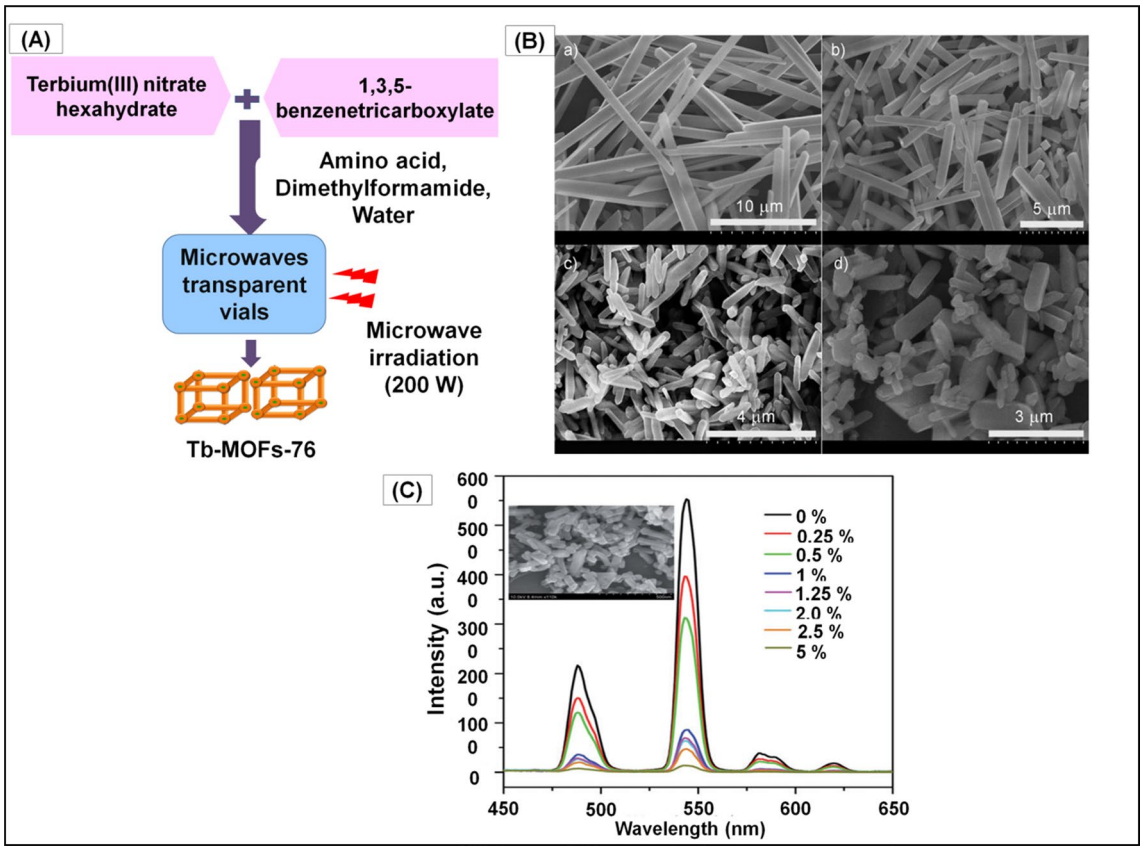

Fig. 7 Synthesis of Tb-MOFs-76 (**A**) and Scanning electron microscopic images of Tb-MOFs-76 in presence of glycine. Presentation of Tb-MOFs-76-based luminescent sensor for acetone sensing (**C**). [Reprinted with permission from reference [151]. Copyright © 2012 Wiley–VCH Verlag GmbH and Co. KGaA, Weinheim.]

and finally complete quench at 5% of acetone concentration (Fig. 7C). Principally, the presence of Tb^{3+} ions in MOFs shows potential for acetone. Overall, the diffusion-controlled was a theoretical mechanism involved in sensing the analyte using Tb-MOFs-76. As a result, the property of MOFs towards the terminal solvent and pore structures can excel in an innovative arena in luminescent microporous small molecular sensors [151]. In the future, a diffusion-controlled sensing mechanism can be used for sensing acetone in provided samples.

For recognition of dimethylformamide (DMF) vapor the Ln-based MOFs namely $Eu_2L_3(H_2O)_4]\cdot 3DMF$ has been developed using 2′,5′-bis(methoxymethyl)-[1,1′:4′,1″-terphenyl]-4,4″-dicarboxylate) as a ligand (L). Luminescence studies demonstrated that the turn-on in response to DMF vapor has been obtained that might be because of DMF–ligand interactions. It sifts the ligand excited-state energy level, which resulted in ligand-to-metal energy transfer. It has been divulged that the prepared $Eu_2L_3(H_2O)_4]\cdot 3DMF$ demonstrates the rapid response and high selectivity for DMF only in presence of other solvents that confirmed the applicability of the sensor in sensing chemical vapors. Taken as a whole, the reported luminescence "Turn-On" mechanism discovered the new strategy for Ln-MOFs sensor by proper ligand design and targeting analyte through ligand– analyte interactions. As a result, it opened up new opportunities for DMF vapor detection utilizing the Ln-MOFs sensor [134]. Wang and co-authors engineered the mixed-ligand Zn-MOFs as highly luminescent sensors using rigid (carboxylic acid) and semirigid ligand for nitro compounds sensing. Briefly, three Zn-MOFs have been constructed using a dual-ligand approach by N-donor ligand namely 1,3,5-tris [1-imidazolyl]-benzene (tib) and biphenyl-3,3′,4,4′-tetracarboxylic acid (carboxylate ligand) by hydrothermal process. These MOFs provide the solvent-dependent photo-luminance phenomenon. Zn-MOFs provide highly sensitive nitroaromatic detection by way of a fluorescence quenching mechanism. Herein, the fluorescence quenching has been obtained that may be due to e- transfer from electron-donating MOFs towards the e- withdrawing nitro group within the nitro (NO_2) compound. Herein, it shows the high selectivity for nitrobenzene as compared to acetone, toluene, carbon tetrachloride, ethanol, etc. Finally, it concluded that these electron-rich MOFs can be used for the detection

of nitro-substituted compounds [152]. Yet another work reported the luminescent lithium (Li)-based MOFs namely Li-MOFs or [{Li_3[Li (DMF)$_2$] (CPMA)$_2$}s·4DMF·H_2O] modified form using a solvothermal process for explosive nitroaromatic compounds selective detection (Fig. 8). A ditopic H_2CPMA = bis [4-carboxyphenyl]-*N*-methylamine] is used as a ligand and it affords the luminescence properties to MOFs. These ligand molecules offered good luminance towards the analyte detection because of the charges transformation from *N*-methyl amino (donor) to the carboxylate group (acceptor). Owing to the strong interaction of MOFs and nitroaromatic explosive compounds, it alters the electronic structure of MOFs. Thus, it exhibited a suitable MOFs-based sensor for the detection of electron-deficient (nitroaromatic compound example like nitrobenzene). Overall, the host–guest interaction and electron donor–acceptor mechanism help to detect the interest analyte in complex samples. In the future, Li-MOFs can be used for the detection of diverse nitroaromatic by electron donor–acceptor transfer mechanisms [153].

It has been divulged that the use of 1D, honeycomb type channels dependent microporous Tb-MOFs namely {[Tb(FDA)$_{1.5}$(DMF)*DMF}n (1·nDMF and DMF: *N*,*N*-dimethylformamide) for sensing application. Tb(FDA)$_{1.5}$(DMF)*DMF demonstrated exceptional separation and adsorption capabilities towards hydrogen, nitrogen, and carbon dioxide. In addition, it provides the selective significant sorption of CO_2 over nitrogen and methane (CH_4). Besides, the separation and recognition of gas molecules have been occurred due to hydrogen bonding, Vander Val forces from MOFs towards the gases. Ultimately, it enhanced the adsorption and detection of small molecules owing to the open metal sites in porous Ln-MOFs (micropore volume: 0.593 cm^3/g, porosity: 1005.6 m^2/g). The emulsion luminescent studies provide the guest-dependent luminescent emissions because of this potential it could be used for benzene and acetone or small molecule pollutant detection. Owing to this, the diffusion-controlled theoretical sensing response mechanism confirmed the application of MOFs for sensing gases molecules with high selectivity and sensitivity. In the future, the application of this prepared MOFs-mediated nonporous sensor in the environment will offer an alternative to currently engaged methods [154]. The exceptionally remarkable azobenzoic acid-functionalized graphene oxide (GO) nano-composites with luminescent Zn-MOFs (A-GO/L–Zn^{2+}) sensor has been developed for revealing high explosives gases such as dinitrotoluene (DNT), and trinitrotoluene. In brief, for these MOFs, stilbene derivative has been selected as a ligand that may be because of its outstanding photo-luminescent

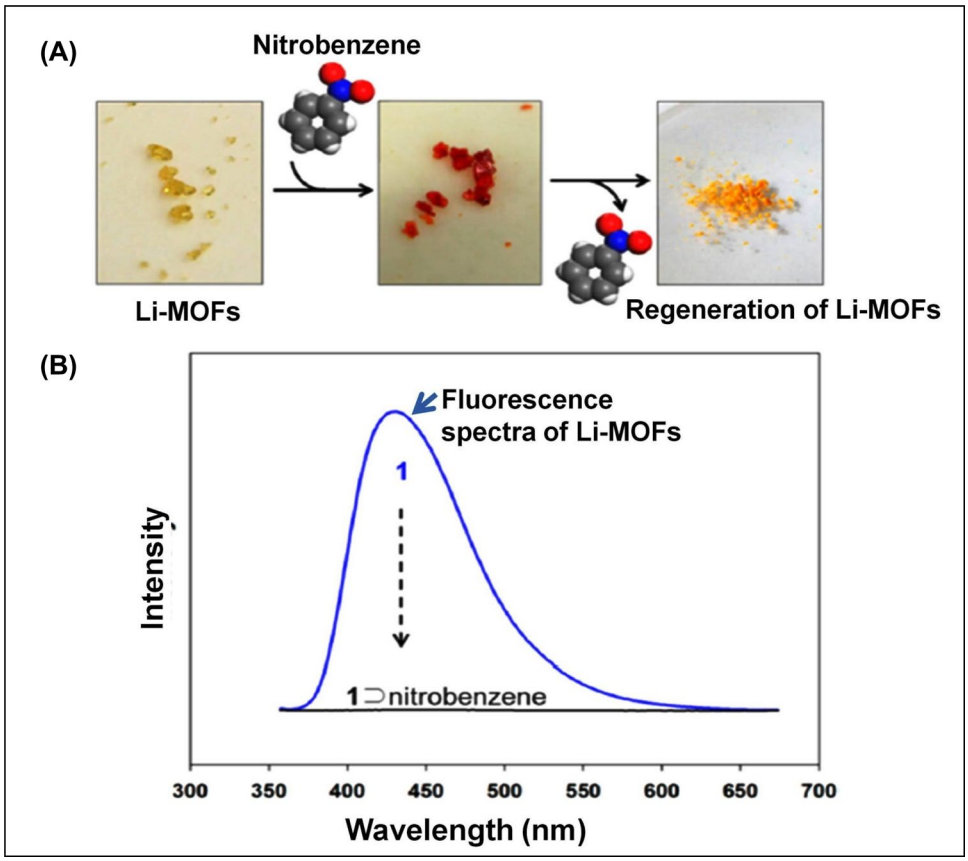

Fig. 8 **a** Detection of nitrobenzene and its regeneration by heating. **b** Fluorescence spectra of Li-MOFs-based sensor in presence of nitrobenzene. [Reprinted with permission from reference [153]. Copyright © 2013, American Chemical Society.]

properties. Importantly, the GO-based MOFs (pore size: 1–2 nm, surface area: 220.03 m^2/g) offered small molecule retention because of their dispersive forces. Moreover, this sensor showed the typical p–p* transition that provides a high fluorescence property. Owing, to the functionalization of graphene-based MOFs, it offered prominent and long-term fluorescence enhancement as compared to the ligand. It has been divulged that the DNT addition into Zn-MOFs (A-GO/L–Zn^{2+}) decreases the fluorescence intensity that may be because of charge transfer interaction. In brief, a ligand of MOFs contains an electron-rich aromatic group that electron gets a transfer from electron-rich ring to electron-deficient DNT. The selectivity study confirmed that the use of a sensor for the identification of gases shows 71 percent quenching in presence of DNT. Therefore, this nanocomposite can be used as a chemosensor in the selective detection of DNT molecules in real-time samples. In the future, it will furnish a new approach for the arena of molecularly designed materials of biology, medicine, and material science [155]. Using a mixed-ligand approach, the isostructural Ln-MOFs, $[Ln_2(BPDC)\text{-}(BDC)_2(H_2O)_2]n$ [Ln = Eu [1] and Tb [2]], have been prepared by Zhou et al. through the hydrothermal method using different ligands, namely 2,2′-bipyridine-3,3′-dicarboxylic acid (H_2BPDC) and H_2BDC. In brief, $BPDC^{2-}$ containing carboxyl groups resulted in bridge formation by two oxygen atoms and metal ions (Eu^{3+}). It generates the edge share binuclear unit with Eu–Eu. Herein, ligands containing aromatic-carboxylic groups mainly phenyl and pyridyl (luminescent chromophore) participate in a function as an antenna for energy transformation to the luminescent component center. Due to the Van der wall radius, explosive organic molecules could arrest MOFs and influence the energy transfer from ligand to the luminescent center of MOFs. These luminescent MOFs showed the selectivity towards the fluoride anion and small molecules including acetone, acetonitrile, as well as formaldehyde. In a nutshell, it could use for the detection of poisonous small molecules as well as anions [156]. The terbium-MOFs, [Tb(1,3,5-BTC)] n has been designed using H_3BTC for picric acid detection. In brief, MOFs synthesis has been achieved via the combined ultrasound-vapor phase diffusion technique. Owing to this technique, nano-scale MOFs crystals have been accomplished with a high yield as compared to the conventional methods, such as solvo-thermal and microwave-assisted synthesis. Principally, nitro-aromatic compounds can accept electrons and substitution of e-withdrawing nitro groups on an aromatic ring, which affects the energy of the orbital. Subsequently, it reduces the energy of p*orbital. In addition, because of this electron transfer (donor and acceptor), quenching of MOFs luminescence has occurred in presence of the target analyte. Ultimately, these prepared MOFs provided more selectivity to the picric acid in the existence of different nitro-aromatic compounds as interfering substances. The limit of detection (LOD) was found to be 8.1×10^{-8} µM, whereas it provides the linearity range from 0.001 to 0.18 mM. Therefore, in the upcoming days, the prepared luminescent MOFs-mediated sensor can offer the potential for highly sensitive and selective identification of picric acid in provided real-time samples [157]. In another work, zinc (II) nodes and luminescent organic ligand 9-phenylcarbazole- 3,6-dicarboxylic acid (H_2PDA) -based MOFs sensor $\{[Zn_4O(C_20H_{11}NO_4)_3(C_4H_9NO)(H_2O)]\cdot(C_4H_9NO)_2(H_2O)_3\}n$ or (Zn−PDA2) for detection of picric acid (Fig. 9). It shows the ellipsoid cavities and the addition of picric acid demonstrated the naked-eye changes in Zn−PDA2 (Fig. 9A. Interestingly, MOFs offered the dual signal emission importantly ligand-based emission and metal–ligand charge transfer-mediated emission. Additionally, intra-ligand charge transfer offers a blue shift that may be because of host–guest effective electron transfer. Thus, it increased the accuracy and sensitivity of the sensor towards picric acid detection. As a result, Zn−PDA2 will offer a new alternative for picric acid detection visually with precise selectivity (Fig. 9B). This sensor provided the naked-eye and luminescent detection limit of 0.45 µg and 25 ppb (Fig. 9C), respectively in favor of picric acid. Owing to synergistic hydrogen bonding and electron transfer, the present sensor demonstrates high selectivity in the occurrence of diverse interfering substances. In conclusion, this sensor will open a new door with boosted accuracy and sensitivity [158].

The pyrene (NU-1000) core-mediated zirconium (Zr)-based luminescent MOFs have been designed using tetraethyl 4,4′,4″,4‴-(pyrene-1,3,6,8-tetrayl) tetra-benzoic acid (TBAPy) for detection and screening of human urinary 1-Hyroxypyrene (1-HP). The ligand structural arrangement in MOFs provides the detection of 1-HP via strong intermolecular π–π interaction. The photoluminescence of a highly conjugated ligand has been confirmed that shows the excitation spectrum at 250–400 nm that may be because of π–π* transition. It shows good stability after the formation of NU100 by co-ordination to Zr (IV). It has been declared that there was no metal–ligand charge transfer as well as ligand metal charge transfer. That assures the emission potential of MOFs has relied on ligand emission. In presence of the analyte, NU-1000 provides the quenching and gives the low detection limit of 48 nM. In addition, it furnishes the high selectivity for 1-HP in presence of plenty of interfering agents, such as urine containing components urea, glucose, uric acid, etc., that may be because of weak host–guest interactions between these interfering molecules and luminescent NU-1000. Consequently, this sensor showed good feasibility for practical application. Besides this, NU-1000 demonstrated a good recovery of human urine containing 1-HP. Concisely, the potential of the developed NU-1000 sensor can provide a fresh option for sensing chemicals and biomarkers in clinical samples [69]. Nagarkar and the

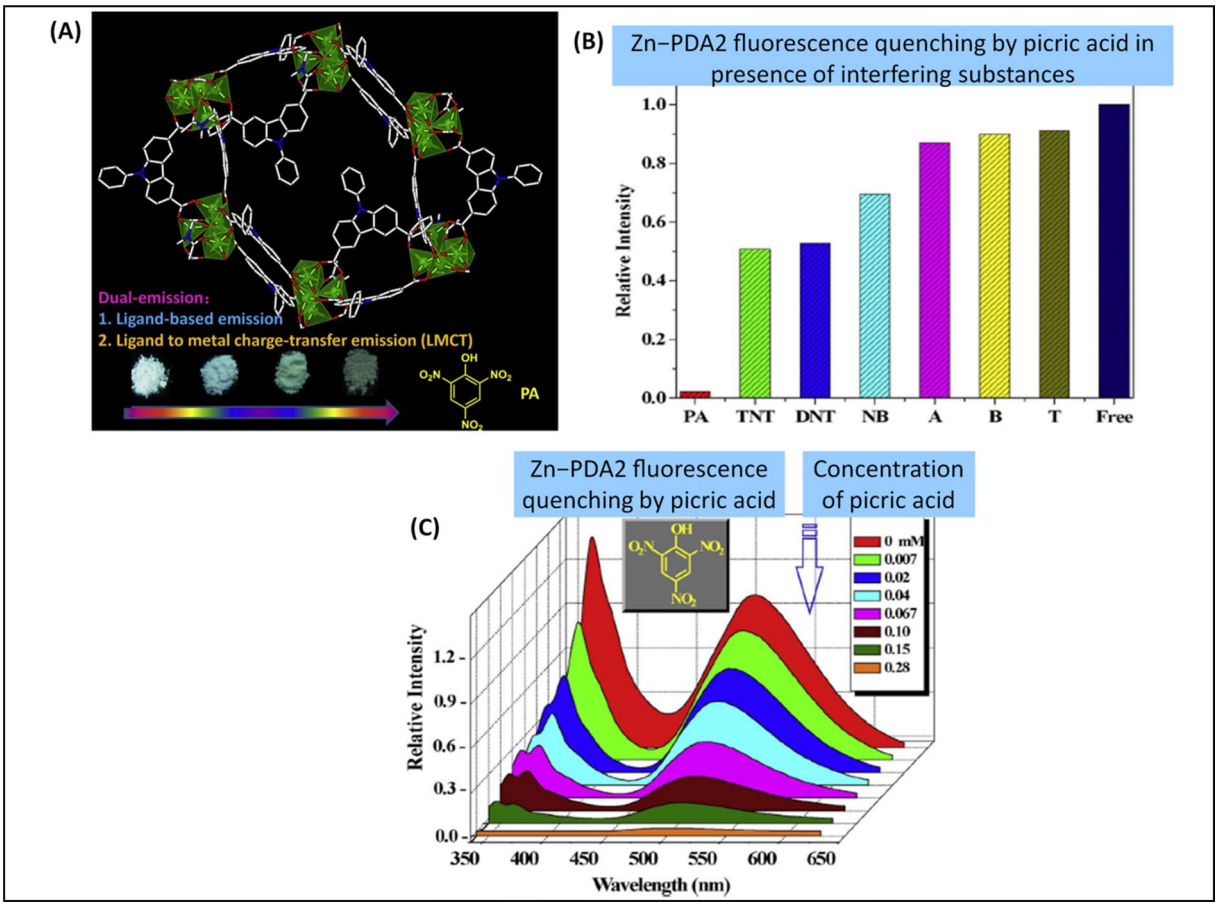

Fig. 9 **A** Crystal packing structure of Zn – PDA2 and visual changes in Zn – PDA2 after addition of picric acid. **B** Quenching of fluorescence of Zn – PDA2 after addition of picric acid (PA) and different interfering substances, such as aniline (**A**), toluene (T), benzene (B), DNT, 2,4,6-TNT; **C** presentation of Zn – PDA2 fluorescence quenching upon adding picric acid up to 0.28 mM. [Reprinted with permission from ref [158]. Copyright © 2017 Elsevier.]

authors reported that the revealing of nitro-explosive mainly 2, 4, 6-trinitrophenol (TNP) using three-dimensional (3D) fluorescent MOFs. Figure 10A depicts the rapid sensing of nitro explosives using 3D porous MOFs. Briefly, [Cd(NDC)0.5(PCA)]·Gx (1G = guest molecules) has been obtained using 2,6-naphthalene dicarboxylic acid (NDC) and 4-pyridine carboxylic acid (PCA as a ligand. In this study, fluorescence quenching titrations have been accomplished using TNT, 1,3-dinitrobenzene, nitrobenzene, 2,6-dinitrotoluene, dinitrobutane (DMNB), 2,3-dimethyl-2,3- nitromethane (NM), etc. It demonstrates the high selectivity due to the surface adsorption of interfering substances (Fig. 10B). Herein, selective recognition of TNP was observed owing to the electrostatic interaction and electron and energy transfer mechanism. Moreover, it shows the high sensitivity to TNT that may be because of spectral overlap that demonstrates the effectual quenching of fluorescence intensity. Moreover, MOFs exhibited more stability with water and enormous electrostatic interaction with TNP can provide a substitute for sensing of target analyte in real-time samples. In the future, this prepared MOFs-mediated luminescence sensor will release a new horizon for the highly selective and sensitive identification of explosives [159].

Tian and co-authors prepared the Cd-MOFs, $[NH_2(CH_3)_2]_2[Cd_{17}(L)_{12}(m_3\text{-}H_2O)_4(DMF)_2(H_2O)_2]$*solvent for recognition of nitroaromatic explosives in a vapor state. Briefly, it has been assembled using a π e^--rich aromatic 2,4,6-tris[1-[3-carboxylphenoxy]ylmethyl]mesitylene (H_3L) as a ligand and cadmium (Cd^{2+}) metal ions via solvothermal conditions. It has been reported that the nitroaromatic containing nitro group provides the electron-withdrawing substituent. Additionally, it enhanced the oxidative stability of the aromatic ring. Due to the electron transfer quenching mechanism, the Cd-MOFs show fluorescence quenching in the presence of nitro explosives (nitrobenzene). As a result, it showed high sensitivity and selectivity for nitroaromatic compounds. For a future point of view, the investigated MOFs-centered new method will open the door for the detection of nitrobenzene and its derivative in solution or vapor state [160]. Song and colleagues reported the single

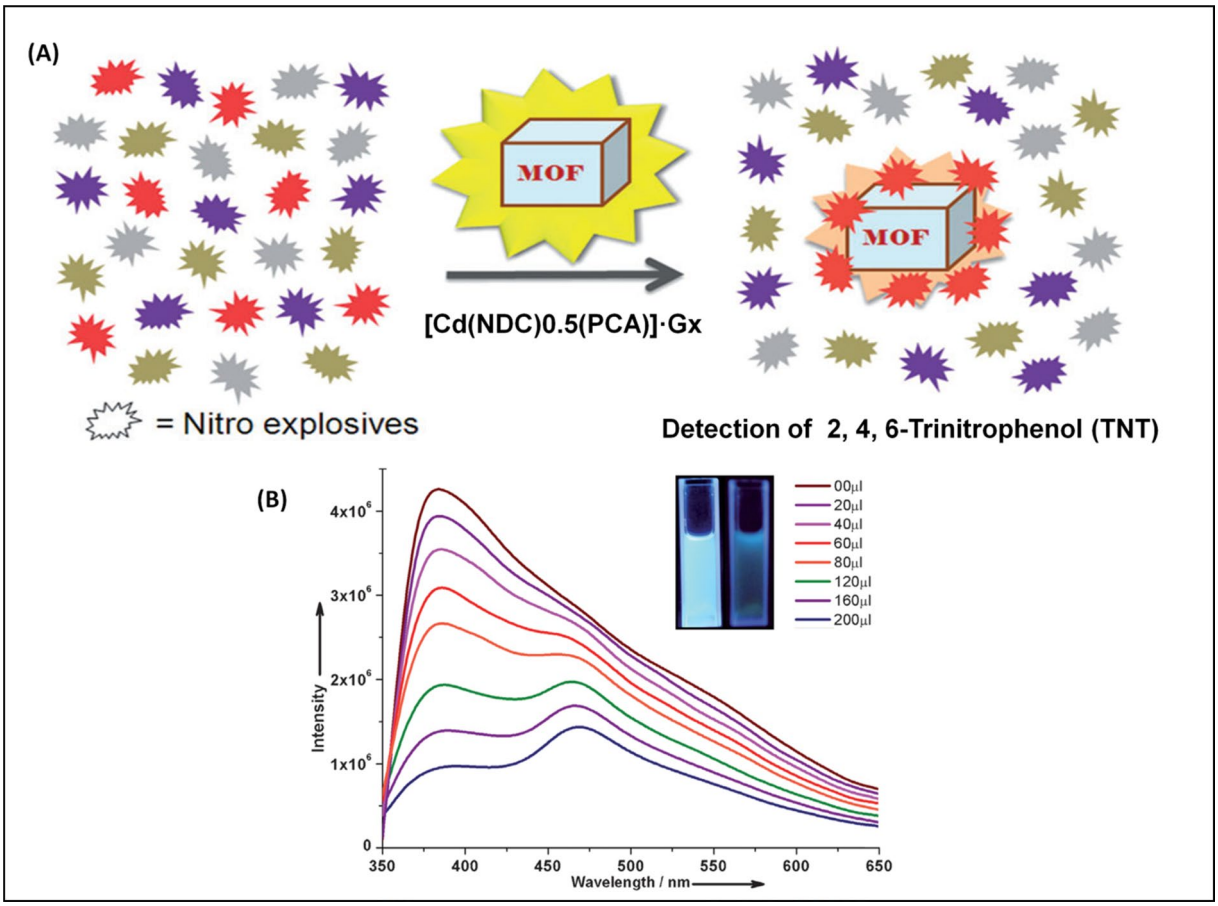

Fig. 10 **A** Presentation of MOFs-mediated sensor for the selective recognition of target nitro explosives in the existence of interfering nitro compounds. **B** Impact of the addition of TNT on luminescence spectra of [Cd(NDC)0.5(PCA)]·Gx [Reprinted with permission from ref [159]. Copyright © 2013 Wiley–VCH Verlag GmbH & Co. KGaA, Weinheim]

crystal to single crystal (SC-SC) transformation mechanism-based Eu-MOFs luminescent sensor using 4,4′-(4,4′-bipyridine-2,6-diyl)dibenzoic acid ($bpydbH_2$) as a ligand. Interestingly, these selected ligands provide intense rigidity which furnishes the porous structure with a combination of transition metal. Also, it has given the high capacity to conquer the low absorption coefficient of single lanthanide ions via the antenna effect. Moreover, ligand conjugated rings with available Lewis-base sites improve the sensitivity of analytes through a variety of host–guest interactions. In this study, guest analyte and host interaction offer the lowest detection limit for aliphatic alcohol. In another case, due to electron transfer from the electron-rich region of the aromatic ring of the abovementioned linker and electron-deficient analyte, it shows the high selectivity towards the nitro compounds. This sensor has been showing the ability the detection of acetone, highly explosive TNP, and selective for aliphatic alcohols. Subsequently, this sensor can serve as a multi-responsive tool for pollutant detection for future environmental applications [161]. Cd(II)-containing MOFs have piqued the curiosity of researchers because of their wide application in photochemistry, and chemical sensors. Novel anionic, 3D metal-based MOFs, such as Cd-MOFs or $\{(CH_3)_2NH_2]_4[Cd^{3+}(H_2L)\}$, have been synthesized for the detection of nitrobenzene (Fig. 11). Briefly, $(CH_3)_2NH_2]_4Cd^{3+}H_2L$ has been prepared using multi-dentate organic carboxylic acid ($H_{12}L$) via a solvo-thermal method. The Cd^{3+} oxidation and reduction are challenging tasks, whereas ligand containing 12 carboxyl groups provides the adequate oxygen atoms to assemble the coordination requirements of metal ions (Cd^{3+}). As result, MOFs provide a novel cage-to-cage connection between 3D Cd-MOFs and 1D channels. It has been declared that the prepared MOFs get quenched due to the nitrobenzene emulsion wherein photoinduced electron transfer plays an imperative role. In this case, electron-deficient nitrobenzene accepts an electron from an electron-rich ligand. Furthermore, it offered complete quenching at 1000 pm concentration of nitrobenzene (Fig. 11a) whereas it exhibited high selectivity towards nitrobenzene in presence of diverse types of interfering substances (Fig. 11b). It

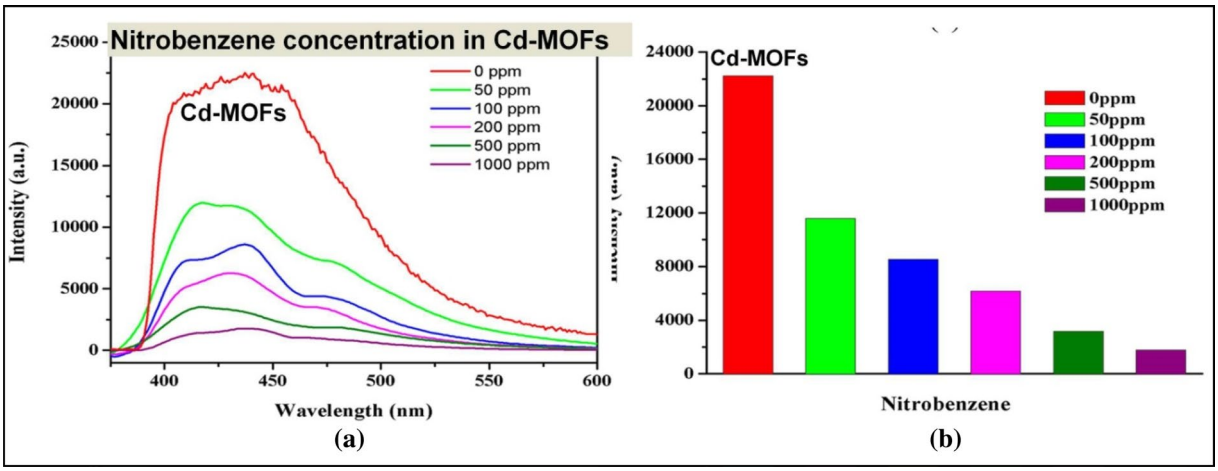

Fig. 11 **a** Emission spectra of MOFs at different concentrations of nitrobenzene, **b** Graph of emission intensity of MOFs at different concentrations (0–1000 ppm) nitrobenzene. [Reprinted with permission from ref. [162]. Copyright © 2014, American Chemical Society]

confirmed the quenching of luminescence by the presence of a nitro group. As a result, it is obvious that the described Cd-MOFs-based sensor can usher in a new age of detecting nitroaromatic explosives in the surroundings [162].

Because of high explosivity and high toxicity, existing nitroaromatic compounds have become significant polluters of groundwater, soils, etc. Wang et al. synthesized the new (Tb) terbium-based MOFs namely UPC-11 or $[Tb_3(NO_3)(BPTA)_2(H_2O)_6]$*3Diox·8$H_2O$ (H_4BPTA: 1,1′-biphenyl]-2, 2′, 5, 5′-tetracarboxylic acid, Diox: = 1,4-dioxane) using tetracarboxylate as a ligand via solvothermal reaction for detection of nitroaromatic compounds. In this study, UPC-11 shows quenching of emission because of the energy transfer from ligand to the electron-deficient molecules. In order, these MOFs augment the potential for the detection of analytes in presence of complex samples. In addition, the UPC-11 exhibited the solvent dependant photoluminescence properties. Finally, the addition of diverse types of interfering molecules in the prepared MOFs solution caused less effect on luminescence whereas the 4-nitrophenol addition shows the complete quenching that confirmed the selectivity of luminescent MOFs. It has been revealed that UPC-11 demonstrated the high sensitivity and selectivity towards the nitroaromatic compounds that may be because of electron transfer among BPTA ligand to nitrobenzene (electron-deficient) molecules. Therefore, in the future, the UPC-11 sensor provides a high potential for the detection of nitroaromatic compounds [163]. In 2014, Dou et al. reported a luminescent MOFs film that offers speedy and reversible detection of oxygen. Briefly, porous MIL-100(In) ⊃ Tb^{3+} and CPM-5 ⊃ Tb^3 MOFs have been prepared using an indium organic framework (Pore size: 4.89 Å). It has been mentioned that the CPM-5 containing every single carboxylate acid of the H_3BTC ligand can be deprotonated. In addition, $(CH_3)_2NH^{2+}$ provided as the variable charge-balancing cation in pores. In the case of MIL-100(In) ⊃ Tb^{3+}, the additional trimesic acid shows a strong interaction with the In_3O trimer by way of the CO – In monodentate coordination. It serves as one of the terminal molecules of the In_3O trimer for MIL-100(In). Besides, the deactivation of the triplet state organic ligand by oxygen demonstrates the oxygen quenching as well as offers some interaction with the excited state of lanthanide atoms. MIL-100(In) ⊃ Tb^{3+} illustrated more energy transfer efficiency as compared to CPM-5 ⊃ Tb^{3+}, and therefore MIL-100(In) ⊃ Tb^{3+} provide high luminescent properties. It has been reported that intra-molecular energy transfer luminescent Ln-centered MOFs demonstrate higher oxygen sensitivities as compared to the MOFs with intermolecular energy transfer. Consequently, prepared MOFs showed great potential to the oxygen sensitivity (Ksv = 7.59) as well as short response or recovery time (6 s/53 s). It will lead the way as an enhanced sensory material for sensing various sorts of chemical moieties in the sensing field [164].

The luminescence-based MOFs namely Zn_2(TCPPE) {TCPPE: tetrakis[4-[4-carboxyphenyl]phenyl]ethene} has been used for the revealing of volatile organic compounds.

Interestingly, tetraphenylethene (TPE) is a fascinating chromophore that shows aggregation-induced emission (AIE). It has been reported as a building block for designing fluorescence sensors. Moreover, it can be decorated with different functional/coordination groups, such as carboxylates/aromatic carboxylates. It offers stiff organic ligands in the arrangement of luminous MOFs. In addition, the selection of TCPPE can form coordinate bonds with single metal ions that furnish the 1D secondary building units (metal carboxylate chain). The vibrations and rotations of phenyl rings from $TCPPE^{4-}$ have been limited in the rigid framework. It has been reported that the tetra-phenyl-ethene-based MOFs

contain small pore size (BET surface area: 1248m^2/g) and low dimensional (Pore dimension: 11.4×9.8 $Å^2$) channels that could saturate the analytes efficiently in the core. It increased the interaction ability among analytes and MOFs and thus, it boost the sensing ability of MOFs towards the analytes. The vapors of nitrobenzene and DNT showed the quenching of luminescence of MOFs. Overall, the MOFs sensor provided strong fluorescence and offered gas adsorption along with towering sensitivity to the volatile organic compounds. Hence, the use of TCPPE as a ligand for the construction of Zn_2(TCPPE) releases an excellent alternative with improved sensor performance, such as high sensitivity, rapid detection, etc. [165]. In 2018, highly luminescent Zn-based porous (BET surface area: 4073.9 m^2/g, Pore size: 7 Å) MOFs (ZnPO-MOFs) have been designed for the detection of pesticides residue (parathion-methyl). Shortly, ZnPO-MOFs have been synthesized using H_4TCPB as a linker via the hydrothermal method. This sensor provides a very wide linear detection range from 1 µg/L to 10 mg/kg and low limit of detection 0.12 µg/kg (0.456 nM) for parathion-methyl. In this study, they proposed the fluorescence quenching mechanism due to the existence of nitroaromatic groups. Herein, the fluorescence of MOFs has been quenched after the addition of parathion-methyl which may be because of an electron-rich group that existed in nitroaromatics. It leads to the transfer of photoinduced electrons. The real-time analysis in irrigation water has been achieved that confirmed the applicability of developed sensory material for sensing diverse kinds of pesticide in water sources, food materials, etc. Finally, it exhibited good selectivity in presence of different organophosphorus pesticides. Therefore, owing to the high selectivity and sensitivity, it would be an excellent example of luminescent MOFs for the identification of pesticides by fluorescent quenching [166]. Liu et al., developed the 3D Cd(II)-MOFs or [$Cd_3(L)_2$(bipy)$(H_2O)_2$]·H_2O, [H_3L: 9-[4-carboxy-phenyl]-9*H*-carbazole-3,6-dicarboxylic acid, bipy: 4,4′-bipyridine] using H_3L and $Cd(NO_3)_2$ via the solvothermal process (Fig. 12A, B). After that, it has been used for the detection of uranyl ions wherein the resonance energy transfer from MOFs to uranyl ions causes fluorescence quenching. Notably, the fluorescence intensity of Cd(II)-MOFs has been declined by uranyl ions

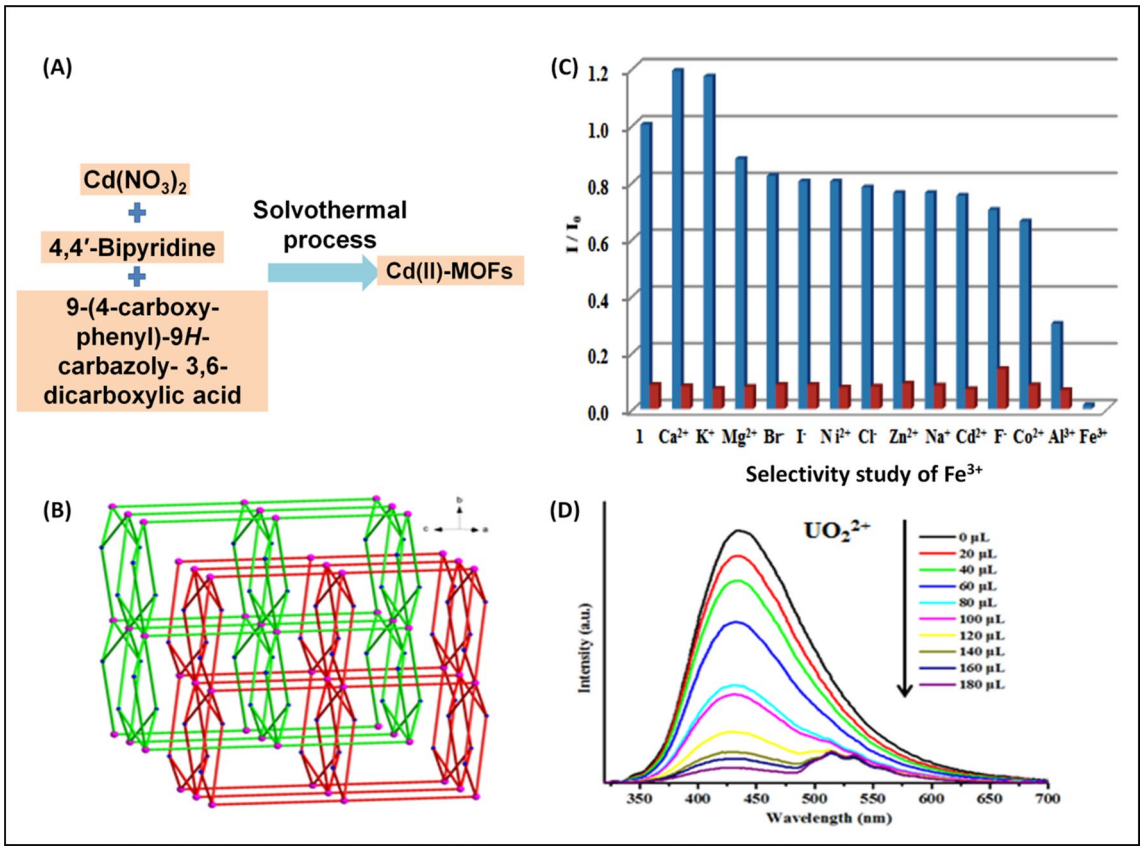

Fig. 12 **A** Synthesis of Cd(II)–MOFs. **B** 3D topology of Cd(II)–MOFs. **C** Selectivity of Cd(II)–MOFs for uranyl ions in presence of interfering substances. Blue color columns indicate the combination of Cd(II)–MOFs and ions and red color columns indicate the combination of Cd(II)–MOFs, ions, and uranyl ions. **D** Emission spectra of Cd(II)–MOFs upon the addition of UO_2^{2+} ions. [Reprinted with permission from reference [167]. Copyright © 2019 Elsevier.]

wherein quenching efficiency of 96%. Interference study of the prepared sensor has been accomplished using different ion that shows the high selectivity towards the uranyl ions (Fig. 12C, D). It demonstrates good recyclability that confirmed the applicability of the sensor 4 times. In a nutshell, in the future, it will open a new vista for sensing uranyl ions in environmental samples [167].

In 2019, Guo reported the detection of $Cr_2O_7^{-2}$ and picric acid using Mn-MOFs. In brief, $Mn_2(HBTC)_2(TIAB)]n$ MOFs has been synthesized using 1,2,4,5-tetrakis[1-imidazolyl] benzene (TIAB), H_3BTC, and Mn(II) via heating. Herein, it furnished the different coordinated atoms, multiform coordination nodes, and rigid framework that are helpful for the synthesis of MOFs. Moreover, these two ligands give the luminescent properties for MOFs sensors that get quench in presence of interest analyte. Interestingly, it provides the LOD of 1.25×10^{-5} mol/L for $Cr_2O_7^{-2}$ whereas 3.08×10^{-5} mol/L for picric acid. Finally, it shows the good recycling performance (up to 4 cycles) that may be due to the excellent structural stability of MOFs. In this investigation, the theoretical sensing mechanism includes the resonance energy transfer, photoinduced electron transfer, electrostatic interaction, etc. Herein, the selected analyte shows the high ability to accept an electron from MOFs that may be because of the electron-deficient group on the surface of the analyte. Moreover, the overlapping between the absorption spectrum of analyte and MOFs emission spectrum resulted in the resonance energy transfer. It has been claimed that non-radioactive energy transfer from luminescent MOFs to an analyte is shown the quenching of fluorescent intensity. Due to these synergistic responses, it shows the high sensitivity and selectivity to interest analyte. In summary, luminescent MOFs can open a new arena for the recognition of analytes, In addition, it can be used as a bifunctional luminescent sensor for detection of $Cr_2O_7^{2-}$ and nitroaromatic compounds [168]. A recently published study reported the $Cr_2O_7^{2-}$ detection through Pb^{II}-MOFs, $\{Pb\ (AIA)_2\}_n$. In short, Pb^{II}-MOFs have been assembled by the assembly of rigid linkers namely 5-aminonicotinic acid (HAIA) and Pb (II) via a hydrothermal condition. It provides the Lewis basic sites and luminescent property in the structure and because of this prepared MOFs could be used as Lewis basic catalysts. These uncoordinated pyridine nitrogen atoms and $–NH_2$ (Lewis basic) in the structure offer the sensing ability to MOFs. It exhibited a good catalytic effect as well as recyclability. Also, it worked as a luminescent sensor for detection of $Cr_2O_7^{2-}$ in presence of a diverse type of ions that confirmed the excellent selectivity of the sensor. Herein, UV–Vis absorption spectra of $Cr_2O_7^{2-}$ demonstrate the overlapping effect. Therefore, the excitation energy can be competitive among the analyte and designed MOFs. Finally, Pb^{II}-MOFs-mediated sensor provides the detection limit of 1.03×10^{-5} mol/L with a good linear relationship ($R^2 = 0.9945$). Additionally, it demonstrates the recyclability of up to 4 cycles that assured the structural stability of the MOFs. As a result, this sensor could be seen as an ideal replacement for sensing various ions in real-time samples [169].

In 2019, He and co-authors reported the recognition of TNT, picric acid, and tetryl using the Eu-MOFs, or $[(CH_3)_2NH_2]$ $[Eu_3(\mu_3\text{-}OH)\ (1,4\text{-}BDC)_3(HCOO)_3]$ as a luminescent sensor. In brief, Eu-MOFs have been synthesized using 1,4-BDC and 'Eu' metal ions. Herein, TNT, picric acid, and tetryl in luminescent MOFs demonstrate the fluorescence intensity near zero. The fluorescent response mechanism has been assured using UV absorption spectral analysis. Herein, the overlap between acetone UV absorption band and MOFs excitation wavelength offers the notable quenching of fluorescence in presence of organic molecules. As a result, it shows the significant quenching effects on the MOFs containing fluorescence intensities that offer high sensitivity and selectivity. It provides the low detection limit for picric acid, TNT, and tetryl from 20 to 140 µg/mL. In addition, the test strip of Eu-MOFs resulted in the quenching of fluorescence in presence of TNT concentration. As a result, in the forthcoming days, it may be the most practical way for sensing various chemical residues in presented samples [170]. As we know, Zr is an outstanding material widely preferred for abundant applications, such as sensing development, biomedical applications, etc. [171]. In this line, Ye et al. developed the new Zr-MOFs using UiO-66 (Pt-TCPP/H_4TCPE@UiO-66) for sensing of NO using platinum meso-tetra[4-carboxyphenyl]porphyrin (Pt-TCPP) and 1,1,2,2-Tetra[4-carboxy phenyl]ethylene (H_4TCPE) and BDC as a co-linkers (Fig. 13). It has been mentioned that the addition of luminescence molecules in MOFs furnishes the improved surface area as well as larger pore size. Interestingly, Pt-TCPP plays the role of signal reported in the existence of NO whereas H_4TCPE acts as a luminescence reference that helps to design the ratiometric sensor. As result, it provides the lowest detection limit of 0.1420 µg/mL for NO. The sensing mechanism has been confirmed using time-resolved emission decay where it shows the static quenching of fluorescence intensity of luminescent MOFs. Moreover, it exhibited good biocompatibility thus it offered the new potential for NO detection in living cells. The Pt-TCPP/H_4TCPE@UiO-66 nanoparticles (NPs) produced had an excellent sensing property toward NO, with an ultrahigh linear correlation of the Stern–Volmer equation. Additionally, it gives a rapid response as short as 2 min. Furthermore, the developed sensor could operate in a wide pH range (7.4, 5.6, and 0). As a result, in the approaching days, Pt-TCPP/H_4TCPE@UiO-66 as a sensory nanomaterial may be a commendable option for clinical NO sensing. [172].

It is crystal clear that MOFs have recently released a new domain for the identification of new chemical moieties,

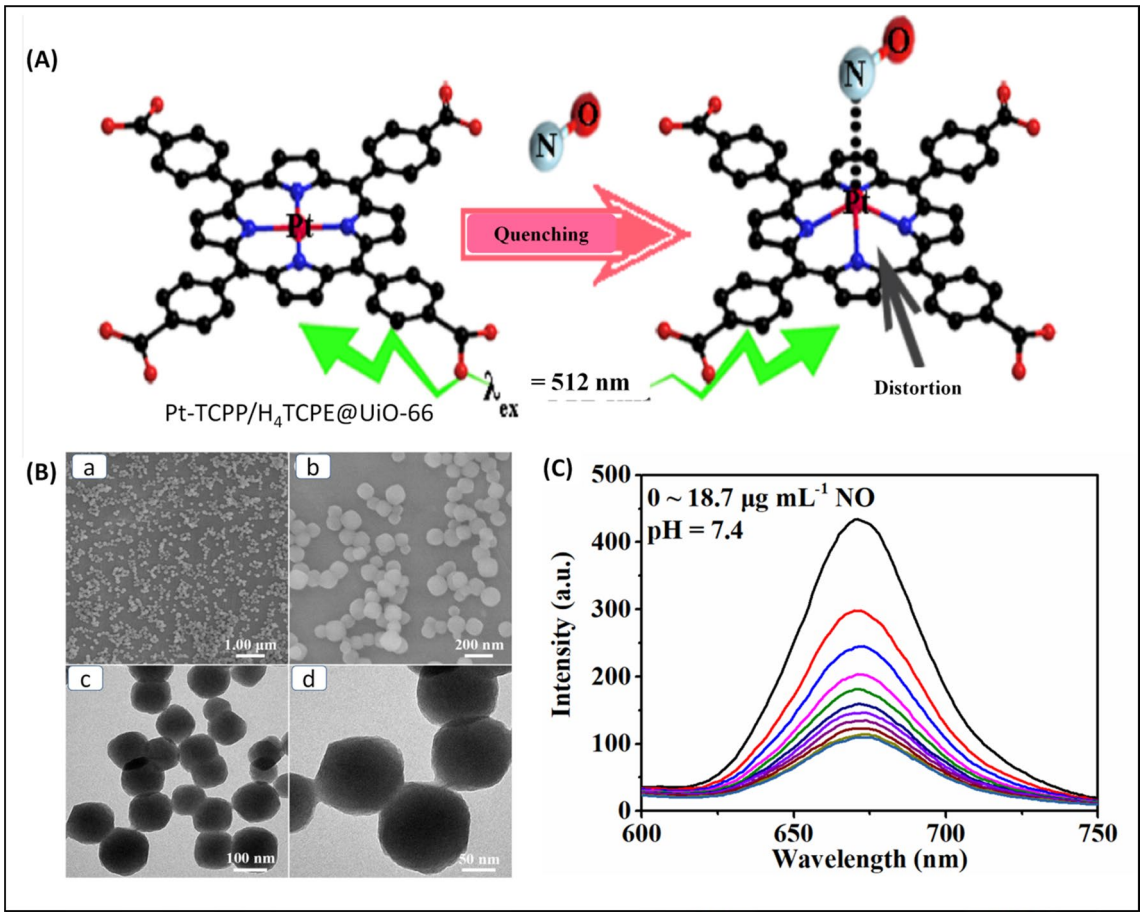

Fig. 13 **A** Presentation of quenching process of Pt-TCPP in presence of NO (donor). **B** Field emission scanning electron microscopic images (a, b) and transmission electron microscopic images (c, d) of Pt-TCPP. **C** The luminescence spectra of the Pt-TCPP as a function of NO concentration from 0 to 18.7 μg/mL(pH = 7.4). [Reprinted with permission from reference [172]. Copyright © 2019 Elsevier.]

antibiotics, and so on. Li and prepared the luminescent mixed matrix membranes (MMMs)-based sensors for detection of antibiotics. Herein, MMMs have been engineered using $\{Eu^2(TDC)_3(CH_3OH)_2 \cdot (CH_3OH)\}n$ (Eu-TDC), (TDC: thiophene-2,5-dicarboxylate) as filler, and 502 glue of the Evo-bond brand (EVOB). Due to the inner filter effect, the fluorescence quenching of the Eu-TDC-MMMs has been observed in the existence of nitroimidazole. Mainly, inner filter effect-based decrease in luminescence intensity has been observed due to the absorption of the excitations and emission of lights of the preferred fluorescent in the sensing method. Moreover, it shows good fluorescence stability that can be more useful for sensing the target analyte. In addition, it exhibited a low detection limit of 0.58 μg/mL and 0.51 μg/mL for metronidazole and dimetridazole, respectively. The real-time analysis confirmed the applicability of the sensor for the recognition of interest analytes in complex samples. Taken as a whole, the potential of the prepared sensor can furnish a new substitute for sensing nitroimidazole [173]. In another study, Zr-MOFs (PCN-128Y) have been reported for sensing tetracycline antibiotics in water. Initially, PCN-128Y has been synthesized using Zr and 4,4′,4″,4‴-(ethene-1,1,2,2-tetrayl) tetrakis ([1,1′-biphenyl]-4-carboxylic acid) (H_4ETTC). Herein, Zr-MOFs play two major parts namely sensing and removal of antibiotics from samples. Herein, the luminescence quenching in presence of tetracycline provides the detection ability whereas the strong metal–ligand bonding resulted in good adsorption ability. The fluorescence turn On–Off sensing mechanism has been observed in presence of tetracycline. Moreover, the theoretical sensing response mechanism involved in sensing of interest analyte was photoinduced electron transfer from ligand to the analyte. Also, the strong absorption of the analyte at the excitation wavelength was responsible for the sensing of tetracycline. In conclusion, such MOFs-mediated dual approaches are useful removal of tetracycline from water and environments. Hence, the current work demonstrates the potential for luminous MOFs materials to be used in the identification of antibiotic contaminations in water. [174]. In 2021 Chen et al. developed a boric acid-modified carbon

quantum dots (B-CQDs)-mediated Tb-MOFs (MOFs-76)-based ratiometric fluorescence sensor for highly sensitive recognition of 2,6-pyridinedicarboxylic acid (DPA). In brief, MOFs-76 has been synthesized using H_3BTC as ligand and Terbium(III) nitrate pentahydrate via the solvo-thermal method. This prepared smooth rod-shaped MOFs fixed with B-CQDs that can be destroyed after the addition of interest analyte. The sensing of DPA exhibited the high selectivity in the existence of other interfering substances that assured the potential of prepared ratiometric fluorescence sensor as compared to the bare fluorescence sensor. It provides the lowest detection limit up to 3.05 µM that may be because of different sensing mechanisms. In brief, the addition of DPA shows the enhancement of MOFs-76 fluorescence that may be because of energy transfer from analyte to MOFs. In this step, the DPA functional groups mainly carboxylate containing oxygen and an aromatic ring containing nitrogen forms the strong coordinate bonding with metal ions of the MOFs. Accordingly, it resulted in energy transfer from analyte to metal ions. In the case of sensing analyte using B-CQDs offers the inner filter effect that gives the quenching of fluorescence. Interestingly, the cross-linked B-CQDs-MOFs-76 demonstrated the quenching of fluorescent of MOFs-76 after the addition of B-CQDs and the fluorescence of B-CQDs remained unchanged. Finally, the incorporation of analyte provides the strong coordination effect with metal ions that resulted in the destruction of MOFs and accordingly recovery of quenched fluorescence. Therefore, in the future, this ratiometric sensor can be an excellent option for sensing DPA with towering sensitivity and selectivity [175]. The sensing of metronidazole has been accomplished using $[Eu_2(dtztp)(OH)_2(DMF)(H_2O)2.5]$ $2H_2O$ wherein H_4dtztp is used as ligand and europium(III) nitrate hydrate through the solvothermal method. This prepared sensing provides the lowest detection limit up to 18.3 ppm. Herein, the addition of metronidazole in prepared sensory materials shows the quenching of fluorescence of MOFs that may be because of framework collapse and adsorption of guest molecules. In brief, photoinduced electron transfer is the possible theoretical mechanism involved in sensing of analyte wherein electron transfer from MOFs conduction band to analytes lowest unoccupied molecular orbital. That resulted in quenching of fluorescence. The real-time analysis of antibiotics in calf serum shows the low concentration range from 0 to 0.008 mM that confirmed the applicability of the sensor for practical sensing. The presence of diverse types of interfering substances with an analyte in MOFs sensor confirmed the high selectivity of MOFs material towards the metronidazole. For upcoming days, this sensor will unlock a new era for pharmaceutical as well as other fields for sensing of concentration of antibiotics in provided samples [176]. In a nutshell, the different types of nanoarchitecture luminescent MOFs have been reported for sensing of chemical moieties including gas, solvent, explosives, antibiotics, etc. Different luminescence sensing response mechanisms are overlapping effects, a ligand-to-metal charge transfer, metal-to-ligand charge transfer, energy transfer, redox interaction, static effect, etc. It provides the lowest detection limit up to nM/ng with a wide linearity range. In addition, MOFs were reported to demonstrate the excellent stability and ability of reuse for several applications. In presence of several interfering substances, designed nano-MOFs offer high selectivity towards the chemical residue. Due to the post-synthetic modifications, MOFs boosted the sensitivity to an analyte. In the future, luminescent MOFs will pave the way for sensing and monitoring of the level of chemicals in real times samples, such as water, food materials, air, soil, etc.

Structural design of MOFs-based luminescent sensor for metal ion sensing

Regular exposure to metal ions is a very well worldwide problem with negative consequences for human health. Tiny dosages of metal ions can pose a multitude of ailments, including cancer, and sometimes even mortality. Hence, there is a need to supervise the level of metal ions in water, food, etc. Also, metal ion sensing is an essential aspect of biological systems. In this case, the detection of metal ions will offer evidence about disease or disorders that may be useful in the treatment of the corresponding disease. Moreover, it is most essential in environmental monitoring. In recently published work, lewis basic pyridyl sites for the precise sensing of metal ions have been reported by Chen. Herein, europium (Eu)-based MOFs namely $[Eu(pdc)_{1.5}(dmf)]\cdot(DMF)_{0.5}(H_2O)_{0.5}\}$, (pdc: pyridine-3,5-dicarboxylate) as a luminescent sensor has been designed via a solvothermal route. It contains Eu-free sites engaged with carboxylate ions that assist stabilization of MOFs. Moreover, because of its one-dimensional (1D) channels, the prepared sensor recognized the new guest analytes or molecules. Additionally, due to the occurrence of free Lewis basic pyridyl sites within the pores, it enhanced the recognition competence towards the metal ions, and an acidic molecule along with that it furnishes the enhanced sensing function of MOFs. In addition, porous MOFs-based Lewis basic sites are expected to participate the foremost role in the recognition of small Lewis acidic molecules as well as metal ions. In the future, the surface modulated functionality of nanosized MOFs can open new-fangled sites for the recognition of real-time samples containing metal ions and chemicals [33]. In another study, Eu-MOFs [Eu(BTB)(phen)0.4.5 DMF*$2H_2O$]n has been synthesized using 1,3,5-benzene-tri benzoate (H_3BTB) that provides high thermal stability and maximum pore volume (56.1%). During sensing of Al^{3+}, preferred ligands absorb the energy from the UV spectrum and then transfer that energy to metal ions (Eu^{3+}). It offers the luminescence

spectrum to prepared MOFs. Unfortunately, Al^{3+} demonstrates minimal photon absorption at the excitation wavelength (300 nm). Therefore, there was no significant cause on the ligand absorption of energy. In this case, the collision interaction among analyte and prepared MOFs might be responsible for sensing wherein it consumes the energy and then reduces the energy transfer from ligand to the metal ion that gives quenching the fluorescence. These MOFs have been provided the highly sensitive detection (Fig. 14A) than other reported luminescent detection of Al^{3+} along with 1.35 ppb as the detection limit. Herein, the collapse of the Eu-MOFs is the probable reason behind the quenching of emission. In addition, collision among ions and MOFs resulted in energy consumption and finally a decline in sensor intensity. Moreover, it demonstrates good recyclability and owing to this, it can be used for several sample analyses also. The anti-interference study confirmed the selectivity towards the Al^{3+} ions in the occurrence of plenty of cationic ions (Fig. 14B). In the future, [Eu(BTB)(phen.4.5 DMF*2H_2O]n might be employed for Al^{3+} sensing in given samples [177].

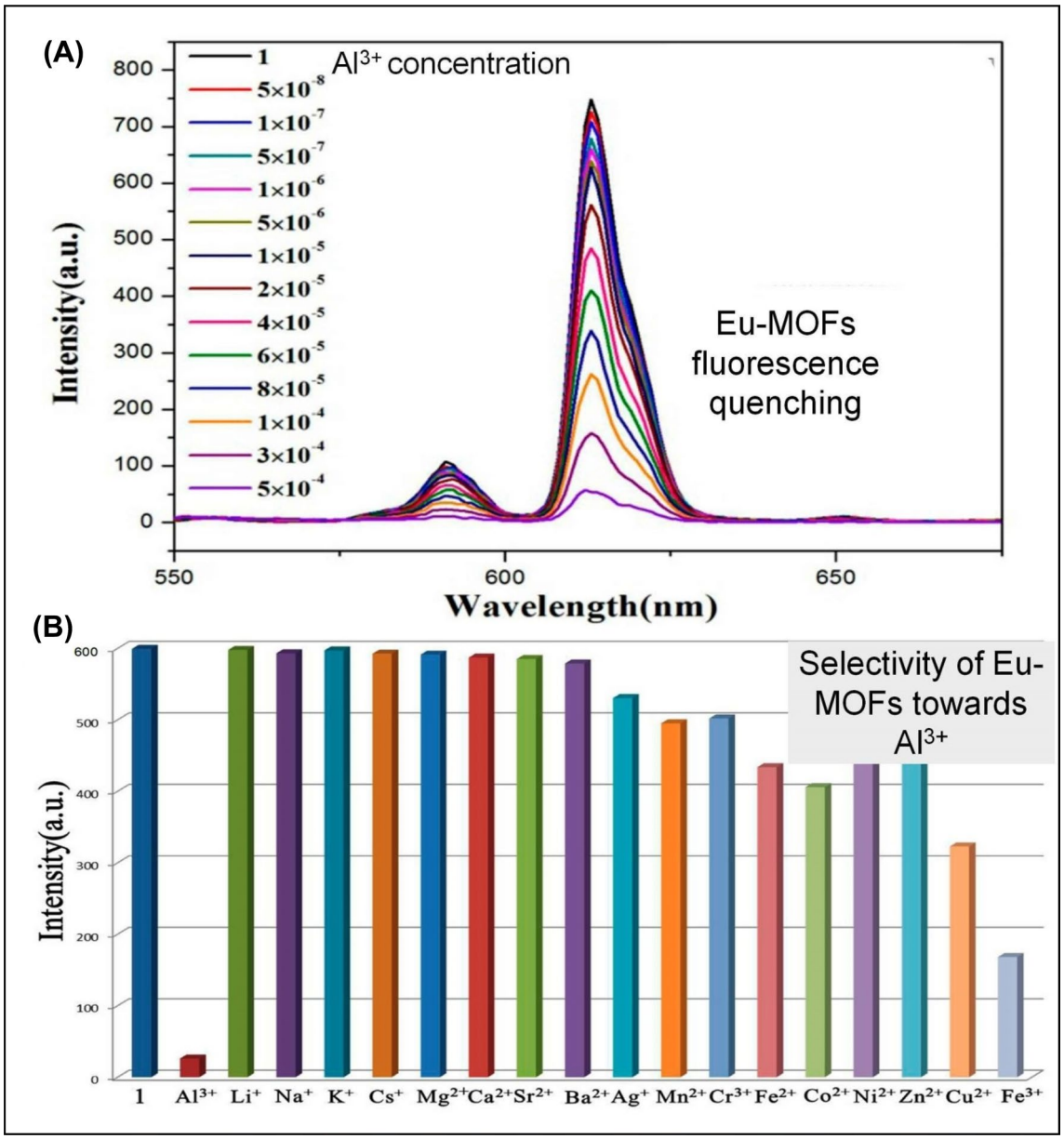

Fig. 14 **A** Presentation of MOFs emission spectra in presence of different concentrations (1 -5*10^{-4}) of Fe^{3+} ions. **B** Presentation of luminescence intensity of MOFs in the presence of different interfering substances (5×10^{-4} M) and Al^{3+} shows the selectivity of prepared sensor [Reprinted with permission from ref [177]. Copyright © 2016, American Chemical Society]

Identifying Fe^{3+} in an aquatic system with excellent sensitivity and high selectivity is critical considering iron is a necessary and pivotal mineral in both the ecosystem and biology. Sun and co-authors developed the double-paned extended 2D network-based Tb-MOFs namely [Tb(Hbtca)$(H_2O)_2$]*H_2O (Tb-MOFs–COOH) using uncoordinated 1,10-biphenyl-2,3,30,50-tetracarboxylic acid (H_4btca) as a ligand. The carboxyl group notes to the inside pore of the MOFs, which generates a luminescent-based MOFs sensor. Furthermore, it offers selectivity and specificity towards the metal ions (Fe^{3+}). When the concentration of Fe^{3+} reached 0.01 mol/L, the luminescence intensities of the Tb-MOFs–COOH get completely quenched. In addition, a strong linear relationship ($R^2 = 0.994$) has been found between luminescence intensity and Fe^{3+} concentration range of 10–1000 mmol/L. Finally, it shows the high selectivity in presence of different cationic metal ions. In this case, the analyte and carboxylate ligands competed for excitation wavelength absorption that resulted in the reduction in excitation energy transfer from Tb^{3+} ions to a ligand. Owing to this, it shows high sensitivity and selectivity to an analyte in presence of interfering agents. Additionally, the small overlapping among Fe^{3+} absorption spectrum and emission band of MOFs also offers the quenching fluorescence intensity of Tb-MOFs–COOH. As a result, Tb-MOFs–COOH would be a potential framework for sensing metal ions in biological systems and environments [178]. In another work, fast response and highly sensitive MOFs nanosheets have been investigated for luminescent sensing of Fe^{3+}. In that, the MOFs (NTU-9-NS) have been synthesized by a solvothermal method using Ti_2(HDOBDC)$_2$ (H_2DOBDC) (H_2DOBDC: 2,5-dihydroxyterephthalic acid), which proposed the high sensitivity for Fe^{3+}. It showed a low detection limit of 0.45 µM. Herein, plenty of accessible active site in MOFs provides high sensitivity and selectivity towards the Fe^{3+}. Fascinatingly, the luminescent quenching effect has been occurred due to the electronic interaction between Fe^{3+} and DOBDC moieties. Moreover, notable competition among absorption of the light source energy may be the responsible sensing mechanism of luminescent MOFs. Principally, the presence of The Fe^{3+} ions shows the ability of filtration of the light adsorbed by ligand followed by quenching of luminescence of NTU-9-NS. In conclusion, NTU-9-NS luminescent sensor offers the high sensitivity and high selectivity that could endow the base for designing and analysis of biological as well as environmental for Fe^{3+} [75].

In another study, Li et al. Fe^{3+} sensing has been reported using luminescent Cd (II)-MOFs-based chemosensor namely {[Cd(L)(2-NTP)]0.25H_2O)}n or t Cd(II)-MOFs. Briefly, bis(benzimidazole) and aromatic dicarboxylate have been used as ligands for the development of chemo-sensors. It has been nanostructured MOFs based on d^{10} metal ions offer superb luminescent properties and that can be preferred for sensory applications. In this study, the ligand exhibited the emission band that because of intra-ligand transition mainly π–*π /π*–n. The prepared MOFs endow with high thermal stability and high sensitivity towards the Fe^{3+}. Also, the ligand-to-metal charge transfer among ligand containing delocalized π bonds and metal ions (Cd^{2+}). It has been suggested that the quenching of luminescence property of MOFs can occur wherein metal ions mantled absorption bands that resulted in the drastic decline. It offered the 3.54 µM detection limits as well as it showed the promising luminescent probes for selective detection of Fe^{3+} ions in the existence of different metal ions. Also, it exhibited good luminescent stability up to 5 cycles that confirmed the reusability of MOFs-mediated luminescent sensor. Taken as a whole, Cd(II)-MOFs can be used as capable luminescent nano-probes for selectively sensing Fe^{3+} in real-time samples [179]. In another work, Fe^{3+} sensing has been achieved using luminescent $[Zr_6o_4(OH)_4][C_{14}H_8O_4]_{5.82}[EuW_{10}O_{36}]_{0.04}\cdot 7H_2O$ (EuW_{10}@UiO-67). In brief, $[EuW_{10}O_{36}]^{9-}$ has been incorporated into the Zr-MOFs(UiO-67) using the direct synthesis method. Importantly, the existence of diverse metal ions resulted in a decrease in luminescent intensity of the metal ions (Eu^{3+}) as compared to the bare MOFs. It shows the strong quenching effect in presence of Fe^{3+} wherein quenching of emission of MOFs was found due to the conversion of non-emissive in the existence of UV light. The LOD was found to be 37 µM. Moreover, it demonstrates the good linear correlation (R^2:0.999) and recyclability. Future point of view, Zr-MOFs(UiO-67) can be utilized as a luminescent sensor for sensing metal ions in biological fluids as well as water samples [180]. In 2018, Zheng et al. synthesized the Ln-MOFs series (Ln: Eu^{3+}) via hydrothermal method using 1,3-adamantanediacetic acid (H_2ADA) as a ligand and 1,10-phenanthroline (phen). It exhibited high thermal stability, high quantum yield, high sensitivity, and selectivity. It shows the quenching effect (fluorescence turn-off) on the luminescence property of MOFs after the addition of Ni^{2+}. It has been reported that the chemosensor exhibited the luminescence "turn-on" for valine by introducing the ligand of 1,3-adamantane acetic acid (H_2ADA). Principally, the luminescence of lanthanide-based MOFs shows the antenna effect that offers the luminescence property to the lanthanide complex. In presence of Ni^{2+}, the prepared Ln-MOFs demonstrate the quenching that may be because of ligand-to-metal charge transfer. Herein, the photon is absorbed by selected ligands, which coordinate the Ln^{3+}. Afterward, the absorbed energy transfer from H_2ADA to lanthanide ions. The LOD for Ni^{2+} sensing was found to be 1.0×10^{-9} M (5.9×10^{-5} mg/L) concludes the high sensitivity value as compared to the World Health Organization and Chinese environmental quality standard. Possibly, the ligand-to-metal charge transfer resulted in quenching of luminescence. It

gives the linear concentration range from 0.2 to 0.6 μM. Finally, it demonstrated the high selectivity in presence of amino acids and metal ions. Therefore, lanthanide-based nanostructured MOFs could be a more convenient method for the detection of Ni^{2+} in provided samples [140]. In 2018, the luminescent Tb-MOFs (TbTATB) for Zn^{2+} sensing and imaging has been designed solvothermal by Fan et al. The use of 4,4′-4″-s-triazine-2,4,6-triyl-tribenzoic acid (H_3TATB) offers plenty of merits for sensing of the target analyte. The use of the H_3TATB ligand shows the emission at 430 nm which may be because ligand molecules absorb the photons with appropriate energy. Herein, π–π* transition is responsible for luminescence wherein radiative transition from initial singlet state to ground singlet state occurs. Mainly, it exhibited the luminescent phenomenon that may be due to the energy transfer from ligand-to-metal ions (Tb^{3+}) (Fig. 15A). In this study, the luminescence of TbTATB has been enhanced after contact with Zn^{2+}. Moreover, Tb-MOFs exhibited high selectivity in presence of different metal ions and other interfering substances. As well, it presents a high sensitivity to target ions. Tb-MOFs furnish the lowest detection limit of 10.5 nM for Zn^{2+} in an aqueous solution. In addition, Tb-MOFs have shown good biocompatibility accordingly, bioimaging of Zn^{2+} was carried out

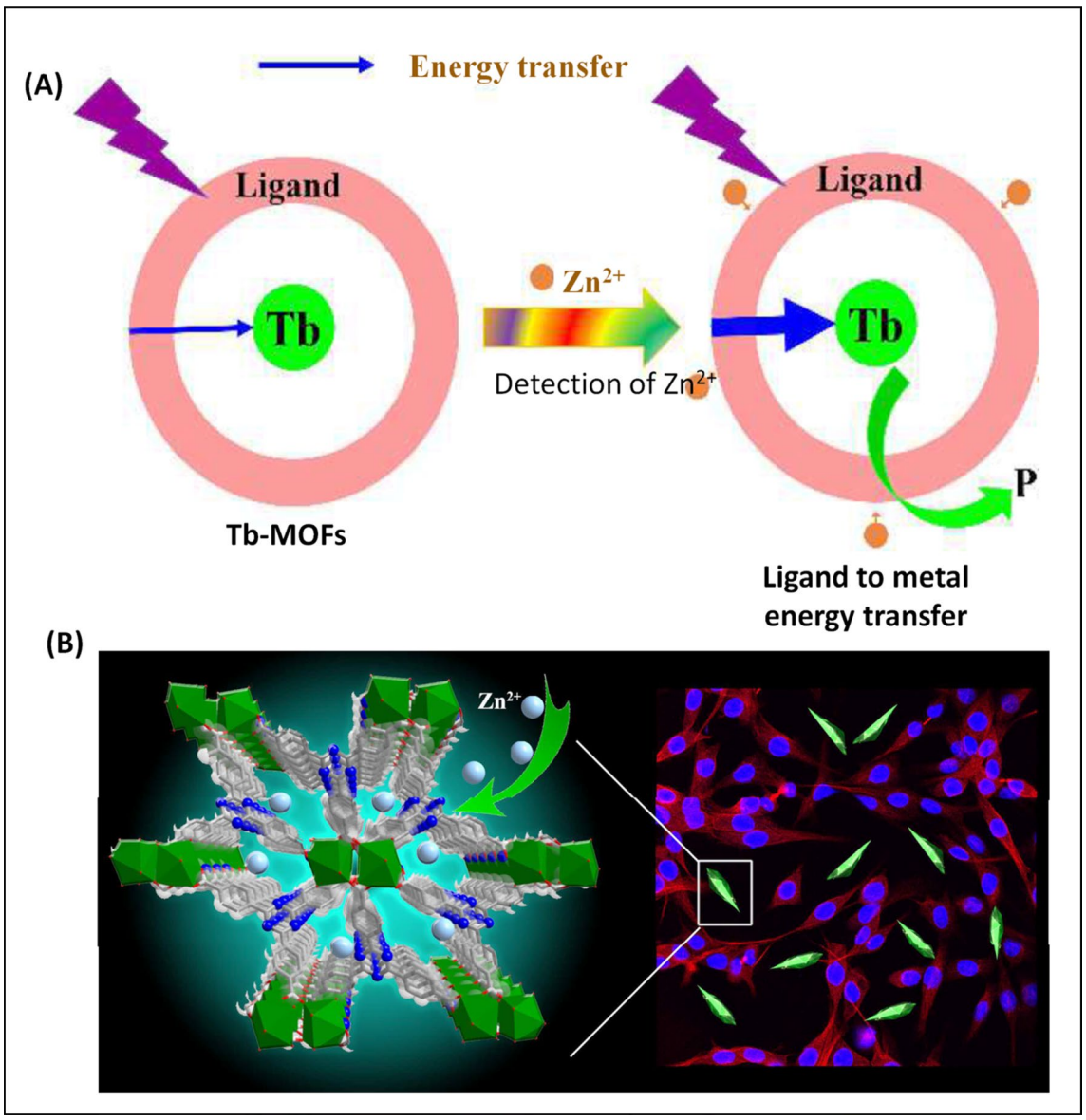

Fig. 15 **A** Scheme for ligand–metal energy transfer process for luminescence emission of Tb-MOFs and influence of Zn^{2+} on the ligand–metal energy transfer process. **B** Detection of Zn^{2+} ions in living cells using Tb-MOFs [Reprinted with permission from reference [76]. Copyright © 2018 Elsevier.]

in living cells (Fig. 15B). As a result, Tb-MOFs can offer the potential for the recognition of Zn^{2+} ions in living cells with high selectivity and sensitivity [76].

The copper ions detection in water has been performed using bonded-luminescent foam based on europium–polyurethane complexes (Eu-PUFs). Herein, Eu-PUFs have been formulated using a co-polycondensation reaction. It has been claimed that the Eu-PUFs exhibited high selectivity in presence of other metal ions in water. Eu-PUFs provide a low detection limit up to 0.28 µM. fascinatingly, the possible mechanism involved in quenching of fluorescence of sensor in presence of Cu^{2+}that may be because of a reduction in the energy transfer efficiency between ligands and Eu^{3+}. Furthermore, Eu-PUFs illustrate the high selectivity in the existence of different interference substances that is extremely important for biomedical applications as well as environmental applications. Owing to the high sensitivity in pure water, the prepared Eu-PUFs-mediated sensor could be an imperative strategy for sensing Cu^{2+} ions in biological and environmental science [181]. In 2021, Wang et al. reported novel luminescent Zn (II)-MOFs associated with twofold interpenetrating Zn(DHT)(BPP)n(GUPT-2) [GUPT: Guangdong University of Petrochemical Technology, H_2DHT: 2,5-dihydroxyterephthalic acid, and BPP:1,3-di[4-pyridyl] propane GUPT-2 for sensing of Fe^{3+} and Al^{3+}. Initially, the MOFs have been synthesized using a hydrothermal method using zinc nitrate hexahydrate as precursor and H_2DHT, BPP as a ligand. The use of their two ligands shows the boosted emissive properties due to their high aromaticity. Owing to the π–π* transition in the H_2DHT, it provides an emission peak similar to the GUPT-2. Accordingly, the prepared MOFs sensor shows good stability at the water and different pH from 3 to 11. The sensing of Fe^{3+} showed a decrease in fluorescence intensity whereas the addition of Al^{3+} improved the intensity of GUPT-2. It provides the detection limit for Fe^{3+} and Al^{3+} up to 0.446 µM and 0.269 µM, respectively. The powdered x-ray diffraction study confirmed that with the addition of Fe^{3+} there was no reaction among GUPT-2 and analyte. In this sensing, the quenching of fluorescence has been reported that may be because of competition among analyte absorption and GUPT-2 excitation. In the context of Al^{3+}, sensing has relied on intermolecular proton transfer. It has been suggested that the selected ligand (H_2DHT) forms the intramolecular hydrogen bonds that may be because of adjacent proton donor and acceptor groups. Afterward, the proton (hydroxyl group) transfer to the acceptor (carboxyl group) during the excited-state intramolecular proton transfer. Herein, the introduction of Al^{3+} ions destroyed these hydrogen bonding shows the stabilization of the proton transfer wherein the redox inertia of analyte resulted in suppression of fluorescence of MOFs. Finally, the presence of different cations in the solution confirmed the selectivity of the sensor towards both metal ions. Owing to its high sensitivity and high selectivity, the prepared MOFs-mediated nano-structured materials can be preferred for sensing Fe^{3+} and Al^{3+} in water samples [182]. In 2021, Thang and co-authors prepared 2D {[Cd(hsb-2)[2-obdc]]·$2H_2O$}n or HSB-W7 constructed using Cd(II) and ligands, namely di-carboxylate 2-obdc [2-hydroxybenzene-1,4-dicarboxylate] and hsb-2 (1,2-bis(4′-pyridylmethylamino)-ethane), which belongs to the category of hydrogenated Schiff base. In this study, different nano-MOFs, such as HSB-W7-Ns (Ns: nano-sheet), HSB-W7-Ns1, and HSB-W7-NR (Nanorods), have been synthesized using ultrasonic irradiation. Herein, the prepared mixed-ligand MOFs show the different shapes including rectangle (HSB-W7-Ns1) wherein the length and width were found to be near about 400 nm and 130 nm. Interestingly, the blue luminescence of nano-MOFs originated from the di-carboxylates ligands. In this work, the adsorption of the analyte has been finished due to the presence of phenolic hydroxyl groups and uncoordinated carboxylate oxygen of 2-obdc. Herein, the presence of different cations does not demonstrate the huge influence of the intensity of MOFs whereas the existence of Fe^{3+} ions shows the quenching of fluorescence intensity. Accordingly, it exhibited the linear concentration range from 0 to 40 µM. Additionally, HSB-W7-Ns, HSB-W7-Ns1, and HSB-W7-NR offer the lower detection limit of 0.21 µM, 0.36 µM, and 0.51 µM, respectively. Hence, the prepared MOFs exhibited towering sensitivity and selectivity towards the Fe^{3+} ions (Fig. 16a). It shows the concentration-dependent fluorescence quenching from 5 to 350 µM (Fig. 16b). The linearity range was reported from 5 to 40 µM ($R^2 = 0.98$, Fig. 16c) Herein, the nano-sized MOFs offer the boosted performance that may be because of the larger surface area and a huge number of active sites for interaction. Herein, the adsorptions of analyte on the surface of MOFs show the competitive absorption of energy from the light source, which resulted in the quenching of fluorescence intensity of MOFs. Moreover, the overlapping effect among the absorption range of MOFs and absorption band of analyte provides the quenching of HSB-W7-Ns fluorescent intensity. In conclusion, HSB-W7-Ns, HSB-W7-Ns1, and HSB-W7-NR offer a new epoch for sensing Fe^{3+} ions. In the future, nano-MOFs can be impending potential for sensing of the analyte with an elevated presentation in terms of precise selectivity [183].

Yu and co-authors developed the dual emitting lanthanide MOFs ($Eu_{0.07}Gd_{0.03}$-MOFs) using functionalized ligands namely 2,3,5,6-tetrafluoroterephthalic acid (H_2tfBDC), and 1,10-phenanthroline. Herein, europium III nitrate hexahydrate and gadolinium nitrate hexahydrate have been preferred as metal ions precursor wherein the prepared mixture was subjected for ultrasound treatment followed by hydrothermal process. Afterward, the prepared $Eu_{0.07}Gd_{0.03}$-MOFs have been employed for sensing of Fe^{3+} ions that provide the lowest detection limit up to 0.091 µM and linear

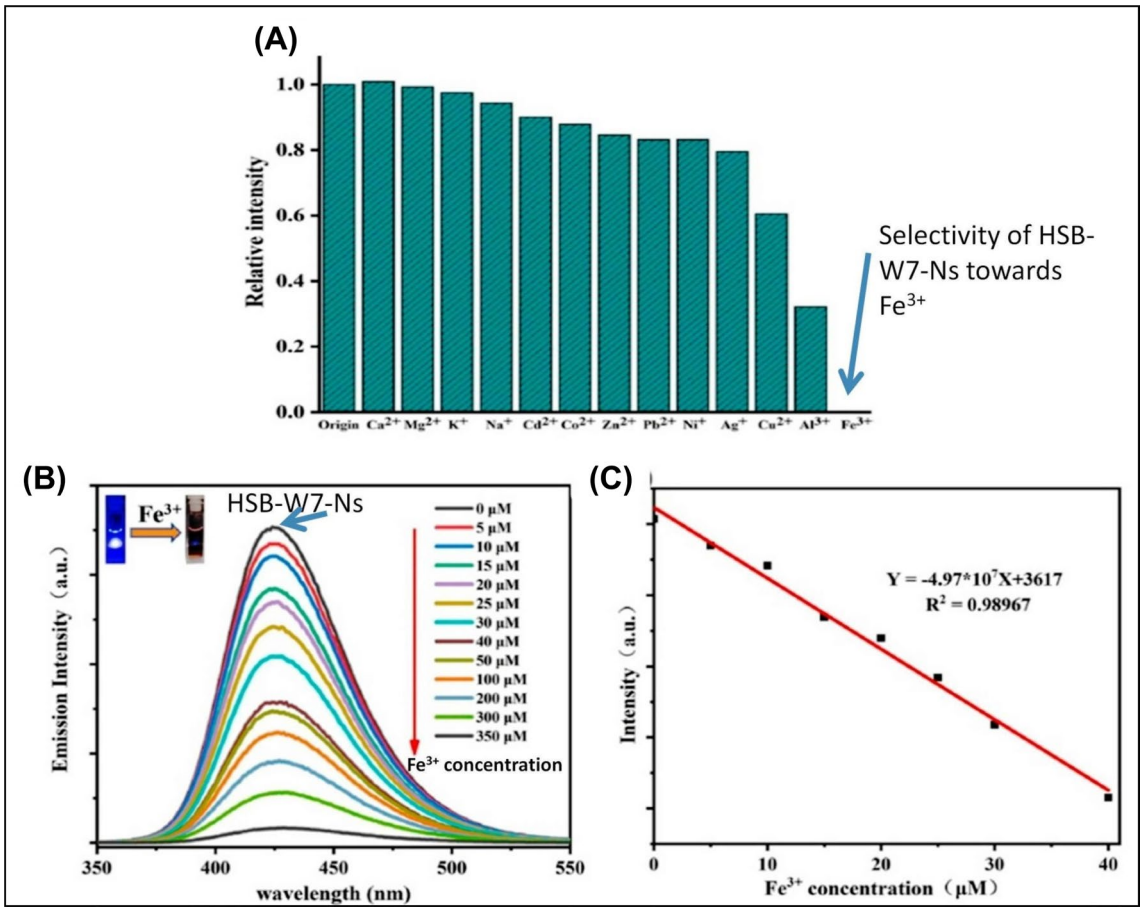

Fig. 16 **a** Selectivity of HSB-W7-Ns suspension in presence of metal. **b** Relative emission of HSB-W7-Ns in the presence of a different concentration of Fe^{3+}. **c** The fitting curve of the emission intensity of HSB-W7-Ns vs Fe^{3+}. [Reprinted with permission from [183]. Copyright © 2021, American Chemical Society]

concentration range from 0.0 to 60 µM. This radiometric $Eu_{0.07}Gd_{0.03}$-MOFs sensor yielded decreased luminescence that confirmed the quenching of fluorescent MOFs. It may be because of the dynamic quenching effect. Herein, overlapping effect between absorption band of analyte and ligands emission and due to this, the competition among analyte resulted in Eu^{3+}-mediated luminescence quenching. The addition of a plethora of cations into the sensory system does not affect the fluorescence of prepared materials that confirmed the high selectivity of $Eu_{0.07}Gd_{0.03}$-MOFs. Also, the recyclability of MOFs shows the application of single MOFs composite for number cycles. Taken as a whole, $Eu_{0.07}Gd_{0.03}$-MOFs can be used for sensing Fe^{3+} in provided samples [184]. In another study, the sensing of Fe^{3+} ions has been accomplished using poly-phenylene sulfide (PPS) paper-mediated Eu-MOFs sensor (Eu-MOFs@ALD-PPS). In this work, the ultrafine PPS fibers (2–6 µm) have been obtained using melt blowing whereas the Atomic layer deposition (ALD) has been used to depot the fibers membrane on the surface of titanium dioxide thin nanolayer that offers the rough surface as well as provides the number of coordinate bonding to the metal precursor (Eu). The Eu-MOFs have been engineered using europium nitrate hexahydrate as a precursor of metal ions and 2,5-dihydroxyterephthalic acid as a ligand through the solvothermal method (Fig. 17). In this method, the prepared PPDS-ALD mixed with MOFs mixture forms the dense layer Eu-MOFs@ALD-PPS. It has been revealed that the Eu-MOFs present strong hypersensitive transitions whereas Eu-MOFs@ALD-PPS demonstrated the red glow in UV (ultraviolet) light. The prepared paper-based MOFs sensory material exhibited the quenching response in presence of Fe^{3+} ions in presence of a variety of cations that may be because of the good porosity of prepared MOFs. This sensor offers the interactions between Lewis acid (Fe^{3+}) and carboxylic acid/hydroxyl group of ligands containing oxygen quenched the fluorescence of paper-centered sensory material. It shows the linear concentration range of 0–3 mM whereas the limit of detection was found to be $1*10^{-6}$ M. Therefore, this research suggests a potential way for fabricating a flexible detector for monitoring Fe^{3+},

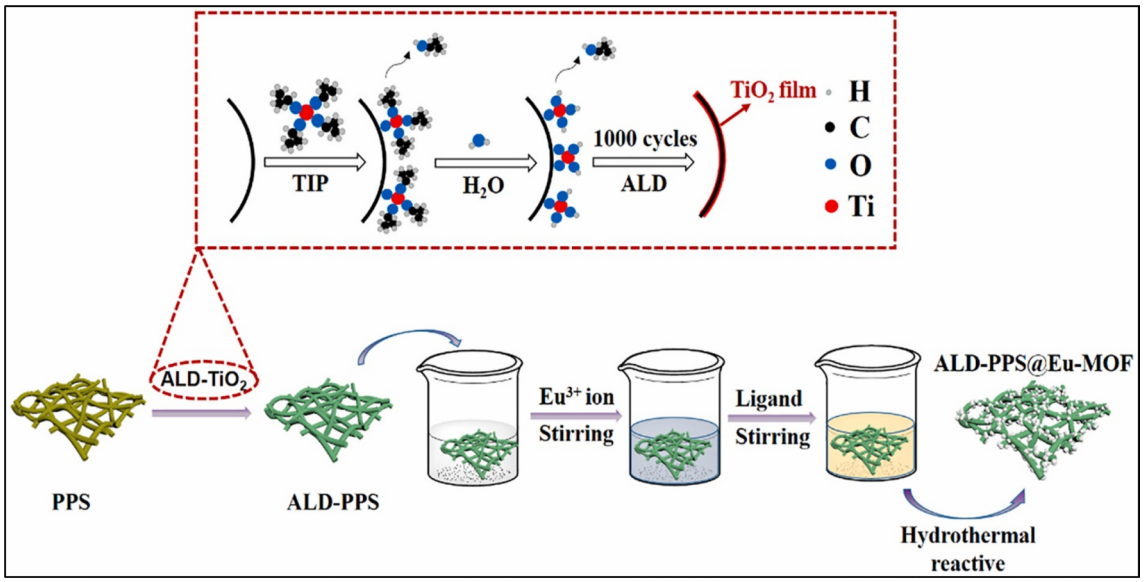

Fig. 17 Schematic presentation of synthesis of paper-based Eu-MOFs@ALD-PPS for sensing of Fe^{3+} ions. [Reprinted with permission from ref. [185]. Copyright © 2021 Elsevier B.V. All rights reserved.]

particularly in hostile environments. In the future, it will complete the demand for simplistic and reliable sensing of different ions in provided samples [185].

In 2021, Li and co-authors developed the nanocage-mediated nitrogen-rich nanosize luminescent MOFs (LCU103) for the recognition of toxic metals. Briefly, it has been designed as an interpenetrating nanostructure (N-rich{Zn6(dttz)4}) using an N-donor ligand namely 4,4′-dipyridylamine. Owing to the plenteous nitrogen functional sites in nanocage LCU103, it aids the interaction with interest metal ions. As a result, this prepared LCU103 luminescence sensory materials offers the lower detection limit of 1.45 and 1.66 µM for Fe^{3+} and Cu^{2+} ions, respectively based on luminescent quenching mechanism. Additionally, it furnishes the recycling stability, rapid luminescence quenching, and high selectivity in presence of different interfering substances. After that, the LCU103-based paper strip confirms real-time application for sensing both metal ions. The possible luminescence quenching mechanism includes the guest-induced quenching and cation-exchange quenching. This interaction could help transfer the energy that resulted in the alteration in luminescent intensity. In the upcoming days, LCU103 can be employed for sensing copper ions and Fe^{3+} in biological as well as environmental applications [186]. Metal–organic compounds with fluorescence "turn-on" detection of metal ions in aqueous are particularly attractive but have received little attention. In this line, Wang and colleagues prepared the binuclear MOFs namely Cu-HBIBA using Cu(I) ions and 4-[bis-[4-imidazol-1-ylphenyl]amino] benzoic acid (HBIBA) via autoclaving for sensing of Fe^{3+} (Fig. 18a) and Bi^{3+} (Fig. 18b) in water. Interestingly, HBIBA shows a strong broad peak due to the intra-ligand transitions. Herein, these prepared sensory materials exhibited good pH stability from a range of 2–12. Therefore, it can be preferred for sensing different pH for a wide range of applications. After the addition of selected trivalent analytes, it shows the enhancement in the luminescent intensity of Cu-HBIBA. It provides the lower detection limit of about 43 nM and 0.16 mM for Bi^{3+} and Fe^{3+}, respectively. The linear concentration for Fe^{3+} was found to be within the range of 0–50 µM ($R^2 = 0.99$, Fig. 18c) whereas 0 nM to 1000 nM for Bi^{3+} ($R^2 = 0.99$, Fig. 18d). Principally, after addition of analyte prepared sensor resulted in adsorption of cations (analyte) that restricts the photoinduced electron transfer process of the preferred ligand. Subsequently, it resulted in the recovery of luminescence. In the case of selectivity study, the addition of different metals ions changes the slight luminescence of sensory material that indicates the selectivity of Cu-HBIBA towards the metal ions (Fig. 18). Concisely, uncoordinated carboxylate group, good hydrolytic stability, reduced ligand-mediated luminescence boosted the final performance of the sensor, and owing to this it provides high sensitivity and selectivity towards the Bi^{3+} and Fe^{3+} in water. For futuristic application, it will release a new option for sensing trivalent metal ions in an aqueous system [187].

Taken as a whole, the application of luminescent MOFs for sensing diverse categories of chemicals and several metal ions can be identified in environmental samples and biological (Table 2). Herein, the stability, porosity, surface functionalities, compatibility among metal ions and ligands, etc., are playing a crucial part in sensor fabrication.

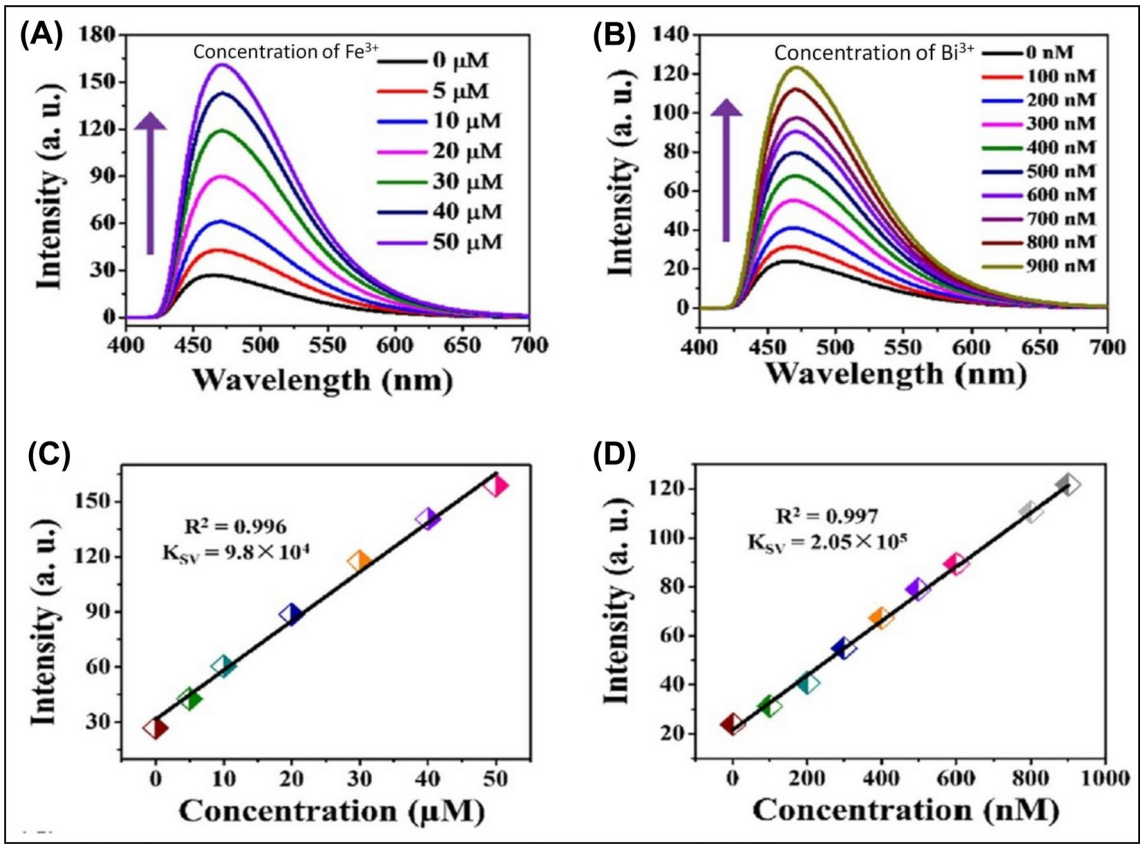

Fig. 18 Cu-HBIBA luminescence intensity spectra *vs* concentrations of selected trivalent ions namely **a** Fe^{3+} and **b** Bi^{3+}. Graphical presentation of linear relationships between the luminescence of sensor materials and different concentrations of **c** Fe^{3+} and **d** Bi^{3+}. [Reprinted with permission from ref [187]. Copyright © 2021 Elsevier.]

Current challenges and future prospects

Over the last decade, MOFs have been classed among the noteworthy kinds of materials for a plethora of analytical applications. To date, more than 20,000 types of MOFs have been reported for biomedical applications. It offers abundant inimitable properties mainly high porosity, versatile functionality, diverse composition, and structural topologies, modifiable pore size, and tunable surface area. Owing to this, it endows with high selectivity, high sensitivity, speedy detection, etc. In addition, it provides both qualitative as well as quantitative information of interest analytes, such as chemicals and metal ions. Using different varieties of MOFs-mediated luminescent sensors can present information on chemical moieties and metal ions. It provides the low detection limit of up to nanogram (ng) or nanomolar (nM), along it shows wide linear ranges. Despite this, there is still a necessary accomplishment of the lowest detection limit of femtogram (fg)/femtomolar (fM). For most of these solvent molecules, detection does not demonstrate the LOD that needs to be overcome using the modified design of MOFs. Linearity range is also with the range of μg/μM for several chemicals and metal ions that can be overcome using new types of MOFs. The dimensions of reported MOFs are crucial for sensing applications. In the future, the discussion of MOFs dimensions will help to design highly sensitive MOFs as well as aid to clear the sensing mechanism. As per described data, the different sensing mechanism is involved in the detection of target ions and chemical traces that includes mainly hydrogen bonding, electrostatic interaction, size exclusion, etc. In addition, the luminescent MOFs-based fluorescent turns "On–Off", and "Off–On" have been reported as a favorable mechanism for most of the analyte sensing in complex samples. Theoretical sensing aspects include energy transfer, electron transfer, FERT, oscillation effect, decomposition, LMCT, photo-induced electron transfer, MMCT, ligand emission, guest emission, etc. In luminescent MOFs sensors, the weak interaction mechanisms or non-covalent interactions for examples linker analyte interactions, multi-interactions, synergistic effects, and hydrogen bonding are helpful for the construction of luminescent MOFs for renewable applications. Such mechanisms can be changeable via water or solvent washing as well as changing other reaction conditions. Afterward, the stability

Table 2 Structural design of MOFs-based luminescent sensor for chemical and metal ion sensing

Sr. No	MOFs	Metal ions	Linker name	Synthesis method	Dimensions	Analyte name	Luminescence turn On/ Off sensing (Theoretical mechanism)	Linearity range	LOD	Refs
Structural design of MOFs-based luminescent sensor for chemical sensing										
1	MMOFs	Zn	bpdc, bpee	Solvothermal	Langmuir surface area of 483 m^2/g	DNT and DMNB	Turn "On–Off" (Host–guest chemistry)	Not reported	Not reported	(149)
2	Cu-TCA	Cu^{2+}	H_3TCA	Solvothermal	Not reporter	NO	Turn "Off –On" (Paramagnetic characteristics of metal ion)	0.1 to 1 mM	Not reported	[150]
3	Tb-MOFs-76	Tb	H_3BTC	Microwave	50 nm (width), 100 nm (length)	Acetone	Turn "On–Off" (Energy exchange between ligand and solvent)	0 to 5%	Not reported	[151]
4	$Eu_2L_3(H_2O)_4]\cdot 3$ DMF	Ln	L	Solvothermal	Not reported	DMF	Turn "Off–On" (Ligand-to-metal energy transfer)	Not reported	Not reported	[134]
5	Zn-MOFs	Zn	tib	Hydrothermal	Not reported	Nitrobenzene	Turn "On–Off" (Electron transfer)	Not reported	Not reported	[152]
6	Li-MOFs	Li	H_2CPMA	Solvothermal		Nitrobenzene	Turn "On–Off" (Intraligand charg e trans-fer)	Not reported	Not reported	[153]
7	Ln-MOFs	Ln	H_2FDA	Hydrothermal	Not reported	Benzene, Acetone	Turn "On–Off" (Diffusion-controlled)	Not reported	Not reported	[154]
8	GO-MOFs	A-GO/L–Zn^{2+}	Stilbene	Solvothermal	Length: 100–130 µm	DNT	Turn "Off–On" (Photoinduced electron transfer)	Not reported	Not reported	[155]
9	Ln-MOFs	Eu and Tb	H_2BPDC, H_2BDC	Hydrothermal	Not reported	Poisonous small molecules	Turn "Off–On" (Energy transfer from the ligand to the lanthanide center)	Not reported	Not reported	[156]

Table 2 (continued)

Sr. No	MOFs	Metal ions	Linker name	Synthesis method	Dimensions	Analyte name	Luminescence turn On/Off sensing (Theoretical mechanism)	Linearity range	LOD	Refs
10	Tb-MOFs	Tb	H_3BTC	Ultrasound-vapor phase diffusion technique	Not reported	Picric acid	Turn "On–Off" (Charge transfer between PA and framework,)	0.001 to 0.18 mM	8.1×10^{-8} µM	[157]
11	Zn-PDA2	Zn	H_2PDA	Solvothermal	Not reported	Picric acid	Turn "On–Off" [Intraligand charge transfer]	0.007 to 0.28 mM	0.45 µg	[158]
12	$Cd(NDC)_{0.5}(PCA)]\cdot Gx$	Cd	NDC, PCA	Not reported	Not reported	TNP	Turn "On–Off" (Electron and energy transfer)	Not reported	Not reported	[159]
13	NU-1000	Zr	TBAPy	Solvothermal	Length: ~ 5 µm	1-HP	Turn "On–Off" (Charge transfer between the 1-HP and pyrene cores within NU-1000)	0.2 to 50 µM	48 nM	[69]
14	Cd-MOFs	Cd	H_3L	Solvothermal	Not reported	nitrobenzene	Turn "On–Off" (Electron transfer quenching Mechanism)	0 to 150 ppm	Not reported	[160]
15	Eu-MOFs	Eu	$bpydbH_2$	Solvothermal	Brunauer Emmett Teller (BET) surface area: 316.20 m^2/g	TNP, acetone	Turn "On–Off" (Electron transfer from the aromatic rings of ligand to the analyte)	Not reported	Not reported	[161]
16	Cd-MOFs	Cd^{3+}	$H_{12}L$	Solvothermal	Not reported	nitrobenzene	Turn "Off–On" (Photoinduced electron transfer mechanism)	Not reported	Not reported	[162]

Table 2 (continued)

Sr. No	MOFs	Metal ions	Linker name	Synthesis method	Dimensions	Analyte name	Luminescence turn On/Off sensing (Theoretical mechanism)	Linearity range	LOD	Refs
17	UPC-11	Tb	H_4BPTA	Solvothermal	Not reported	4-Nitrophenol	Turn "On–Off" (Electron transfer from the BPTA ligands to the electron-deficient molecules)	Not reported	Not reported	[163]
18	MIL-100(In) ⊃ Tb^{3+}	Ln	H_3BTC, BTC	Solvothermal	Not reported	O_2	Turn "On–Off" (Intramolecular energy transfer)	Not reported	Not reported	[164]
19	TPE-MOFs	Zn	H_4TCPPE	Solvothermal	Not reported	Volatile organic	Turn "On–Off" (Interaction between guest to MOFs)	Not reported	Not reported	[165]
20	ZnPO-MOFs	Zn	H_4TCPB	Solvothermal	0.13 μm	parathion-methyl	Turn "On–Off" (Photo-induced electron transfer)	1.0 μg/Kg–10 mg/Kg	0.45 nM	[166]
21	Cd(II)-MOFs	Cd	H_3L	Solvothermal	Not reported	Uranyl ions	Turn "On–Off" (Resonance energy transfer)	Not reported	Not reported	[167]
22	$Mn_2(HBTC)_2(TIAB)n$	Mn	TIAB, H3BTC	Solvothermal	Not reported	$Cr_2O_7^{2-}$, Picric acid	Turn "Off–On" (Ligand-to-metal and the intraligand transition)	Not reported	For $Cr_2O_7^{2-}$: 1.25×10^{-5} mol/L	[168]
23	Pb^{II}-MOFs	Pb	HAIA	Hydrothermal	Not reported	$Cr_2O_7^{2-}$	Turn "On–Off" (Excitation energy competitive between MOFs to the analyte)	Not reported	1.03×10^{-5} mol/L	[169]

Table 2 (continued)

Sr. No	MOFs	Metal ions	Linker name	Synthesis method	Dimensions	Analyte name	Luminescence turn On/Off sensing (Theoretical mechanism)	Linearity range	LOD	Refs
24	Eu-MOFs	Eu	1,4-BDC	Solvothermal	Not reported	Picric acid TNT, tetryl	Turn "On–Off" (Competitive absorption between Eu-MOFs and analytes)	0 to 100 µM	20–140 µg/mL	[170]
25	Pt-TCPP/H_4TCPE@UiO-66	Pt	H_4TCPE, Pt-TCPP	Solvothermal	100 nm	NO	Turn "On–Off" (Static quenching process)	0.48 to 18.7 µg/mL	0.1420 µg/mL	[172]
26	MMMs	Eu	2,5-TDC	Not reported	Not reported	Metronidazole, Dimetridazole	Turn "On–Off" (Inner filter effect)	0 to 60 µM	0.58 µg/mL, 0.51 µg/mL	[173]
27	Zr-MOFs	Zr	H_4ETTC	Solvothermal	0.5–1.5 µm	Tetracycline	Turn "On–Off" (Photoinduced electron Transfer from ligand to metal)	0.10 to 0.95 µM	30 nM	[174]
28	MOFs-76	Tb	H_3BTC	Solvothermal	Not reported	DPA	Turn "On–Off" (Energy transfer, Inner filter effect)	10–100 µM	3.05 µM	[175]
29	[Eu_2(dtztp)$(OH)_2$(DMF)$(H_2O)2.5]\cdot 2H_2O$	Eu	H_4dtztp	Solvothermal	Not reported	Metronidazole,	Turn "On–Off" (Adsorption of guest molecules	0–0.008 mM	18.3 ppm	[176]
Structural design of MOFs-based luminescent sensor for metal ion sensing										
30	Eu-MOFs	Eu	H_2pdc	Solvothermal	Not reported	Na^+, K^+, Mg^{2+}, Ca^{2+}, Mn^{2+}, Co^{2+}, Cu^{2+}, Zn^{2+}, etc	Turn "On–Off" (Ligand-to-metal energy transfer)	NA	NA	[33]
31	[Eu(BTB)(phen).4.5 DMF*$2H_2O$]n	Eu	H_3BTB	Hydrothermal	Not reported	Al^{3+}	Turn "On–Off" (Ligand-to-metal energy transfer)	-	1.35 ppb	[177]

Table 2 (continued)

Sr. No	MOFs	Metal ions	Linker name	Synthesis method	Dimensions	Analyte name	Luminescence turn On/ Off sensing (Theoretical mechanism)	Linearity range	LOD	Refs
32	Tb-MOFs–COOH	Tb	H_4btca	Hydrothermal	Not reported	Fe^{3+}	Turn "On–Off" (Overlapping effect, Metal to ligand energy transfer)	10 to 1000 mmol/L	0.01 mol/L	[178]
33	NTU-9-NS	Ti	DOBDC	Solvothermal	11 X 11 $Å^2$	Fe^{3+}	Turn "On–Off" (Electron transfer between Fe^{3+} and the MOFs nanosheets)	–	0.45 µM	[75]
34	Cd (II)-MOFs	Cd	Bis(benzimidazole), dicarboxylate	Hydrothermal	10.485 × 11.007 Å	Fe^{3+}	Turn "On–Off" (Ligand-to-metal charge transfer)	–	3.54 µM	[179]
35	EuW_{10}@UiO-67	Eu	Biphenyl-dicarboxylic acid	Direct synthesis	9 Å	Fe^{3+}	Turn "On–Off" (Ligand-to-metal charge transfer)	Not reported	37 µM	[180]
36	$Ln(ADA)_{1.5}(phen)]n$ MOFs	Ln	H_2ADA	Hydrothermal	Not reported	Ni^{2+}	Turn "On–Off" (Ligand-to-metal charge transfer)	0.2 to 0.6 µM	5.9×10^{-5} mg/L	[140]
37	TbTATB	Ln	H_3TATB	Solvothermal	Not reported	Zn^{2+}	Turn-On (Ligand-to-metal electron transfer)	0 to 10 µM	10.5 nM	[76]
38	Eu-PUFs	Eu^{3+}	5- amino -1,10-phenanthroline	co-polycondensation reaction	Not reported	Cu^{2+}	Turn "On–Off" (Cu^{2+} ions reduces the energy transfer efficiency between Eu^{3+} and ligands)	$1–12*10^{-5}$	0.28 µM	[181]

Table 2 (continued)

Sr. No	MOFs	Metal ions	Linker name	Synthesis method	Dimensions	Analyte name	Luminescence turn On/ Off sensing (Theoretical mechanism)	Linearity range	LOD	Refs
39	Zn(II)-MOFs	Zn	H_2DHT	hydrothermal method	Not reported	Fe^{3+} and Al^{3+}	For Fe^{3+}: Turn "On–Off" (Competition between the absorption of analyte and the excitation of GUPT-2) For Al^{3+}: Turn On (Intermolecular proton transfer)	For Fe^{3+}: 1–7 µM For Al^{3+}: 0–40 µM	Fe^{3+} and Al^{3+} up to 0.446 µM and 0.269 µM,	[182]
40	$Eu_{0.07}Gd_{0.03}$-MOFs	Eu	H_2tfBDC, 1,10-phenanthroline	Hydrothermal	Not reported	Fe^{3+}	Turn "On–Off" (Dynamic quenching effect)	0.0 µM -60 µM	0.091 µM	[184]
41	HSB-W7-Ns, HSB-W7-Ns1, HSB-W7-NR	Cd	Dicarboxylate 2-obdc, hsb-2	Ultrasonic irradiation	Length: 400 nm Width: 130 nm	Fe^{3+}	Turn "On–Off" (Surface adsorption, overlapping effect)	0–40 µM	0.21 µM, 0.36 µM and 0.51 µM	[183]
42	Eu-MOFs@ALD-PPS	Eu	2,5-dihydroxyterephthalic acid	solvothermal method	Not reported	Fe^{3+}	Turn "On–Off" (Interaction between analyte and ligand)	0–3 mM	10^{-6} M	[185]
43	LCU103	Zn	Hdpa	Hydrothermal	Not reported	Fe^{3+} and Cu^{2+}	Turn "On–Off" (Guest-induced and cation-exchange Quenching)	0–520 µM (Fe^{3+}) and 0–540 µM (Cu^{2+})	1.45 and 1.66 µM	[186]
44	Cu-HBIBA	Cu	HBIBA	Autoclaving	Not reported	Fe^{3+} and Bi^{3+}	Turn On (surface adsorption)	0–50 µM (Fe^{3+}), 0–900 nM (Bi^{3+})	0.16 µM, and 0.043 µM	[187]

of luminescent MOFs structural stability and luminescent stability in solvent mainly is a major critical task for scientific fraternities. In the future, there is a tremendous need to improve the biocompatibility, sensitivity, and selectivity of luminescent MOFs towards the biomolecules that could be more beneficial for clinical applications. The surface area of a few reported MOFs has been reported from 300 to 500 m^2/g by different methods. In the future, there is a huge urge to depict the surface area and sensing correlation. In the upcoming days, MOFs can design with adequate porosity and magnetic property using suitable building blocks that can furnish the highly promising stimuli-sensitive platform. As a result, it will provide diverse magnetic properties in the existence of guest targets within their nano-size pore of MOFs. Despite abundant benefits of MOFs, the chemical stability, as well as thermo-stability of MOFs, is a challenging issue for the field of separation and detection. The room temperature stability, as well as different pH stability, is a rising concern in MOFs. Moreover, designed MOFs must be stable in the sample with chemicals, such as nitrobenzene, ethanol, DMF, etc. Also, that used MOFs can be reusable for the next sensing of the same analyte. In this regard, the use of linker/ligand modification for structural strength improvement can be an excellent alternative. Besides this, the use of cooperative combination along with engineered material mainly utilization of metal nanoparticles, polymers, silica, quantum dots, carbon-based materials, metal oxides, etc. can offer good stability in chemicals and diverse temperatures. For use of such advanced materials, there is a suggestion to optimize the concentration ratio for a good result in terms of high sensitivity, and selectivity. Presently, Tb, Eu, Cu, Zn, Zr, Pt, etc. have been reported for a luminescent sensor for metal ions and chemical traces sensing. Herein, the selection criteria of metal ions, such as the ability of electron donor/accepter, charge transfer/donor, oscillation effect, etc., necessitate for further development of MOFs. Therefore, there is huge scope to utilize the different metal ions for the development of ultrasensitive MOFs. Even though several issues remain unresolved, we believe that metal nanoparticles and MOFs-mediated nano-conjugates would have a promising future; therefore, thanks to the constant attempts of scientists around the globe. In addition, the use of a suitable linker with the coordination of new metal ions could release a highly sensitive sensor that can provide the detection limit of up to pictogram (pg) to attogram (ag). The doped MOFs and metal-centric MOFs can be an excellent option for the identification of metal ions and chemical ions at low concentrations. Also, total removal of metal ions and chemical residues can be possible. Moreover, there is much need for more clarification regarding sensing mechanisms involved in the detection of metal ions and chemical residues. The detailed emphasis on a limit of detection and linearity range, stability, reusability, and real-time applications of MOFs is required to assist burgeoning researchers. In a nutshell, the selection of adequate proportions of organic ligands and metals ions needs to optimize to construct intended building blocks with a specific framework. In addition, reaction time, temperature conditions, types of solvents, magnetic stirring, etc., parameters must consider during the engineering of nano-size MOFs with unique topology. Abundant MOFs derivatives with metal nanoparticles, carbon nanomaterials, etc. can be synthesized via adjusting the different parameters that include temperature, gas atmosphere, annealing steps, etc. Moreover, several MOFs are required high costs and complex synthetic pathways that avert them from reaching considerable quantity and commercialization. Therefore, in the upcoming days, it should be proposed to produce economic, large-scale, and trouble-free manufacturing processes. Overall, the modified advanced MOFs generations will endow industrial development as well as social advancement.

Conclusion

Luminescent MOFs have always been a dynamic and astounding class of crystalline functional materials, with several attractive characteristics. A good summarization of the design and engineering of nano-size luminescent MOFs using a diverse class of metal ions and organic resulted in rapid expansion, augmentation, and widespread innovations in materials science. Principally, remarkable progress has been made in the nano-architecture and fabrication of a fresh category of nanostructured MOFs using modern synthesis methods. Presently, the detection of explosives and other explosive-like molecules is a genuinely exciting application of luminescence-MOFs-based sensing. The rational design of nano-architectured MOFs-mediated sensory materials with strong electron transfer, energy transfers, appropriate porosity, particle size, specific functional groups, and tunable electronic structures can lead to an efficient fluorescence response in the vapor and/or liquid phases. The combined approach based on accessible porosity and luminescence property of MOFs provides the transducing potential from host–guest chemistry to recognizable amend in nano-size MOFs luminescence that can be preferred as a suitable candidate for sensing applications. Moreover, MOFs with excellent balance among emission rate, energy transfer, and absorption could offer the sensing property at the physiological as well as real-time sample pH range. The present review summarizes the detection of interest analyte using nano-architectured MOFs that relied on hydrogen bonding, electrostatic interaction, size exclusion, etc. In addition, the existence of basic pyridyl sites (free Lewis) within the MOFs pores provides the aptitude of sensing metal ions and chemicals also. Moreover, the post-synthetic modification

of luminescent MOFs furnishes the high selectivity towards analyte as compared to the plain MOFs. Therefore, many composite formulas published in the literature could facilitate the design and synthesis of new nano-architectured MOFs-based materials. In this line, the tiny differences in the method of synthesis are offering the emergence of nano-MOFs with various framework topologies that provide the lowest detection limit of up to ng/nM for metal ions as well as chemical residues. Hence, the present review assures that the surface functionality that existed on the surface of luminescent MOFs furnishes the site for the identification of target metal ions and chemicals in the presence of interfering substances. And at last, an evident understanding of the rapidly expanding field is provided. Main obstacles and recommendations for further research are summarized and prophesied. Concisely, the nano-architectured MOFs based on luminescent sensors demonstrate high sensitivity and high selectivity for chemical traces and metal ions in the existence of diverse substances.

Acknowledgements The authors are thankful to H. R. Patel Institute of Pharmaceutical Education and Research, Shirpur for providing the necessary facilities.

Declarations

Conflict of interest None to declare.

References

1. Carter, K.P., Young, A.M., Palmer, A.E.: Fluorescent sensors for measuring metal ions in living systems. Chem. Rev. **114**, 4564–4601 (2014)
2. Mei, C.J., Ahmad, S.A.A.: A review on the determination heavy metals ions using calixarene-based electrochemical sensors. Arab. J. Chem. **14**, 103303 (2021)
3. Fan, L., Zhao, D., Zhang, H., Wang, F., Li, B., Yang, L., Deng, Y., Zhang, X.: A hydrolytically stable amino-functionalized Zinc (II) metal-organic framework containing nanocages for selective gas adsorption and luminescent sensing. Microporous Mesoporous Mater. **326**, 111396 (2021)
4. Scharf, B., Clement, C.C., Zolla, V., Perino, G., Yan, B., Elci, S.G., Purdue, E., Goldring, S., Macaluso, F., Cobelli, N.: Molecular analysis of chromium and cobalt-related toxicity. Sci. Rep. **4**, 1–12 (2014)
5. Kim, H.S., Kim, Y.J., Seo, Y.R.: An overview of carcinogenic heavy metal: molecular toxicity mechanism and prevention. J. Cancer Prev. **20**, 232 (2015)
6. Sun, K., Song, Y., He, F., Jing, M., Tang, J., Liu, R.: A review of human and animals exposure to polycyclic aromatic hydrocarbons: Health risk and adverse effects, photo-induced toxicity and regulating effect of microplastics. Sci. Total Environ. 145403 (2021).
7. Nangare, S. N., Patil, S. R., Patil, A. G., Khan, Z. G., Deshmukh, P. K., Tade, R. S., Mahajan, M. R., Bari, S. B., Patil, P. O.: Structural design of nanosize-metal–organic framework-based sensors for detection of organophosphorus pesticides in food and water samples: current challenges and future prospects. J. Nanostruct. Chem. (2021). https://doi.org/10.1007/s40097-021-00449-y.
8. Zhang, Z., Lou, Y., Guo, C., Jia, Q., Song, Y., Tian, J.-Y., Zhang, S., Wang, M., He, L., Du, M.: Metal–organic frameworks (MOFs) based chemosensors/biosensors for analysis of food contaminants. Trends Food Sci Technol. **118**, 569–588 (2021)
9. Lebelo, K., Malebo, N., Mochane, M.J., Masinde, M.: Chemical contamination pathways and the food safety implications along the various stages of food production: a review. Int. J. Environ. Res. Public Health. **18**, 5795 (2021)
10. Zhang, Z., Zhang, X., Rajh, T., Guha, S.: Photonic microresonator based sensor for selective nitrate ion detection. Sens. Actuators B Chem. **328**, 129027 (2021)
11. Seenan, S., Sathiyanarayanan, K.I.: A multisensing ratiometric fluorescent sensor for recognition of Al3+, Th4+ and picric acid. Inorg. Chem. Commun. **132**, 108825 (2021)
12. Wei, Y.-B., Wang, M.-J., Luo, D., Huang, Y.-L., Xie, M., Lu, W., Shu, X., Li, D.: Ultrasensitive and highly selective detection of formaldehyde via an adenine-based biological metal–organic framework. Mater. Chem. Front. **5**, 2416–2424 (2021)
13. McRae, R., Bagchi, P., Sumalekshmy, S., Fahrni, C.J.: In situ imaging of metals in cells and tissues. Chem. Rev. **109**, 4780–4827 (2009)
14. Mi, X., Sheng, D., Yu, Ye., Wang, Y., Zhao, L., Lu, J., Li, Y., Li, D., Dou, J., Duan, J.: Tunable light emission and multiresponsive luminescent sensitivities in aqueous solutions of two series of lanthanide metal–organic frameworks based on structurally related ligands. ACS Appl. Mater. Interfaces. **11**, 7914–7926 (2019)
15. Banerjee, D., Hu, Z., Li, J.: Luminescent metal–organic frameworks as explosive sensors. Dalton Trans. **43**, 10668–10685 (2014)
16. Sun, J., Du, H., Chen, Z., Wang, L., Shen, G.: MXene quantum dot within natural 3D watermelon peel matrix for biocompatible flexible sensing platform. Nano Res. 1–7 (2021).
17. Mu, S., Liu, Q., Kidkhunthod, P., Zhou, X., Wang, W., Tang, Y.: Molecular grafting towards high-fraction active nanodots implanted in N-doped carbon for sodium dual-ion batteries. Natl. Sci. Rev. **8**, 78 (2021)
18. Guan, H., Huang, S., Ding, J., Tian, F., Xu, Q., Zhao, J.: Chemical environment and magnetic moment effects on point defect formations in CoCrNi-based concentrated solid-solution alloys. Acta Mater. **187**, 122–134 (2020)
19. Wang, T., Liu, W., Zhao, J., Guo, X., Terzija, V.: A rough set-based bio-inspired fault diagnosis method for electrical substations. Int J. Electr. Power Energy Syst. **119**, 105961 (2020)
20. Tang, X., Wu, J., Wu, W., Zhang, Z., Zhang, W., Zhang, Q., Zhang, W., Chen, X., Li, P.: Anal. Chem. **92**, 3563–3571 (2020)
21. He, H., Zhu, Q.-Q., Yan, Y., Zhang, H.-W., Han, Z.-Y., Sun, H., Chen, J., Li, C.-P., Zhang, Z., Du, M.: Metal–organic framework supported Au nanoparticles with organosilicone coating for high-efficiency electrocatalytic N_2 reduction to NH_3. Appl. Catal. B: Environ. **302**, 120840 (2021)
22. Hu, K., Wang, F., Shen, Z., Liu, H., Xiong, J.: Ternary heterojunctions synthesis and sensing mechanism of Pd/ZnO–SnO_2 hollow nanofibers with enhanced H_2 gas sensing properties. J. Alloys Compd. **850**, 156663 (2021)
23. Saha, S., De, A., Ghosh, A., Ghosh, A., Bera, K., Das, K.S., Akhtar, S., Maiti, N.C., Das, A.K., Das, B.B.: Pyridine-pyrazole based Al (iii)'turn on'sensor for MCF7 cancer cell imaging and detection of picric acid. RSC Adv. **11**, 10094–10109 (2021)
24. Liang, Z., Qiu, T., Gao, S., Zhong, R., Zou, R.: Multi-scale design of metal–organic framework-derived materials for energy electrocatalysis. Adv. Energy Mater. (2021). https://doi.org/10.1002/aenm.202003410

25. Zhao, D., Yu, K., Han, X., He, Y., Chen, B.: Recent progress on porous MOFs for process-efficient hydrocarbon separation, luminescent sensing, and information encryption. Chem. Commun. **58**, 747–770 (2022)
26. Chakraborty, G., Park, I.-H., Medishetty, R., Vittal, J.J.: Two-dimensional metal-organic framework materials: synthesis, structures, properties and applications. Chem. Rev. **121**, 3751–3891 (2021)
27. Nangare, S. N., Sangale, P., Patil, A. G., Boddu, S. H., Deshmuk, P. K., Jadhav, N. R., Tade, R. S., Patil, D. R., Pandey, A., Mutalik, S.: Surface architectured metal organic frameworks-based biosensor for ultrasensitive detection of uric acid: Recent advancement and future perspective. Microchem J. 106567 (2021).
28. Yu, S., Pang, H., Huang, S., Tang, H., Wang, S., Qiu, M., Chen, Z., Yang, H., Song, G., Fu, D.: Recent advances in metal-organic framework membranes for water treatment: a review. Sci. Total Environ. **800**, 149662 (2021)
29. Li, X.-Y., Song, Y., Zhang, C.-X., Zhao, C.-X., He, C.: Inverse CO_2/C_2H_2 separation in a pillared-layer framework featuring a chlorine-modified channel by quadrupole-moment sieving. Sep. Purif. Technol. **279**, 119608 (2021)
30. Liu, J., Huang, J., Zhang, L., Lei, J.: Multifunctional metal–organic framework heterostructures for enhanced cancer therapy. Chem. Soc. Rev. **50**, 1188–1218 (2021)
31. Wang, R., He, C., Chen, W., Fu, L., Zhao, C., Huo, J., Sun, C.: Design strategies of two-dimensional metal–organic frameworks toward efficient electrocatalysts for N_2 reduction: cooperativity of transition metals and organic linkers. Nanoscale **13**, 19247–19254 (2021)
32. Zhou, J., Zeng, C., Ou, H., Yang, Q., Xie, Q., Zeb, A., Lin, X., Ali, Z., Hu, L.: Metal-organic framework-based materials for full cell systems: a review. J. Mater. Chem. C. **9**, 11030–11058 (2021)
33. Chen, B., Wang, L., Xiao, Y., Fronczek, F.R., Xue, M., Cui, Y., Qian, G.: A luminescent metal–organic framework with Lewis basic pyridyl sites for the sensing of metal ions. Angew. Chem. Int. Ed. **48**, 500–503 (2009)
34. Rani, S., Kataria, N.: Metal− organic framework and its nanocomposites as chemical sensors, in metal− organic frameworks for environmental sensing. Metal− Organic Framework and Its Nanocomposites as Chemical Sensors, ACS Publications, pp. 83–124 (2021). https://doi.org/10.1021/bk-2021-1394.ch004.
35. Ma, L., Lin, W.: Designing metal-organic frameworks for catalytic applications. Top. Curr. Chem. **293**, 175–205 (2009)
36. Zhu, Q.-L., Xu, Q.: Metal–organic framework composites. Chem. Soc. Rev **43**, 5468–5512 (2014)
37. Liu, C.-S., Li, J., Pang, H.: Metal-organic framework-based materials as an emerging platform for advanced electrochemical sensing. Coord. Chem. Rev. **410**, 213222 (2020)
38. Bennett, T.D., Cheetham, A.K.: Amorphous metal–organic frameworks. Acc Chem. Res. **47**, 1555–1562 (2014)
39. Fonseca, J., Gong, T., Jiao, L., Jiang, H.-L.: Metal-organic frameworks (MOFs) beyond crystallinity: amorphous MOFs, MOF liquids and MOF glasses. J. Mater. Chem. A. **9**, 10562–10611 (2021)
40. Orellana-Tavra, C., Baxter, E.F., Tian, T., Bennett, T.D., Slater, N.K., Cheetham, A.K., Fairen-Jimenez, D.: Amorphous metal–organic frameworks for drug delivery. Chem. Commun. **51**, 13878–13881 (2015)
41. Lee, T., Liu, Z.X., Lee, H.L.: A biomimetic nose by microcrystals and oriented films of luminescent porous metal–organic frameworks. Cryst. Growth Des. **11**, 4146–4154 (2011)
42. Bennett, T.D., Goodwin, A.L., Dove, M.T., Keen, D.A., Tucker, M.G., Barney, E.R., Soper, A.K., Bithell, E.G., Tan, J.-C., Cheetham, A.K.: Structure and properties of an amorphous metal-organic framework. Phys. Rev. Lett. **104**, 115503 (2010)
43. Zhang, L., Yan, Z., Chen, X., Yu, M., Liu, F., Cheng, F., Chen, J.: Facile synthesis of amorphous MoS x–Fe anchored on Zr-MOFs towards efficient and stable electrocatalytic hydrogen evolution. Chem. Commun. **56**, 2763–2766 (2020)
44. Fonseca, J., Choi, S.: Synthesis of a novel amorphous metal organic framework with hierarchical porosity for adsorptive gas separation. Microporous Mesoporous Mater. **310**, 110600 (2021)
45. Fonseca, J., Choi, S.: Flexible amorphous metal–organic frameworks with π Lewis acidic pore surface for selective adsorptive separations. Dalton Trans. **50**, 3145–3154 (2021)
46. Garg, N., Deep, A., Sharma, A.L.: Metal-organic frameworks based nanostructure platforms for chemo-resistive sensing of gases. Coord. Chem. Rev. **445**, 214073 (2021)
47. Dang, S., Zhu, Q.-L., Xu, Q.: Nanomaterials derived from metal–organic frameworks. Nat. Rev. Mater. **3**, 1–14 (2017)
48. Cui, Y., Chen, B., Qian, G.: Lanthanide metal-organic frameworks for luminescent sensing and light-emitting applications. Coord. Chem. Rev. **273**, 76–86 (2014)
49. Deng, Y., Wu, Y., Chen, G., Zheng, X., Dai, M., Peng, C.: Metal-organic framework membranes: recent development in the synthesis strategies and their application in oil-water separation. Chem. Eng. J. **405**, 127004 (2021)
50. Zhang, L., Kang, Z., Xin, X., Sun, D.: Metal–organic frameworks based luminescent materials for nitroaromatics sensing. CrystEngComm **18**, 193–206 (2016)
51. Zhang, X.-P., Wang, D.-G., Su, Y., Tian, H.-R., Lin, J.-J., Feng, Y.-L., Cheng, J.-W.: Luminescent 2D bismuth–cadmium–organic frameworks with tunable and white light emission by doping different lanthanide ion. Dalton Trans. **42**, 10384–10387 (2013)
52. Li, L., Zhang, S., Han, L., Sun, Z., Luo, J., Hong, M.: A noncentrosymmetric dual-emissive metal–organic framework with distinct nonlinear optical and tunable photoluminescence properties. Crys. Growth Design. **13**, 106–110 (2013)
53. Wang, S.-J., Li, Q., Xiu, G.-L., You, L.-X., Ding, F., Van Deun, R., Dragutan, I., Dragutan, V., Sun, Y.-G.: New Ln-MOFs based on mixed organic ligands: synthesis, structure and efficient luminescence sensing of the Hg^{2+} ions in aqueous solutions. Dalton Trans. **50**, 15612–15619 (2021)
54. Asad, M., Wang, S., Wang, Q.-Y., Li, L.-K., Anwar, M.I., Younas, A., Zang, S.-Q.: Aqueous media ultra-sensitive detection of antibiotics via highly stable luminescent 3D Cadmium-based MOF. New J. Chem. **45**, 20887–20894 (2021)
55. Feng, P.L., Leong, K., Allendorf, M.D.: Charge-transfer guest interactions in luminescent MOFs: implications for solid-state temperature and environmental sensing. Dalton Trans. **41**, 8869–8877 (2012)
56. Guo, Z., Xu, H., Su, S., Cai, J., Dang, S., Xiang, S., Qian, G., Zhang, H., O'keeffe, M., Chen, B.: A robust near infrared luminescent ytterbium metal–organic framework for sensing of small molecules. Chem. Commun. **47**, 5551–5553 (2011)
57. Xiao, J., Liu, J., Liu, M., Ji, G., Liu, Z.: Fabrication of a luminescence-silent system based on a post-synthetic modification Cd-MOFs: a highly selective and sensitive turn-on luminescent probe for ascorbic acid detection. Inorg. Chem. **58**, 6167–6174 (2019)
58. Cadiau, A., Brites, C.D., Costa, P.M., Ferreira, R.A., Rocha, J., Carlos, L.D.: Ratiometric nanothermometer based on an emissive Ln^{3+}-organic framework. ACS Nano **7**, 7213–7218 (2013)
59. Lin, Z.-G., Song, F.-Q., Wang, H., Song, X.-Q., Yu, X.-X., Liu, W.-S.: The construction of a novel luminescent lanthanide framework for the selective sensing of Cu^{2+} and 4-nitrophenol in water. Dalton Trans. **50**, 1874–1886 (2021)

60. Yang, H., Wang, F., Tan, Y.X., Kang, Y., Li, T.H., Zhang, J.: Charge matching on designing neutral cadmium–lanthanide–organic open frameworks for luminescence sensing. Chem Asian J. **7**, 1069–1073 (2012)
61. Kim, T.K., Lee, J.H., Moon, D., Moon, H.R.: Luminescent Li-based metal–organic framework tailored for the selective detection of explosive nitroaromatic compounds: direct observation of interaction sites. Inorg. Chem. **52**, 589–595 (2013)
62. Lei, M., Ge, F., Gao, X., Shi, Z., Zheng, H.: A water-stable Tb-MOF as a rapid, accurate, and highly sensitive ratiometric luminescent sensor for the discriminative sensing of antibiotics and D_2O in H_2O. Inorg. Chem. **60**, 10513–10521 (2021)
63. Gutierrez, M., Martín, C., Souza, B.E., Van der Auweraer, M., Hofkens, J., Tan, J.-C.: Highly luminescent silver-based MOFs: scalable eco-friendly synthesis paving the way for photonics sensors and electroluminescent devices. Appl. Mater. Today. **21**, 100817 (2020)
64. Shustova, N. B., Cozzolino, A. F., Reineke, S., Baldo, M., Dincă, M.: Selective turn-on ammonia sensing enabled by high-temperature fluorescence in metal–organic frameworks with open metal sites. J. Am. Chem. Soc.. **135**, 13326–13329 (2013).
65. He, Q.-Q., Yao, S.-L., Zheng, T.-F., Xu, H., Liu, S.-J., Chen, J.-L., Li, N., Wen, H.-R.: Multi-responsive luminescent sensor based on a stable Eu (III) metal-organic framework for sensing Fe^{3+}, MnO^{4-}, and $Cr^2O_7^{2-}$ in aqueous solution. CrystEngComm (2022). https://doi.org/10.1039/D1CE01503F
66. Shan, X.-C., Jiang, F.-L., Yuan, D.-Q., Zhang, H.-B., Wu, M.-Y., Chen, L., Wei, J., Zhang, S.-Q., Pan, J., Hong, M.-C.: A multi-metal-cluster MOF with Cu_4I_4 and Cu_6S_6 as functional groups exhibiting dual emission with both thermochromic and near-IR character. Chem. Sci. **4**, 1484–1489 (2013)
67. Vlad, A., Zaltariov, M.-F., Shova, S., Novitchi, G., Varganici, C.-D., Train, C., Cazacu, M.: Flexible linkers and dinuclear metallic nodes build up an original metal–organic framework. CrystEngComm **15**, 5368–5375 (2013)
68. Ferrando-Soria, J., Khajavi, H., Serra-Crespo, P., Gascon, J., Kapteijn, F., Julve, M., Lloret, F., Pasán, J., Ruiz-Pérez, C., Journaux, Y.: Highly selective chemical sensing in a luminescent nanoporous magnet. Adv. Mater. **24**, 5625–5629 (2012)
69. Zhou, Y., Yang, Q., Cuan, J., Wang, Y., Gan, N., Cao, Y., Li, T.: A pyrene-involved luminescent MOF for monitoring 1-hydroxypyrene, a biomarker for human intoxication of PAH carcinogens. Analyst. **143**, 3628–3634 (2018)
70. Liu, W., Chen, C., Wu, Z., Pan, Y., Ye, C., Mu, Z., Luo, X., Chen, W., Liu, W.: Construction of multifunctional luminescent lanthanide MOFs by hydrogen bond functionalization for picric acid detection and fluorescent dyes encapsulation. ACS Sustain. Chem. Eng. **8**, 13497–13506 (2020)
71. Kent, C.A., Liu, D., Meyer, T.J., Lin, W.: Amplified luminescence quenching of phosphorescent metal–organic frameworks. J. Am. Chem. Soc. **134**, 3991–3994 (2012)
72. Li, C., Hai, J., Li, S., Wang, B., Yang, Z.: Luminescent magnetic nanoparticles encapsulated in MOFs for highly selective and sensitive detection of ClO−/SCN− and anti-counterfeiting. Nanoscale **10**, 8667–8676 (2018)
73. Lee, H. L., Lee, T., Liu, Z. X., Tsai, M. H., Tsai, Y. C., Lin, T. Y., Cheng, S. L., Lee, S. W., Hu, J. C., Chen, L. T.: A taste and odor sensing by photoluminescence responses of luminescent metal organic frameworks, Trans Tech Publ. 392–397(2013).
74. Han, Y.-H., Tian, C.-B., Li, Q.-H., Du, S.-W.: Highly chemical and thermally stable luminescent Eu_xTb_{1-x} MOF materials for broad-range pH and temperature sensors. J. Mater. Chem. C. **2**, 8065–8070 (2014)
75. Xu, H., Gao, J., Qian, X., Wang, J., He, H., Cui, Y., Yang, Y., Wang, Z., Qian, G.: Metal–organic framework nanosheets for fast-response and highly sensitive luminescent sensing of Fe^{3+}. J. Mater. Chem. A. **4**, 10900–10905 (2016)
76. Fan, T., Xia, T., Zhang, Q., Cui, Y., Yang, Y., Qian, G.: A porous and luminescent metal-organic framework containing triazine group for sensing and imaging of Zn^{2+}. Microporous Mesoporous Mater. **266**, 1–6 (2018)
77. He, H., Sun, F., Borjigin, T., Zhao, N., Zhu, G.: Tunable colors and white-light emission based on a microporous luminescent Zn (II)-MOF: Dalton Trans. **43**, 3716–3721 (2014).
78. Pandey, A., Dhas, N., Deshmukh, P., Caro, C., Patil, P., García-Martín, M.L., Padya, B., Nikam, A., Mehta, T., Mutalik, S.: Heterogeneous surface architectured metal-organic frameworks for cancer therapy, imaging, and biosensing: a state-of-the-art review. Coord. Chem. Rev. **409**, 213212 (2020)
79. Shu, J.C., Cao, W.Q., Cao, M.S.: Diverse metal–organic framework architectures for electromagnetic absorbers and shielding. Adv. Funct. Mater. (2021). https://doi.org/10.1002/adfm.202100470
80. Yoo, Y., Varela-Guerrero, V., Jeong, H.-K.: Isoreticular metal−organic frameworks and their membranes with enhanced crack resistance and moisture stability by surfactant-assisted drying. Langmuir **27**, 2652–2657 (2011)
81. Dey, C., Kundu, T., Biswal, B. P., Mallick, A., Banerjee, R.: Crystalline metal-organic frameworks (MOFs): synthesis, structure and function. Acta Crystallogr. B Struct. Sci. Cryst. Eng. Mater. **70**, 3–10 (2014).
82. Butova, V.V.E., Soldatov, M.A., Guda, A.A., Lomachenko, K.A., Lamberti, C.: Metal-organic frameworks: structure, properties, methods of synthesis and characterization. Russ. Chem. Rev. **85**, 280 (2016)
83. Huang, L., Wang, H., Chen, J., Wang, Z., Sun, J., Zhao, D., Yan, Y.: Synthesis, morphology control, and properties of porous metal–organic coordination polymers. Microporous Mesoporous Mater. **58**, 105–114 (2003)
84. Huang, X.C., Lin, Y.Y., Zhang, J.P., Chen, X.M.: Ligand-directed strategy for zeolite-type metal–organic frameworks: zinc (II) imidazolates with unusual zeolitic topologies. Angew. Chem. Int. Ed. **45**, 1557–1559 (2006)
85. Qiu, L.-G., Li, Z.-Q., Wu, Y., Wang, W., Xu, T., Jiang, X.: Facile synthesis of nanocrystals of a microporous metal–organic framework by an ultrasonic method and selective sensing of organoamines. Chem Comm. (2008). https://doi.org/10.1039/B804126A
86. Garay, A.L., Pichon, A., James, S.L.: Solvent-free synthesis of metal complexes. Chem. Soc. Rev. **36**, 846–855 (2007)
87. Friščić, T., Reid, D.G., Halasz, I., Stein, R.S., Dinnebier, R.E., Duer, M.J.: Ion-and liquid-assisted grinding: improved mechanochemical synthesis of metal–organic frameworks reveals salt inclusion and anion templating. Angew. Chem. **122**, 724–727 (2010)
88. Yuan, W., Friščić, T., Apperley, D., James, S.L.: High reactivity of metal–organic frameworks under grinding conditions: parallels with organic molecular materials. Angew. Chem Int. Ed. **49**, 3916–3919 (2010)
89. Li, P.-Z., Wang, X.-J., Li, Y., Zhang, Q., Tan, R.H.D., Lim, W.Q., Ganguly, R., Zhao, Y.: Co (II)-tricarboxylate metal–organic frameworks constructed from solvent-directed assembly for CO_2 adsorption. Microporous Mesoporous Mater. **176**, 194–198 (2013)
90. Ahmadi, M., Ayyoubzadeh, S.M., Ghorbani-Bidkorbeh, F., Shahhosseini, S., Dadashzadeh, S., Asadian, E., Mosayebnia, M., Siavashy, S.: An investigation of affecting factors on MOF characteristics for biomedical applications: a systematic review. Heliyon. **7**, e06914 (2021)
91. Chen, L., Jia, H.-Y., Hong, X.-J., Chen, D.-H., Zheng, Z.-P., Jin, H.-G., Gu, Z.-G., Cai, Y.-P.: Construction of one pH-independent

3-D pillar-layer lead-organic framework containing tetrazole-1-acetic acid. Inorg. Chem. Commun. **27**, 22–25 (2013)
92. Sun, Y.-X., Sun, W.-Y.: Influence of temperature on metal-organic frameworks. Chin. Chem. Lett. **25**, 823–828 (2014)
93. Seetharaj, R., Vandana, P., Arya, P., Mathew, S.: Dependence of solvents, pH, molar ratio and temperature in tuning metal organic framework architecture. Arab. J. Chem. **12**, 295–315 (2019)
94. Hu, X., Wang, C., Wang, L., Liu, Z., Wu, L., Zhang, G., Yu, L., Ren, X., York, P., Sun, L.: Nanoporous CD-MOF particles with uniform and inhalable size for pulmonary delivery of budesonide. Int. J. Pharm. **564**, 153–161 (2019)
95. Abazari, R., Mahjoub, A.R., Slawin, A.M., Carpenter-Warren, C.L.: Morphology-and size-controlled synthesis of a metal-organic framework under ultrasound irradiation: an efficient carrier for pH responsive release of anti-cancer drugs and their applicability for adsorption of amoxicillin from aqueous solution. Ultrason. Sonochem. **42**, 594–608 (2018)
96. Li, L., Wang, S., Chen, T., Sun, Z., Luo, J., Hong, M.: Solvent-dependent formation of Cd (II) coordination polymers based on a C 2-symmetric tricarboxylate linker. Crys. Growth Des. **12**, 4109–4115 (2012)
97. Gao, X., Cui, R., Ji, G., Liu, Z.: Size and surface controllable metal–organic frameworks (MOFs) for fluorescence imaging and cancer therapy. Nanoscale **10**, 6205–6211 (2018)
98. Luo, L., Lv, G.-C., Wang, P., Liu, Q., Chen, K., Sun, W.-Y.: pH-Dependent cobalt (ii) frameworks with mixed 3, 3′, 5, 5′-tetra (1 H-imidazol-1-yl)-1, 1′-biphenyl and 1, 3, 5-benzenetricarboxylate ligands: synthesis, structure and sorption property. CrystEngComm **15**, 9537–9543 (2013)
99. Gupta, G., Thakur, A.: A comprehensive review on luminescent metal–organic framework detectors. Mater. Today. Proc. (2021). https://doi.org/10.1016/j.matpr.2021.09.170
100. Ge, Y., Yao, S., Sun, X., Yu, C., Li, G., Liu, Y.: A luminescent metal-organic framework with helical SBUs for highly effective detection of Fe^{3+} ions. Inorg. Chem. Comm. **93**, 52–55 (2018)
101. Guo, J., Wan, Y., Zhu, Y., Zhao, M., Tang, Z.: Advanced photocatalysts based on metal nanoparticle/metal-organic framework composites. Nano Res. **14**, 2037–2052 (2021)
102. Schoedel, A., Rajeh, S.: Why design matters: From decorated metal-oxide clusters to functional metal-organic frameworks. Metal-Organic Framework. 1–55 (2020).
103. Zhang, X., Chen, Z., Liu, X., Hanna, S.L., Wang, X., Taheri-Ledari, R., Maleki, A., Li, P., Farha, O.K.: Chem. Soc. Rev. **49**, 7406–7427 (2020)
104. Kanan, S.M., Malkawi, A.: Recent advances in nanocomposite luminescent metal-organic framework sensors for detecting metal ions. Comments Inorg. Chem. **41**, 1–66 (2021)
105. Wang, S., Gong, M., Han, X., Zhao, D., Liu, J., Lu, Y., Li, C., Chen, B.: Embedding red emitters in the NbO-type metal-organic frameworks for highly sensitive luminescence thermometry over tunable temperature range. ACS Appl. Mater. Interfaces **13**, 11078–11088 (2021)
106. Pashazadeh-Panahi, P., Belali, S., Sohrabi, H., Oroojalian, F., Hashemzaei, M., Mokhtarzadeh, A., de la Guardia, M.: Metal-organic frameworks conjugated with biomolecules as efficient platforms for development of biosensors. TrAC Trends in Analytical Chemistry. 116285 (2021).
107. Sanati, S., Abazari, R., Albero, J., Morsali, A., García, H., Liang, Z., Zou, R.: Metal–organic framework derived bimetallic materials for electrochemical energy storage. Angew. Chem. Int. Ed. **60**, 11048–11067 (2021)
108. Kukkar, D., Vellingiri, K., Kim, K.-H., Deep, A.: Recent progress in biological and chemical sensing by luminescent metal-organic frameworks. Sens. Actuators B Chem. **273**, 1346–1370 (2018)
109. Bosch, M., Zhang, M., Zhou, H.-C.: Increasing the stability of metal-organic frameworks. Adv. Chem. **2014**, 1155 (2014)
110. Ding, M., Cai, X., Jiang, H.-L.: Improving MOF stability: approaches and applications. Chem. Sci. **10**, 10209–10230 (2019)
111. Li, N., Xu, J., Feng, R., Hu, T.-L., Bu, X.-H.: Governing metal–organic frameworks towards high stability. Chem. Commun. **52**, 8501–8513 (2016)
112. Chughtai, A.H., Ahmad, N., Younus, H.A., Laypkov, A., Verpoort, F.: Metal–organic frameworks: versatile heterogeneous catalysts for efficient catalytic organic transformations. Chem. Soc. Rev. **44**, 6804–6849 (2015)
113. Soni, S., Bajpai, P. K., Arora, C.: A review on metal-organic framework: synthesis, properties and application. Charact. Appl. Nanomater. **3**, (2020).
114. Bazargan, M., Ghaemi, F., Amiri, A., Mirzaei, M.: Metal–organic framework-based sorbents in analytical sample preparation. Coord. Chem. Rev. **445**, 214107 (2021)
115. Li, H., Eddaoudi, M., O'Keeffe, M., Yaghi, O.M.: Design and synthesis of an exceptionally stable and highly porous metal-organic framework. Nature **402**, 276–279 (1999)
116. Kumar, S., Jain, S., Nehra, M., Dilbaghi, N., Marrazza, G., Kim, K.-H.: Green synthesis of metal–organic frameworks: as state-of-the-art review of potential environmental and medical applications Coord. Chem. Rev. **420**, 213407 (2020)
117. Dapaah, M.F., Liu, B.: Recent advances of supercritical CO_2 in green synthesis and activation of metal–organic frameworks, journal of inorganic and organometallic polymers and materials. J. Inorg. Organomet. Polym. Mater. **30**, 581–595 (2020)
118. Dašić, M., Stanković, I., Gkagkas, K.: Molecular dynamics investigation of the influence of the shape of the cation on the structure and lubrication properties of ionic liquids. Phys. Chem. Chem. Phys. **21**, 4375–4386 (2019)
119. Jiao, L., Seow, J.Y.R., Skinner, W.S., Wang, Z.U., Jiang, H.-L.: Metal–organic frameworks: Structures and functional applications. Mater. Today. **27**, 43–68 (2019)
120. Zhang, Y., Yuan, S., Day, G., Wang, X., Yang, X., Zhou, H.-C.: Luminescent sensors based on metal-organic frameworks. Coord. Chem. Rev. **354**, 28–45 (2018)
121. Zhao, D., Cui, Y., Yang, Y., Qian, G.: Sensing-functional luminescent metal–organic frameworks. CrystEngComm **18**, 3746–3759 (2016)
122. Farahani, Y.D., Safarifard, V.: A luminescent metal-organic framework with pre-designed functionalized ligands as an efficient fluorescence sensing for Fe^{3+} ions. J. Solid State Chem. **270**, 428–435 (2019)
123. Han, X., Gu, C., Ding, Y., Yu, J., Li, K., Zhao, D., Chen, B.: Stable Eu^{3+}/Cu^{2+}-functionalized supramolecular Zinc (II) complexes as fluorescent probes for turn-on and ratiometric detection of hydrogen sulfide. ACS Appl. Mater. Interfaces. **13**, 20371–20379 (2021)
124. Ding, Y., Lu, Y., Yu, K., Wang, S., Zhao, D., Chen, B.: MOF-nanocomposite mixed-matrix membrane for dual-luminescence ratiometric temperature sensing. Adv. Optic. Mater. **9**, 2100945 (2021)
125. Kumar, P., Deep, A., Kim, K.-H.: Metal organic frameworks for sensing applications. TrAC, Trends Anal. Chem. **73**, 39–53 (2015)
126. Allendorf, M.D., Bauer, C.A., Bhakta, R., Houk, R.: Luminescent metal–organic frameworks. Chem. Soc. Rev. **38**, 1330–1352 (2009)
127. Kreno, L.E., Leong, K., Farha, O.K., Allendorf, M., Van Duyne, R.P., Hupp, J.T.: Metal–organic framework materials as chemical sensors. Chem. Rev. **112**, 1105–1125 (2012)
128. Amiripour, F., Ghasemi, S., Azizi, S.N.: Design of turn-on luminescent sensor based on nanostructured molecularly imprinted polymer-coated zirconium metal–organic framework

for selective detection of chloramphenicol residues in milk and honey. Food Chem. **347**, 129034 (2021)
129. Lei, J., Qian, R., Ling, P., Cui, L., Ju, H.: Design and sensing applications of metal–organic framework composites. TrAC Trend. Anal. Chem. **58**, 71–78 (2014)
130. Huangfu, M., Wang, M., Lin, C., Wang, J., Wu, P.: Luminescent metal–organic frameworks as chemical sensors based on "mechanism–response": a review. Dalton Transac. **50**, 3429–3449 (2021)
131. Zeng, G., Xing, S., Wang, X., Yang, Y., Ma, D., Liang, H., Gao, L., Hua, J., Li, G., Shi, Z.: 3d–4f metal–organic framework with dual luminescent centers that efficiently discriminates the isomer and homologues of small organic molecules. Inorg. Chem. **55**, 1089–1095 (2016)
132. Pramanik, S., Zheng, C., Zhang, X., Emge, T.J., Li, J.: New microporous metal− organic framework demonstrating unique selectivity for detection of high explosives and aromatic compounds. J. Am. Chem. Soc. **133**, 4153–4155 (2011)
133. Buragohain, A., Yousufuddin, M., Sarma, M., Biswas, S.: 3D luminescent amide-functionalized cadmium tetrazolate framework for selective detection of 2, 4, 6-trinitrophenol. Cryst. Growth Des. **16**, 842–851 (2016)
134. Li, Y., Zhang, S., Song, D.: A Luminescent metal–organic framework as a turn-on sensor for DMF vapor. Angew. Chem. Int. Ed. **52**, 710–713 (2013)
135. Zeng, C.-H., Meng, X.-T., Xu, S.-S., Han, L.-J., Zhong, S., Jia, M.-Y.: A polymorphic lanthanide complex as selective Co^{2+} sensor and luminescent timer. Sens. Actuators B Chem. **221**, 127–135 (2015)
136. Yang, M.-Q., Zhou, C.-P., Chen, Y., Li, J.-J., Zeng, C.-H., Zhong, S.: Highly sensitive and selective sensing of CH_3Hg^+ via oscillation effect in Eu-cluster. Sens. Actuators B Chem. **248**, 589–596 (2017)
137. Zheng, K., Liu, Z., Jiang, Y., Guo, P., Li, H., Zeng, C., Ng, S.W., Zhong, S.: Ultrahigh luminescence quantum yield lanthanide coordination polymer as a multifunctional sensor. Dalton Transac. **47**, 17432–17440 (2018)
138. Li, C., Zeng, C., Chen, Z., Jiang, Y., Yao, H., Yang, Y., Wong, W.-T.: Luminescent lanthanide metal-organic framework test strip for immediate detection of tetracycline antibiotics in water. J. Hazard. Mater. **384**, 121498 (2020)
139. Liu, M., Li, H., Bai, L., Zheng, K., Zhao, Z., Chen, Z., Ng, S.W., Ding, L., Zeng, C.: Real-time and visual sensing devices based on pH-control assembled lanthanide-barium nano-cluster. J. Hazard. Mater. **413**, 125291 (2021)
140. Zheng, K., Liu, Z.-Q., Huang, Y., Chen, F., Zeng, C.-H., Zhong, S., Ng, S.W.: Highly luminescent Ln-MOFs based on 1, 3-adamantanediacetic acid as bifunctional sensor. Sens. Actuators B Chem. **257**, 705–713 (2018)
141. Liu, J., Han, X., Lu, Y., Wang, S., Zhao, D., Li, C.: Isostructural single-and dual-lanthanide metal-organic frameworks based on substituent-group-modifying tetracarboxylate ligands for ratiometric temperature sensing. Inorg. Chem. **60**, 4133–4143 (2021)
142. Dai, Y., Zhou, H., Song, X.-D., Zhang, J.-J., Hao, C., Di, L., Wang, Y.-X., Ni, J., Wang, H.-L.: Two (5, 5)-connected isomeric frameworks as highly selective and sensitive photoluminescent probes of nitroaromatics. CrystEngComm **19**, 2786–2794 (2017)
143. Xu, H., Liu, F., Cui, Y., Chen, B., Qian, G.: A luminescent nanoscale metal–organic framework for sensing of nitroaromatic explosives. Chem. Comm. **47**, 3153–3155 (2011)
144. Xin, R., Yu, X.-Y., Gao, W.-P., Wang, N., Yang, J.-J., Qu, X.-S., Zhang, X.: Hydrothermal syntheses, crystal structures and luminescence properties of Cd (II) coordination polymers based on 2-(pyridine-2-yl)-1H-imidazole-4, 5-dicarboxylic acid. Inorg. Chem. Comm. **35**, 38–41 (2013)
145. Wang, H., Yuan, X., Zeng, G., Wu, Y., Liu, Y., Jiang, Q., Gu, S.: Three dimensional graphene based materials: synthesis and applications from energy storage and conversion to electrochemical sensor and environmental remediation. Adv. Colloid Interface Sci. **221**, 41–59 (2015)
146. Xu, W.-X., Li, J., Liu, R.-P., Zhou, W.-X., Ma, W.-Y., Zhang, F.-X.: A novel 1D linear zinc (II) coordination polymer based 2, 2′-bipyridine-4, 4′-dicarboxylic acid: synthesis, crystal structure and photoluminescence property. Inorg. Chem. Comm. **28**, 12–15 (2013)
147. Li, B., Chrzanowski, M., Zhang, Y., Ma, S.: Applications of metal-organic frameworks featuring multi-functional sites. Coord. Chem. Rev. **307**, 106–129 (2016)
148. Gangu, K.K., Maddila, S., Mukkamala, S.B., Jonnalagadda, S.B.: A review on contemporary metal–organic framework materials. Inorg. Chim. Acta. **446**, 61–74 (2016)
149. Lan, A., Li, K., Wu, H., Olson, D.H., Emge, T.J., Ki, W., Hong, M., Li, J.: A luminescent microporous metal–organic framework for the fast and reversible detection of high explosives. Angew. Chem. Int. Ed. **48**, 2334–2338 (2009)
150. Wu, P., Wang, J., He, C., Zhang, X., Wang, Y., Liu, T., Duan, C.: Luminescent metalorganic frameworks for selectively sensing nitric oxide in an aqueous solution and in living cells. Adv. Funct. Mater. **22**, 1698–1703 (2012)
151. Yang, W., Feng, J., Song, S., Zhang, H.: Microwave-assisted modular fabrication of nanoscale luminescent metal-organic framework for molecular sensing. ChemPhysChem **13**, 2734–2738 (2012)
152. Wang, H., Yang, W., Sun, Z.M.: Mixed-ligand Zn-MOFs for highly luminescent sensing of nitro compounds. Chem. Asian J. **8**, 982–989 (2013)
153. Kim, T.K., Lee, J.H., Moon, D., Moon, H.R.: Luminescent Li-based metal–organic framework tailored for the selective detection of explosive nitroaromatic compounds: direct observation of interaction sites. Inorg. Chem. **52**, 589–595 (2012)
154. Li, H., Shi, W., Zhao, K., Niu, Z., Li, H., Cheng, P.: Highly selective sorption and luminescent sensing of small molecules demonstrated in a multifunctional lanthanide microporous metal–organic framework containing 1D honeycomb-type channels. Chem. Eur. J. **19**, 3358–3365 (2013)
155. Lee, J.H., Jaworski, J., Jung, J.H.: Luminescent metal–organic framework-functionalized graphene oxide nanocomposites and the reversible detection of high explosives. Nanoscale **5**, 8533–8540 (2013)
156. Zhou, J.-M., Shi, W., Xu, N., Cheng, P.: Highly selective luminescent sensing of fluoride and organic small-molecule pollutants based on novel lanthanide metal–organic frameworks. Inorg Chem. **52**, 8082–8090 (2013)
157. Xiao, J.-D., Qiu, L.-G., Ke, F., Yuan, Y.-P., Xu, G.-S., Wang, Y.-M., Jiang, X.: Rapid synthesis of nanoscale terbium-based metal–organic frameworks by a combined ultrasound-vapour phase diffusion method for highly selective sensing of picric acid. J. Mater. Chem. A. **1**, 8745–8752 (2013)
158. Wang, J., Zhang, L., Bao, L., Zhou, L., Liu, Y., Wu, P.: A novel dual-emitting luminescent metal-organic framework for naked-eye and microgram detection of picric acid. Dyes Pigm. **150**, 301–305 (2018)
159. Nagarkar, S.S., Joarder, B., Chaudhari, A.K., Mukherjee, S., Ghosh, S.K.: Highly selective detection of nitro explosives by a luminescent metal–organic framework. Angew. Chem. Int. Ed. **52**, 2881–2885 (2013)
160. Tian, D., Li, Y., Chen, R.-Y., Chang, Z., Wang, G.-Y., Bu, X.-H.: A luminescent metal–organic framework demonstrating ideal detection ability for nitroaromatic explosives. J. Mater. Chem. A. **2**, 1465–1470 (2014)
161. Song, X.Z., Song, S.Y., Zhao, S.N., Hao, Z.M., Zhu, M., Meng, X., Wu, L.L., Zhang, H.J.: Single-Crystal-to-single-crystal transformation of a europium (III) metal–organic framework

producing a multi-responsive luminescent sensor. Adv. Funct. Mater. **24**, 4034–4041 (2014)
162. He, Y.-C., Zhang, H.-M., Liu, Y.-Y., Zhai, Q.-Y., Shen, Q.-T., Song, S.-Y., Ma, J.-F.: Luminescent anionic metal–organic framework with potential nitrobenzene sensing. Cryst. Growth Des. **14**, 3174–3178 (2014)
163. Wang, W., Yang, J., Wang, R., Zhang, L., Yu, J., Sun, D.: Luminescent terbium-organic framework exhibiting selective sensing of nitroaromatic compounds (NACs). Cryst. Growth Des. **15**, 2589–2592 (2015)
164. Dou, Z., Yu, J., Cui, Y., Yang, Y., Wang, Z., Yang, D., Qian, G.: Luminescent metal–organic framework films as highly sensitive and fast-response oxygen sensors. J. Am. Chem. Soc. **136**, 5527–5530 (2014)
165. Liu, X.-G., Wang, H., Chen, B., Zou, Y., Gu, Z.-G., Zhao, Z., Shen, L.: A luminescent metal–organic framework constructed using a tetraphenylethene-based ligand for sensing volatile organic compounds. Chem. Commun. **51**, 1677–1680 (2015)
166. Xu, X., Guo, Y., Wang, X., Li, W., Qi, P., Wang, Z., Wang, X., Gunasekaran, S., Wang, Q.: Sensitive detection of pesticides by a highly luminescent metal-organic framework. Sens. Actuators B Chem. **260**, 339–345 (2018)
167. Liu, J., Hou, J.-X., Gao, J.-P., Liu, J.-M., Jing, X., Li, L.-J., Du, J.-L.: Stable Cd (II)-MOF as a fluorescent sensor for efficient detection of uranyl ions. Mater. Lett. **241**, 184–186 (2019)
168. Guo, F.: A novel metal-organic framework based on mixed ligands as a highly-selective luminescent sensor for $Cr_2O_7^{2-}$ and nitroaromatic compounds. Inorg. Chem. Comm. **102**, 108–112 (2019)
169. Lin, M.:A bi-functional 3D PbII–organic framework for Knoevenagel condensation reaction and highly selective luminescent sensing of $Cr_2O_7^{2-}$. Inorg. Chem. Comm. (2019).
170. He, N., Gao, M., Shen, D., Li, H., Han, Z., Zhao, P.: Rapid visual detection of nitroaromatic explosives using a luminescent europium-organic framework material. Forensic Sci Int. **297**, 1–7 (2019)
171. Fu, Y., Chen, H., Guo, R., Huang, Y., Toroghinejad, M.R.: Extraordinary strength-ductility in gradient amorphous structured Zr-based alloy. J. Alloys Compd. **888**, 161507 (2021)
172. Ye, Y., Liu, H., Li, Y., Zhuang, Q., Liu, P., Gu, J.: One-pot doping platinum porphyrin recognition centers in Zr-based MOFs for ratiometric luminescent monitoring of nitric oxide in living cells. Talanta **200**, 472–479 (2019)
173. Li, C., Zhang, F., Li, X., Zhang, G., Yang, Y.: A luminescent Ln-MOF thin film for highly selective detection of nitroimidazoles in aqueous solutions based on inner filter effect. J. Lumin. **205**, 23–29 (2019)
174. Zhou, Y., Yang, Q., Zhang, D., Gan, N., Li, Q., Cuan, J.: Detection and removal of antibiotic tetracycline in water with a highly stable luminescent MOF. Sens. Actuators B Chem. **262**, 137–143 (2018)
175. Chen, L., Liu, D., Zheng, L., Yi, S., He, H.: A structure-dependent ratiometric fluorescence sensor based on metal-organic framework for detection of 2, 6-pyridinedicarboxylic acid. Anal. Bioanal. Chem. **413**, 4227–4236 (2021)
176. Wang, G.-D., Li, Y.-Z., Shi, W.-J., Zhang, B., Hou, L., Wang, Y.-Y.: A robust cluster-based Eu-MOF as multi-functional fluorescence sensor for detection of antibiotics and pesticides in water. Sens. Actuators B Chem. **331**, 129377 (2021)
177. Xu, H., Gao, J., Qian, X., Wang, J., He, H., Cui, Y., Yang, Y., Wang, Z., Qian, G.: Metal–organic framework nanosheets for fast-response and highly sensitive luminescent sensing of F^{3+}. J. Mater. Chem. A. **4**, 10900–10905 (2016)
178. Sun, W., Wang, J., Zhang, G., Liu, Z.: A luminescent terbium MOF containing uncoordinated carboxyl groups exhibits highly selective sensing for Fe^{3+} ions. RSC Adv. **4**, 55252–55255 (2014)
179. Li, J.-X., Qin, Z.-B., Li, Y.-H., Cui, G.-H.: Two luminescent Cd (II)-MOFs based on bis (benzimidazole) and aromatic dicarboxylate ligands as chemosensor for highly selective sensing of Fe^{3+}. Polyhedron **151**, 530–536 (2018)
180. Salomon, W., Dolbecq, A., Roch-Marchal, C., Paille, G., Dessapt, R., Mialane, P., Serier-Brault, H.: A multifunctional dual-luminescent polyoxometalate@ metal-organic framework EuW10@ UiO-67 composite as chemical probe and temperature sensor. Front. Chem. **6**, (2018).
181. Su, Y., Zhang, D., Jia, P., Gao, W., Li, Y., He, J., Wang, C., Zheng, X., Yang, Q., Yang, C.: Bonded-luminescent foam based on europium complexes as a reversible copper (II) ions sensor in pure water. Eur. Polym. J. **112**, 461–465 (2019)
182. Wang, S.-T., Zheng, X., Zhang, S.-H., Li, G., Xiao, Y.: A study of GUPT-2, a water-stable zinc-based metal–organic framework as a highly selective and sensitive fluorescent sensor in the detection of Al^{3+} and Fe^{3+} ions. CrystEngComm **23**, 4059–4068 (2021)
183. Tang, J., Huang, M., Liang, Z., Yang, Y., Wen, Y., Zhu, Q.-L., Wu, X.-T.: Water-Stable two-dimensional metal–organic framework nanostructures for Fe^{3+} ions detection. Cryst. Growth Des. **21**, 5275–5282 (2021)
184. Yu, H., Liu, Q., Li, J., Su, Z.-M., Li, X., Wang, X., Sun, J., Zhou, C., Hu, X.: A dual-emitting mixed-lanthanide MOF with high water-stability for ratiometric fluorescence sensing of Fe^{3+} and ascorbic acid. J. Mater. Chem. C. **9**, 562–568 (2021)
185. Yu, Y., Pan, D., Qiu, S., Ren, L., Huang, S., Liu, R., Wang, L., Wang, H.: Polyphenylene sulfide paper-based sensor modified by Eu-MOF for efficient detection of Fe^{3+}. React Funct Polym. **165**, 104954 (2021)
186. Li, Y.-W., Li, J., Wan, X.-Y., Sheng, D.-F., Yan, H., Zhang, S.-S., Ma, H.-Y., Wang, S.-N., Li, D.-C., Gao, Z.-Y.: Nanocage-based N-rich metal–organic framework for luminescence sensing toward Fe^{3+} and Cu^{2+} Ions. Inorg. Chem. **60**, 671–681 (2021)
187. Wang, G.-Q., Huang, X.-F., Wu, C.-H., Shen, Y., Cai, S.-L., Fan, J., Zhang, W.-G., Zheng, S.-R.: A hydrolytically stable hydrogen-bonded inorganic-organic network as a luminescence turn-on sensor for the detection of Bi^{3+} and Fe^{3+} cations in water. Polyhedron **205**, 115284 (2021)